THE EFFECT OF ENVIRONMENTAL CONDITIONS ON THE HYDROSTATIC BURST PRESSURE AND IMPACT PERFORMANCE OF GLASS FIBER REINFORCED THERMOSET PIPES

BY

MOHAMMED KHALIQ NAIK

A Thesis Presented to the
DEANSHIP OF GRADUATE STUDIES

KING FAHD UNIVERSITY OF PETROLEUM & MINERALS

DHAHRAN, SAUDI ARABIA

In Partial Fulfillment of the
Requirements for the Degree of

MASTER OF SCIENCE

In

MECHANICAL ENGINEERING

DECEMBER 2005

KING FAHD UNIVERSITY OF PETROLEUM AND MINERALS
DHAHRAN 31261, SAUDI ARABIA

DEANSHIP OF GRADUATE STUDIES

This thesis, written by **MOHAMMED KHALIQ NAIK** under the direction of his Thesis Advisor and approved by his Thesis Committee, has been presented to and accepted by the Dean of Graduate Studies, in partial fulfillment of the requirements for the degree of **MASTER OF SCIENCE IN MECHANICAL ENGINEERING.**

Thesis Committee

Dr. Faleh A. Al-.Sulaiman (Advisor)

Dr. Zafarullah Khan (Member)

Dr. Nesar Merah (Member)

Dr. Amro M. Al- Qutub
Department Chairman

Dr. Mohammed A. Al- Ohali
Dean of Graduate Studies

١٤٢٧/٦/١٤

Date 10-7-2006

Dedicated to My Beloved Father, Mother, Brothers and Sisters whose constant prayers, sacrifice and inspiration led to this wonderful accomplishment

ACKNOWLEDGEMENTS

First and foremost, all praise to Allah *subhana-wa-ta'ala* for bestowing me with health, knowledge and patience to complete this work The Almighty, Who alone made this accomplishment possible. I seek His mercy, favor and forgiveness. Acknowledgements are due to King Fahd University of Petroleum & Minerals for the support in carrying out this research.

I acknowledge, with deep gratitude and appreciation, the inspiration, encouragement, remarkable assistance and continuous support given to me by my thesis advisor, Dr. Faleh Al-.Sulaiman. His guidance and assistance changed my thinking from pessimistic to optimistic one. I greatly appreciate dedication, attention and patience provided by him throughout the course of this study. Working with him was an opportunity of great learning and experience. Thanks are due to my thesis committee members, Dr. Zafarullah Khan and Dr. Nesar Merah for their constructive guidance, technical support and also for giving permissions to work in the Mechanical Engineering Workshop, advanced materials science lab (AMSL) and materials science lab (MSL) respectively.

I appreciate the assistance and encouragement received from the Chairman of ME Department, Dr. Faleh Al-Sulaiman for giving permission to work in after hours in the AMSL.

I owe very deep appreciations to Dr. Anwar Khaleel Shaikh, Director ME workshop and supervisor Mr. Abdulaziz including other staff of the ME workshop for their prompt and timely help and technical advice in experimental work.

The technical support and help provided by Engr. Mr. Zainulabdeen in conducting experimental work in AMSL is highly appreciated. The sincere and untiring efforts by him in preparing the experimental program and set-ups utilized in this study are also highly acknowledged.

Special thanks are due to my senior colleagues at the University Shaik Arifussalam, Syed Imran, Fasi, Farrukh, Sami, Qaiyum, Saad, Gayazullah, and Mujahid who were always there to help me in my work. I am indebted to my friends Khaleel, Asif, Zahid, Muqtadir, Kaleem, Imran, Manzoor, Nazeer, Adil, Shujath, Shafeeq, Omer and Rizwan for their encouragement and support throughout my stay at KFUPM. I am also thankful to all those who ever came to me for Da'waa and Tableegh.

Last but not the least I am grateful to my parents, brothers, and sisters for their extreme moral support, encouragement and patience during the course of my studies at KFUPM as well as throughout my academic career. No personal development can ever take place without the proper guidance of parents. This work is dedicated to my parents for their constant prayers and never ending love.

TABLE OF CONTENTS

LIST OF TABLES

LIST OF FIGURES

THESIS ABSTRACT

NAME: **MOHAMMED KHALIQ NAIK**

TITLE: **THE EFFECT OF ENVIRONMENTAL CONDITIONS ON THE HYDROSTATIC BURST PRESSURE AND IMPACT PEROFORMANCE OF GLASS FIBER REINFORCED THERMOSET PIPES**

MAJOR: **MECHANICAL ENGINEERING**

DATE: **DECEMBER, 2005**

During the long-term exposure of through Glass fiber reinforced plastic (GFRP) pipes, material degradation is expected to occur in the matrix, fiber, and the fiber-matrix interfacial regions. The degradation rate may be constant or increase/decrease with time and can be gradual and abrupt. Changes in the degradation mechanisms may also occur during the course of long-term exposure. All of these issues raise serious concerns regarding the long-term durability of the GFRP pipes and constitute problems that require solutions before extensive use of the GFRP pipes in applications such as oil/gas gathering and transportation networks.

In this study the effect of a variant natural and accelerated exposure conditions hydrostatic burst and low velocity impact tests on the 150 mm diameter GFRP pipes have been investigated. An in-house hydrostatic burst testing system and an instrumented impact tester were used for the testing. Pipe specimens of 150 mm internal diameter, 6 mm thickness and 1000 mm long were used for burst tests where as, for impact tests pipe sections of 160 mm length were used. Pipes were exposed to selected environments ranging from outdoor exposures (upto 12 months) to accelerated exposures of dry heat, humidity, seawater, and salt fog for periods ranging from 100 to 1000 hours. Pressure performance of the GFRP pipes reduces to almost 80 % for high energies impact. The energy absorbing capability of GFRV pipes exposed to dry heat first increases and decreases thereafter, due to curing effect. For salt spray exposure conditions decrease in impact resistance was observed. A similar trend of decrease in impact resistance was observed for humidity ambient. For humidity 100% exposure, an increase in impact resistance was noticed.

MASTER OF SCIENCE DEGREE

KING FAHD UNIVERSITY OF PETROLEUM & MINERALS

Dhahran, Saudi Arabia

THESIS ABSTRACT (ARABIC)

ملخص الرسالة

الاســـــــــم: محمد خليق نيك.

عنوان الرسالة: تأثير الظروف البيئية على خصائص الاصطدام والضغوط الهيدروستاتيكية الانفجارية على انابيب الالياف الزجاجية المقواة حراريا.

التخصـــــص: الهندسة الميكانيكية.

تاريخ التخـرج: ديسمبر / 2005

خلال عمليات النقل طويل المدى للغاز والزيوت في انابيب الالياف الزجاجية المقواة بالبلاستيك يتوقع ان يحدث تفسخ للانسجة والالياف في مناطق التقاء هذه الانسجة والالياف. معدل التفسخ قد يكون ثابتا او متغيرا صعودا وهبوطا مع الزمن كما يمكن ان يكون تدريجيا او مفاجئا. التغيرات في ميكانيكيات التفسخ قد تحدث خلال التعرض طويل المدى للظروف المتغيرة. جميع هذه القضايا تطرح اهتمامات جدية ووجود مشاكل متعددة تتعلق بالاستخدام طويل المدى لهذه الانابيب والتي تتطلب وجود حلول عملية لتحسين استخدام هذا النوع من الانابيب خاصة في التطبيقات العملية المتعلقة بنقل الزيوت و الغازات.

في هذه الدراسة تم فحص تاثير الظروف الطبيعية و المتسارعة على انبوب من الالياف الزجاجية المقواة بالبلاستيك بقطر 150 ملم عند اجراء فحصي الاصطدام و الانفجار الهيدروستاتيكي. وتم استخدام كلا من جهاز الانفجار الهيدروستاتيكي الداخلي وفاحص الاصطدام في هذه الدراسة. استخدمت عينة بقطر داخلي مقداره 150 ملم وسماكة 6 ملم وطول 1000 ملم في فحص الانفجار واستخدمت عينة اخرى بنفس المواصفات ولكن بطول 160 ملم في فحص الاصطدام. الانابيب تم تعريضها لبيئة مختارة مشابهة اولا للبيئة والظروف الجوية الخارجية (لمدة تصل تقريبا السنة) واخرى متسارعة من حيث الرطوبة والجفاف ومياه البحار والضباب الناتج من مياه مالحة بعد تعريضها للظروف والبيئة المطلوبة لمدة تتراوح من 100 الى 1000 ساعة . الخصائص المتعلقة بالضغط لهذه الانابيب قلت بنسبة 80% عند طاقات الاصطدام العالية , قابلية امتصاص الطاقة لهذه العينات زادت ومن ثم عادت ونقصت نتيجة تأثيرات "التمليح" . تم ملاحظة وجود نقص في القمة التي تصل اليها القوة لعينة معرضة لضباب ملحي و بطريقة مشابهة تم ملاحظة وجود نقص في مقاومة الاصطدام لعينة معرضة لرطوبة عالية بالاضافة لملاحظة زيادة في مقاومة الاصطدام في بيئة تصل الرطوبة فيها الى 100%.

درجة الماجستير في العلوم

جامعة الملك فهد للبترول والمعادن

الظهران- المملكة العربية السعودية

CHAPTER 1

INTRODUCTION

A 'composite' is a heterogeneous combination of two or more materials (reinforcing agents & matrix), differing in form or composition on a macroscale. The combination results in a material that maximizes specific performance properties. The constituents do not dissolve or merge completely and therefore normally exhibit an interface between one another. In this form, both reinforcing agents and matrix retain their physical and chemical identities, yet they produce a combination of properties that cannot be achieved with either of the constituents acting alone. Composites are commonly classified based on the type of matrix used: polymer, metallic and ceramic. In fiber - reinforced composites, fibers are the principal load carrying members, while the surrounding matrix keeps them in the desired location and orientation. Matrix also acts as a load transfer medium between the fibers, and protects them from environmental damages due to elevated temperatures, humidity and corrosion. The principal fibers in commercial use are various types of glass, carbon and Kevlar. All these fibers can be incorporated into a matrix either in continuous or discontinuous form. Composites have unique properties as follows:

- Composite materials are 30-45% lighter than aluminium structures designed for the same functional requirements

- Pipes/cylinders made of composites, with lower weight compared to the metallic ones, can withstand high internal pressures
- Excellent corrosion resistance
- Appropriate inhibitors/additives can impart very good fire retardance properties in composites
- Improved torsional stiffness and impact resistance properties
- Higher fatigue endurance limit (up to 60% of the ultimate tensile strength)
- Design flexibility (composites are more versatile than metals and can be tailored to meet performance needs and complex design requirements)
- Composites exhibit higher internal damping capacity
- Composites have better dimensional stability over temperature fluctuations due to low coefficient of thermal expansion
- Composites enjoy lower life cycle cost compared to metals
- Composite parts can eliminate joints/fasteners, providing part simplification and integrated design compared to conventional metallic parts
- Improved appearance with smooth surfaces

In spite of many potential advantages of Fiber Reinforced Plastics (FRPs) over their metallic counterparts, a general lack of confidence in the ability of these materials to withstand the full range of environmental conditions experienced during service has prevented their widespread use in oil/gas production and transportation systems. Although extensive research has been undertaken during the past two decades, several major issues remain unresolved in predicting the performance of these materials under long-term exposure to environmental conditions such as seasonal changes in ambient

temperatures, humidity, UV radiation, rain, salt water, precipitation of air-borne contaminants, and other corrosive agents such as crude oil.

During the long-term exposure of oil/gas transportation through GFRP pipes, material degradation is expected to occur in the matrix, fiber, and the fiber-matrix interfacial regions. The degradation rate may be constant or increase/decrease with time. The changes in the degradation rate may be gradual or abrupt. Changes in the degradation mechanisms may also occur during the course of long-term exposure. All of these issues raise serious concerns regarding the long term durability of the GFRP pipes and constitute problems that require solutions before extensive use of the GFRP pipes can be made to replace their metallic counterparts. It is the view of many design engineers, manufacturers, and end users of GFRPs that without finding reliable answers with respect to these issues, many remarkable engineering and economic benefits that the GFRP material can offer may remain unexploited to the disadvantage of the oil production industry. It is hoped that the findings of this study will bring substantial help in expanding the use of GFRPs in many new areas of application, improving operational standards, and providing better maintenance and repair guidelines.

1.1 NEED FOR GFRP PIPES

The potential cost savings associated with replacing steel pipes with vinyl esters GFRP pipes are considerable. However, durability of these pipes for an extended lifetime is very important from the point of view of the end-users. GFRP pipe suppliers may overestimate their maximum allowable temperature and pressure service conditions and often underestimate the effects of the long-term service environment on the mechanical

properties. Hence, the issue of long term behavior and aging of GFRP pipes must be appropriately addressed before extensive use of GFRP pipes in transporting organic liquids such as crude oil, especially when contaminated with water, H_2S, and chemically active solvents. Therefore, long-term GFRP material degradation is an imperative concern to the manufacturer and the end-user.

The environments that the GFRP material production/transportation piping system are expected to encounter can be divided into routine service environments, and those which could be present under specific and unusual circumstances. Routine environments to which the pipe could be exposed involve a range of seasonal temperatures up to 70^{o}C, the amount of moisture in air, rain water, solar radiation in the ultra violet (UV) to visible light ranges, salt-laden air (in costal regions), marine water, and the fluid flowing through the pipes. The pipes in addition to the above environmental conditions would also be exposed to sustain static and variable (fluctuating) mechanical stresses. Thus the synergistic interaction of environmental and mechanical factors will be considered. Under specific and unusual circumstances, the pipes may encounter elevated temperatures, pressure surges, and impact loading.

It is evident that the above listed environmental factors will have a detrimental effect on many critical mechanical and physical properties of the GFRP material. This degradation of material properties will have a consequent influence on the long-term performance and durability of the piping systems. Among these, of major concern are: the loss of tensile, flexural, fatigue, creep rupture, and impact strengths, and decrease in storage modulus and glass transition temperature of the material and the hydrostatic

pressure it can resist. The degradation in these properties will have a substantial effect on the long-term performance capability of the pipes.

1.2 GLASS-FIBER REINFORCED PLASTIC (GFRP)

Glass-fiber reinforced-plastic (GFRP) pipes are excellent candidates for transporting corrosive liquids due to their superior corrosion resistance, higher strength-to-weight ratio, low coefficient of friction, and lower maintenance cost compared to conventional steel pipes. There have been ample studies on the suitability of thermosetting-based resin pipes with glass reinforcement for various applications including water storage tanks and desalination, chemical and process industry, and oil and gas industries.

In the oil and gas industries, for example, SHELL had more than 600 km of epoxy-based GFRP piping installed by 1990 with 37% of the piping used for onshore hydrocarbon flow lines. SHELL had 10 years successful experience with pipe diameters smaller than 150 mm where the highest pressure used was 95 bar and the maximum temperature was up to 65°C. Significant cost savings were obtained in comparison with carbon steel when considering corrosion protection cost. A more recent study presented on 1999 indicated that SHELL had over 2250 km of FRP piping in service.

1.2.1 Fiber Reinforcement

The fiber is an important constituent in composites. A great deal of research and development has been done with the fibers on the effects in the types, volume fraction, architecture, and orientations. The fiber generally occupies 30%-70% of the matrix volume in the composites. The fibers can be chopped, woven, stitched, and/or braided.

They are usually treated with sizings such as starch, gelatin, oil or wax to improve the bond as well as binders to improve the handling. The most common types of fibers used in advanced composites for structural applications are the fiberglass, aramid, and carbon. The fiberglass is the least expensive and carbon being the most expensive. The cost of aramid fibers is about the same as the lower grades of the carbon fiber. Other high-strength high-modulus fibers such as boron are at the present time considered to be economically prohibitive.

1.2.2 Glass Fibers

The most widely used reinforcement is fiberglass because of its low cost, high tensile and impact strength, light weight, and good corrosion resistance. Hence, vinyl ester resin reinforced with fiberglass represents a potential composite materials for the oil and gas industry.

The glass fibers are divided into three classes E-glass, S-glass and C-glass. The E-glass is designated for electrical use and the S-glass for high strength. The C-glass is for high corrosion resistance, and it is uncommon for civil engineering application. Of the three fibers, the E-glass is the most common reinforcement material used in civil structures. It is produced from lime-alumina-borosilicate which can be easily obtained from abundance of raw materials like sand. The fibers are drawn into very fine filaments with diameters ranging from 2 to 13 X 10^{-6} m. The glass fiber strength and modulus can degrade with increasing temperature. Although the glass material creeps under a sustained load, it can be designed to perform satisfactorily. The fiber itself is regarded as an isotropic material and has a lower thermal expansion coefficient than that of steel.

1.2.3 Resin Systems

The resin is another important constituents in composites. The two classes of resins are the thermoplastics and thermosets. A thermoplastic resin remains a solid at room temperature. It melts when heated and solidifies when cooled. The long-chain polymers do not chemically cross link. Because they do not cure permanently, they are undesirable for structural application. Conversely, a thermosetting resin will cure permanently by irreversible cross linking at elevated temperatures. This characteristic makes the thermoset resin composites very desirable for structural applications. The most common resins used in composites are the unsaturated polyesters, epoxies, and vinyl esters; the least common ones are the polyurethanes and phenolics.

One of the important aspects to consider in the durability issues of composites is the role of the polymer matrix and its change. The primary role of the matrix in the composites is for it to transfer stresses between the fibers, to provide a barrier against an adverse environment, and to protect the surface of the fibers from mechanical abrasion. Although its role in tensile load-carrying capacity is minor, it has a major influence on the inter-laminar and in-plane shear load transfer.

1.2.4 Vinyl Esters Resins

The vinyl ester resins were developed to take advantage of both the workability of the epoxy resins and the fast curing of the polyesters. The vinyl ester has higher physical properties than polyesters but costs less than epoxies. The acrylic esters are dissolved in a styrene monomer to produce vinyl ester resins which are cured with organic peroxides. A

composite product containing a vinyl ester resin can withstand high toughness demand and offer excellent corrosion resistance.

The Figure 1.1 shows the idealised chemical structure of a typical vinylester. As the whole length of the molecular chain is available to absorb shock loadings this makes vinylester resins tougher and more resilient than polyesters. The vinylester molecule also features fewer ester groups. These ester groups are susceptible to water degradation by hydrolysis which means that vinylesters exhibit better resistance to water and many other chemicals than their polyester counterparts, and are frequently found in applications such as pipelines and chemical storage tanks.

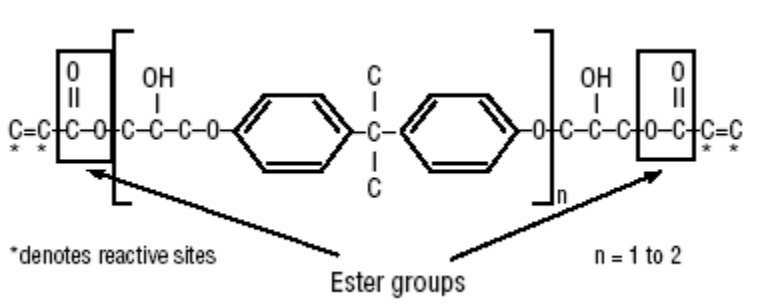

Figure 1.1 Idealised chemical structure of typical epoxy based vinylester

Vinyl esters based GFRP is generally preferred for moderate temperature applications in reinforced thermoset piping systems because of it's:

- Improved corrosion resistance to strong acids, bases, and salt solutions up to a temperature of 93° C.
- Improved impact resistance and greater tolerance to temperature and pressure fluctuations and mechanical shock than the polyesters.

- Excellent fiber wet-out and good adhesion to the glass fiber.
- Rapid curing and superior creep resistance.

Vinyl ester based composites have demonstrated economy and better price to performance characteristics than steel and its alloys in many corrosive environments. Low maintenance requirements, design flexibility and ease of installation.

Vinyl esters cost a bit more than polyesters and so specific applications where vinyl-esters surpass polyesters include chemically corrosive environments (such as filament wound glass/vinyl ester chemical tanks) and in structural laminates where a high degree of moisture resistance is desired.

1.2.5 Epoxy Resins

Epoxy resins are among the best matrix materials for many fiber composites. Epoxy resins are characterized by the presence of epoxide (or oxirane) functionality are an important industrial class of thermosets due to their chemical resistance, outstanding adhesive and good physical and mechanical properties which include high tensile strength, high modulus, and good fatigue resistance.

Epoxy resins adhere well to a wide variety of fillers, reinforcing agents and substrates. The chemical reaction between epoxy resins and the curing agent does not release any volatiles and water. It is also air curable, highly fillable, possesses low cure shrinkage, low susceptibility to stress formation. They also have good chemical resistance and temperature resistance up to 1400°C (wet)/2200°C (dry).

Epoxy resins are widely used for many important applications such as surface coatings, adhesives, reinforced plastics, printed circuit boards, etc. The large family of epoxy resins represents some of the highest performance resins of those available at this time. Epoxies generally out-perform most other resin types in terms of mechanical properties and resistance to environmental degradation. As a laminating resin, they have increased adhesive properties and are resistant to water degradation.

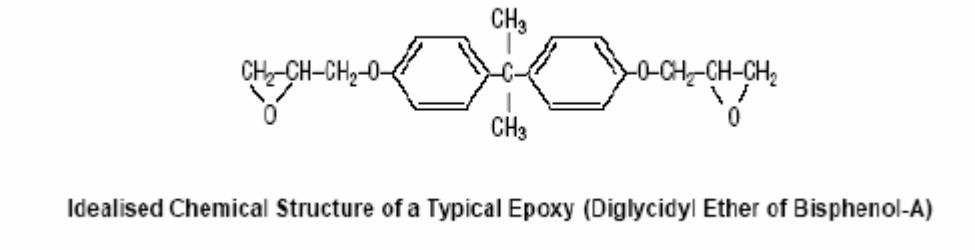

Figure 1.2 Idealised chemical structure of typical epoxy

1.3 TYPES OF ENVIRONMENTAL DEGRADATIONS

Long-term data on glass-fiber reinforced polymeric composites subjected to cyclic loading has not been well documented and is still poorly understood. During the fatigue test, four damage modes were typically observed at various stages of the test: transverse matrix cracking, delamination, fiber/matrix debonding and fiber fracture. While matrix cracking and delamination occur early in the test, the latter two damage modes typically initiate and develop rapidly towards the end of life.

Environment effects on composite materials are considered in the early stages of a system design. Failure to do so can lead to expensive design iterations during the later design stages or a great increase in the cost of ownership because of failures caused by

the environment. Many studies on GFRP degradations are reported in the literature that includes Corrosion, Electromagnetic effects, fatigue, moisture, fire, impact damage, weathering, temperature, rain erosion etc. Among them, four major environmental agents that could significantly degrade GFRPs are.

- Temperature
- UV radiations
- Moisture absorption.
- Oxidation

1.3.1 Temperature

It is well known that temperature has a strong effect on the mechanical properties of polymers. When temperature is increased, energy continues to be added to the polymer chains, and eventually weak chemical bonds begin to break. This bond breakage leads to chain cleavage and cross linking, especially when the thermoset polymer is not fully cured after processing. Cold temperatures tend to make polymers less flexible and thus susceptible to damage due to fatigue induced by mechanical loading. High temperatures can cause resins to chemical reactions are accelerated by an increase in temperature. When large temperature differential exists, sufficiently large stresses may include micro cracking in the material, which in turn reduce the stiffness of the composite, increase permeability and water ingression through fiber/matrix interface, and thus finally contribute to the degradation processes. Another very important effect of lower temperatures is the accompanying change in matrix strength and stiffness. Most resin materials become stiffer and stronger as they are cooled.

Unless a composite contains a significant percentage of interconnected voids, which are filled with water, the freeze-thaw effects on the strength, within the normal temperature range (+30°C to -20°C) are insignificant. Commercially available glass fiber composites usually contain about 0.4 percent voids, which does not allow any appreciable frozen moisture to cause any serious damage. However, low temperature thermal cycling has other effects on composites. Residual stresses occur in composite materials due to differences in coefficients of thermal expansion of constituent elements in the material microstructure. The amount of contraction, or expansion, can be determined by multiplying the coefficient of thermal expansion (CTE), denoted by α, and the change in temperature. Composite manufacture is often completed at elevated temperatures. It is common for a composite to see a change in temperature of –150°C from processing to room temperature. Thus, internal stresses are established in the material even before an external load is applied. Under extreme low temperature conditions, these stresses can result in the formation of micro cracks in the resin matrix or in the resin-fiber interface.

1.3.2 UV Radiation

Another important degradation factor is due to the UV radiation. While the atmosphere absorbs much of the sun's high-energy radiation, some radiation in the 280 to 400 nm (UV) range reaches the earth's surface. Since the energy of this radiation is 72 to 100 kcal, it is sufficiently strong to cleave covalent bonds and cause embrittlement of organic polymers. Some degradation occurs when polymers are irradiated, but cross-linking is the predominant reaction. Although cross-linking is a useful reaction in making poly (vinyl ester) materials that are dimensionally stable at high temperatures, there may

be undesirable consequences when it occurs after the materials are in service. The modulus increases with cross-linking, but the energy-absorbing capability goes through a maximum and decreases thereafter. A rubbery polymer system generally becomes brittle as a result. Another typical pattern accompanying cross-linking is a decrease in compatibility, so that plasticizers exude, system shrinks, and delamination occurs.

1.3.3 Oxidation

The third type of degradation is caused by oxidation. The oxidative degradation of an organic polymer generally proceeds through free-radical reactions. Free radicals are formed by the thermal or photolytic cleavage of bonds. The radicals then react with oxygen to yield peroxides and hydro peroxides. Such reactions lead to both chain cleavage and to cross-linking. Cross-linking is visualized as a result from the combination of radical sites on adjacent chains. Many synthetic organic polymers are oxidized in contact with the atmosphere. At room temperature in the absence of light, the reaction may be very slow. Nevertheless, at elevated temperatures or during exposure to UV light the rate of oxidation is often quite rapid.

1.3.4 Water Absorption

Pipes are often in contact with water either due to weathering by rain or by carrying moisture containing fluids and chemicals. Vinyl esters containing the ester group in their chain molecules are susceptible to hydrolysis of the side group, which might lead to cross-linking. Moisture has potentially degrading effect on matrix materials. Moisture in

many of its forms-acidic, basic, neutral are known to affect the durability of composites Moisture present in many forms and eventually penetrates all organic materials by a diffusion controlled or by instantaneous absorption until the moisture equilibrium concentration is achieved. Usually the moisture concentration increases initially with time and finally approaches the saturation point (equilibrium) after several days of exposure to humid atmosphere. The time to reach the saturation point depends on the thickness of the composite and the ambient temperature. Drying can reverse the process but may not result in complete attainment of original properties. The uptake of water by polymer composites in general follows the generalized Fick's law of diffusion.

1.4 PRESENT STUDY

The main objectives of the present study are to investigate the effect of environmental conditions on the hydrostatic burst pressure and impact performance of the glass fiber reinforced thermoset pipes along with the post-impact hydrostatic burst pressure performance.

The thesis is divided into five chapters. Chapter 1 gives the introduction of the study which includes basic information regarding composites and its properties, glass fibers, Vinyl and epoxy resins and the effects of different types of environmental degradations. Chapter 2 includes the literature review that covers previous work done by researchers on the hydrostatic burst and impact testing on the composite materials. The experimental procedure adopted for the specimen preparation and testing along with the details of testing apparatus are provided in chapter 3. The results for the hydrostatic burst tests and impacts tests performed on glass fiber reinforced vinylester and glass fiber reinforced

epoxy composite pipes are discussed in chapter 4. This chapter also includes results for the seawater immersion and oil filled pipes exposed to natural conditions and impact test results for different accelerated natural conditions of dry heat, salt spray, humidity ambient and humidity 100%. Finally, conclusions drawn from this study and recommendations for future work are given in chapter 5.

CHAPTER 2

LITERATURE REVIEW

This chapter describes the literature review which covers relevant previous and ongoing work done by different researchers on the hydrostatic burst pressure test and impact characteristics of GFRP vinyl ester pipes. First, the literature review regarding the effect of environmental conditions on the mechanical properties of GFRP is presented in section 2.1. Then the hydrostatic burst test and impact damage characteristics of GFRP is discussed in section 2.2. At the end of the chapter the summary of the literature review and status of the present problem is discussed.

2.1 EFFECTS OF DIFFERENT ENVIRONMENTAL CONDITIONS ON GFRP PERFORMANCE

GFRP composites may last many years before showing signs of wear or degradation. However, they can deteriorate when exposed to sunlight, smog, acid rain, hot and cold temperatures, and long-term exposure to, or immersion in, ocean water. Seawater exposures, either salt fog or oxygen-rich salt water, have been shown to result in the most severe degradation of material properties.

As reported by Liao et al., [1] higher the temperature and the longer the exposure time to fluids, the larger is the decrease in strength and modulus of FRP. They have also

reported that the tensile strength, compressive strength and modulus of GFRP degraded upon exposure to various moist and aqueous environments.

Chin et al. [2] designed an integrating sphere UV-chamber which appears to be capable of greatly mitigating known sources of systematic errors like human/machine interactions, high specimen temperature, non-uniform spatial irradiance over the dimensions of a specimen and from specimen-to-specimen. Preliminary evaluations of the integrating sphere based UV-chamber were very promising.

Sampath et al. [3] studied two fiber-reinforced polymer composites for susceptibility to degradation when exposed to aggressive environments. Composites and fibers were then exposed to a mixed inoculum of aerobic bacteria and to an anaerobic sulfate reducing bacteria. Fiberglass-reinforced vinyl ester and isophthalic ester composites, as well as the individual glass fibers, were extensively degraded due to the bacterial attack. The composite samples underwent degradation in the form of fiber pullout, as well as matrix cracking, leading to subsequent reduction in the mechanical properties.

Signor [4] studied the chemical and mechanical properties due to effects of ultraviolet radiation exposure on vinyl ester matrix resins. The degradation may be limited to a thin surface layer, bulk mechanical properties like tensile strength along with strain and toughness of the material is greatly reduced.

Liau [5] studied the individual and combined effects of ultraviolet light and thermal shock on the physical properties of polymer matrix composites in air and in a near vacuum system. It was found that the irradiated surface of the composites would be most

damaged by UV and weight loss increases with irradiation time and the damage would be higher when specimens were exposed in air than in the near vacuum system.

Marsh et al. [6] investigated the solubility and kinetics of moisture transport mechanisms over a range of partial pressure and temperature. He carried out studies on moisture adsorption and diffusion into epoxy and epoxy-glass composites and demonstrated solubility follows Henry's law. The diffusion is best described as non-Fickian. One of the most interesting observations of this work is that the small concentration of H_2O molecules absorbed has an anomalously large effect on those yet to be absorbed.

Springer [7] investigated the effects of environmental on glass fiber reinforced polyester and vinylester composites immersed in liquids and in humid air and found that the weight loss and changes in material strength will depend on the temperature and environment.

Sarkar [8] characterized glass fiber reinforced vinylester resin composites incorporating varying amounts of fibers (63.5, 55.75, 48.48, 38.63 and 27.48 wt %) for their mechanical properties both as prepared and after treatment with boiling water for 2, 4, 6, 8 and 24 h. Weights of the samples were found to increase to a saturation at about 8 h with boiling water treatment. Heavy fibre pullout was observed in the tensile zone while shear fracture of the fiber bundles was predominant at the compressive zone of the samples tested. The fracture surfaces revealed heavy debonded surfaces between the reinforcement and the matrix. The debonded areas joined to form continuous long cracks weakening the composites.

Amateau et al. [9] studied the effects of seawater immersion on the impact resistance of glass fiber reinforced epoxy composites. The energy for incipient damage increased significantly following the seawater immersion due to plasticization of the matrix by the absorbed moisture. The composite experienced substantial reductions in peak load and energy absorbed at peak load as a result of moisture-induced degradation of the fibers and fiber/matrix interface.

Zheng [10] conducted experiments to measure the changes in weight of neat epoxy resins and carbon fiber reinforced epoxy composites during immersion in distilled water in temperature range from 0.5°C to 80 °C. Water absorption in epoxy resin and its fiber composite shows that the water solubility in resin forms two bounds. The absorption lower bound was obtained from initially dry samples and the higher bound (reverse thermal effect i.e, the amount of water absorbed increases when a water-saturated specimen is transferred from a high temperature to a lower temperature water bath) was observed when the saturated samples were transferred from higher to lower temperatures while still exposed to moisture.

Monney [11] studied mechanical behaviour of an epoxy-glass composite under photo-oxidation and concluded that the conjugated actions of the mechanical stress of the photo-oxidation and of the temperature accelerate the weakening of the material by cracking at the surface. Thus making the material weak externally as well as internally.

Kumar [12] did experimental investigation on cyclic exposure of carbon epoxy composite to UV radiation and condensation which resulted in extensive physical degradation and deterioration of mechanical properties. A continuous weight loss was

observed which indicated the presence of synergistic degradation mechanism, which resulted in extensive matrix erosion, void formation and fiber matrix debonding. The synergy between the degrading environmental will cause enough damage that the load transfer between the fibers may not be possible owing to matrix erosion. This will lead to deterioration of even fiber-dominated properties; result in catastrophic structural failure due to internal pressure.

Fernand Ellyin et al. [13] investigated the effects of moisture absorption and exposure to elevated temperature on the mechanical properties of glass fiber reinforced epoxy composite tubes. Filament wound tubular composite specimens were immersed in distilled water at two different temperatures for approximately four months and their moisture absorption was recorded. The rate of moisture absorption was greater for the group of specimens immersed in distilled water at an elevated temperature (50ºC) than those at room temperature (20ºC) and observed that the strength and stiffness decreased to some extent with the presence of moisture and increasing temperature. Microscopically, the greatest water damage was apparent in the matrix, fiber–matrix interface where there was less resin adhesion to the fibers with increasing water temperature. Fiber strength negatively affected, possibly due to either leaching out of the glass fibers interface layer or glass fiber embrittlement, and less effective bonding and load distribution at the fiber–matrix interface.

Kwang Bok Shin [14] exposed the graphite epoxy composite material to natural environments for 5 years and accelerated environmental conditions including temperature, ultraviolet radiation and moisture for 2000 h, in order to evaluate the

degradation of the mechanical and physical properties of graphite epoxy composite material. Decrease in strength and stiffness of the material was observed for both the natural and accelerated environmental conditions. He predicted an accelerating factor for long term performance of the material.

Chin [15] characterized the chemical and physical changes in polymeric matrix resins like vinylester following exposure to UV radiation, moisture, temperature and high pH environments. No significant changes were observed in tensile and hydrostatic strength for vinylester resins following immersion in water, salt solution and surface oxidation was observed as evidenced by the increase in oxygen containing functional groups.

Karbhari et al**.** [16] characterizes the mechanical response of E-glass/vinyl ester quadric axial composites immersed in de ionized water, seawater, and synthetic seawater. They observed substantial differences based on the solution type, with de ionized water immersion causing the maximum drop in inter laminar shear performance and seawater causing the maximum reduction in tensile performance. Drying of specimens, even over prolonged periods, does not result in complete regain of performance degradation due to sorption processes.

Karbhari et al. [17] exposed E-glass Vinyl ester samples to fresh water, seawater, cold, and freeze-thaw and found that the changes in mechanical characteristics such as strength and modulus, and thermo-mechanical dynamic characteristics such as storage and loss moduli, and glass-transition temperature were measured and concluded that the sea water exposure to be most detrimental. The presence of moisture/solution has a significant effect; both in terms of physical and chemical aging and in terms of micro

cracking and fiber–matrix debond initiation. It was shown that degradation due to alkali exposure is more severe than due to the deionized water. Data from accelerated tests is used to provide long-term predictions, which are shown to correlate well with experiments in the short-term.

Kootsookos et al [18] have investigated the durability of glass/ vinyl ester composite when immersed in the seawater at a temperature of 30˚C for about 2 yrs. The experiment was conducted for different immersion times using a 4-point bend load. Considerable amount of moisture absorption as well as the chemical degradation of the resin matrix and fiber/ matrix interface region occurred due to immersion. Hence, this resulted in degradation of flexural modulus and strength. Despite the superior chemical stability of vinyl ester based composites, the flexural properties degraded to a similar extent to that of polyester materials.

Mizoguchi [19] investigated the degradation behaviors of E glass and C glass fiber reinforced plastics concerning acid stress corrosion, measuring the residual strength after environmental pre-stressing using acoustic emission. C glass fiber reinforced plastics have extremely longer lifetime in contrast of E glass fiber reinforced plastics, this result reflect the difference of the durability of reinforcement, that E glass fiber corroded under acid environment, but C glass fiber resist. Residual strength decreases.

2.2 HYDROSTATIC BURST TEST

Hydrostatic testing is universally known and accepted as a means of demonstrating the fitness of a pressurized component for service. After a test, a pipeline or pressure

vessel can be expected to safely contain its intended operating pressure. The confidence level that a pipeline or pressure vessel is fit for safe service increases as the ratio of test pressure to operating pressure increases. This highly beneficial aspect of hydrostatic testing applies not only to a new component to be placed in service for the first time. A similar benefit accrues to an in-service component if that component is taken out of service after a period of time and subjected to a hydrostatic test. A “revalidation” test of the latter type assures either that no significant time dependent deterioration of the component has taken place or that any segment that has been significantly degraded will be revealed and eliminated.

A test reveals weaknesses by causing ruptures or leaks; it does not indicate, for example, other areas where active corrosion may be taking place. A limitation that has both technical and economic implications is that a level of test pressure to operating pressure sufficient to generate high confidence may result in numerous test breaks or leaks. Repeated test failures may actually reduce confidence in the final margin of safety demonstrated by the test, and such failures will certainly add significantly to the cost of the test and the time out of service.

Pressure failure occurs due to ductile yielding of the material when the stress in the pipe wall exceeds the yield stress of the material. Typically the failure proceeds via the following mechanism: the stress on the pipe wall results in uniform creep expansion. When the yield stress of the polymer is exceeded, localized yielding occurs which results in the thinning of the wall in a localized region of the pipe (typically at the point where the wall thickness is lowest). This is followed by localized expansion (or "ballooning") at

the thin wall section. Final failure occurs across the newly oriented polymer structure in the 'balloon' to result in the typical "Parrot's Beak Failure".

Hydrostatic pressure testing is conducted to determine a material's performance. Burst Testing (ASTM D1599) is conducted to determine a material's short term strength. Pipe samples are pressurized such that a ductile failure occurs in 60 - 70 seconds. The pressure required to result in such a failure is known as the 'burst pressure'. Actual pipe samples are pressurized with water as the internal medium and either air or water as the external medium. The internal pressure in the pipe samples results in both an axial and a hoop stress. As the hoop stress is twice the axial stress, it is the stress in the hoop direction that results in failure. The hoop stress is given by

for outside diameter controlled pipe

$$S = \frac{P(D - t)}{2t} \tag{2.1}$$

Or

for inside diameter controlled pipe

$$S = \frac{P(d + t)}{2t} \tag{2.2}$$

Muscati [20] carried out full scale hydraulic pressure tests on GRP pipes with flanged joints under conditions simulating an actual pipework installation. The results show the flanges to have a much lower strength than the basic pipe and demonstrate the need for serious considerations to be given, at the design stage, to the strength of GRP flanged joints under pressure.

Nakai et al. [21] carried out hydrostatic burst tests of steels pipes with and without HIC (hydrogen induced cracking). The pipes with large amount of HIC burst immediately over the yield pressure, showing a little expansion whereas with small amount of HIC burst at the approximately similar pressure to the maximum burst pressure of the reference pipes. The fractured surfaces were smooth for the reference pipes but were rough with HIC. Many small cracks parallel to the axial direction of pipes were observed on the inner surfaces of the fractured parts of burst pipes with the large amount of HIC.

Ghorbel and Spiteri [22] studied the mechanical behaviour of the E glass fiber reinforced polyester resin and an ECR glass fiber reinforced vinylester resin pipes before and after exposure to water for different duration through internal pressurizing tests with closed end procedure. The internal pressure was increased at the rate of 0.5 MPa per second. The results indicate that in the hoop direction, fibers carry the complete load while in the axial direction there is a substantial contribution from the matrix. The fibers are degraded by water penetration explaining the fact that pipes failure occurs by bursting instead of weeping. The failure will occur by bursting when the tensile stress in the pipe reaches the fibers failure strength otherwise weeping occurs. The failure of the pipe take place at much lower pressure after exposure than the design pressure of the pipe material before exposure.

Nagesh [23] conducted finite element analysis of the composite pressure vessels and compared with the experimental hydroburst tests. The finite element analysis predicted burst pressure between 10.5 MPa and 11 MPa is in good agreement with mean burst

pressure of 10.59 MPa from the hydrostatic burst pressure tests. The burst in the pressure vessel is indicated by unusually large displacement and infeasible stress profile in consequence to a substantial degradation in the fibre material of the composite.

Chang et al [24] conducted a test program to investigate the failure modes of damaged and undamaged graphite-epoxy cylindrical tubes subject to burst tests. The specimens were damaged in one of two ways: either a longitudinal line cut or a single-point impact. Impact damaged tubes, showed that the burst pressure decreases with increasing impact load. The incipient damage load was 185 lb. at this load, the damage tube had a burst pressure approximately 24% lower than the undamaged tube. At an impact load of 335 lb, the burst pressure decreases by 32% from the undamaged.

Glover et al [25] conducted burst testing on a carbon steel vessel containing flaws. The vessel was pressurized with water in a controlled ramp approach and the failure pressure observed was nearly five times the design operating pressure even in the severe case where the vessel had several flaws and had been retired from service. Fracture analysis was performed to predict the critical pressure to cause failure from the existing flaws in the vessel. The detailed analysis predicted failure by small amounts of ductile crack growth followed by plastic collapse. After the burst test, a failure analysis was conducted to measure the actual flaw sizes and compared with the fracture analysis.

Chang et al [26] performed an experimental and analytical program to elucidate the failure process of filament-wound graphite-epoxy tubes, especially the effects of wrinkled fibers and of proof testing on tube burst strength. Hoop wrinkles and severe helical wrinkles caused a reduction in burst pressure. Hoop wrinkles caused an average

reduction in burst pressure of 14%; severe helical wrinkles caused an average reduction of 8%. Minor helical wrinkles had no effect. Proof pressures up to 95% of burst and number of proof testing cycles had no noticeable effect on the average ultimate burst pressures of the tubes.

John Smith [27] conducted a number of hydrostatic tests on selected cylinders with various sizes of flaws to determine the burst pressure of cylinder containing flaws. Cylinders without flaws were hydrostatically pressurized to burst to establish the burst pressure to be used to calculate the measured RSF (residual strength factor), which is the ratio of burst pressure with flaw to burst pressure without flaw.

Yang [28] developed a analytical model for predicting the bucking load for fiberglass reinforced thermoset composite pipe under external pressure. This model can be applied to pipe or pressure vessels made of both traditional isotropic materials like steels and composite materials. Thin wall structures as well as thick wall structures ca be analyzed by this model.

Yang [29] also developed an analytical model for predicting the mechanical behavior of the fiberglass composite pipe joints under tensile loading. This model can be used to reduce the peak interfacial stresses by selecting the appropriate joint length and the appropriate coupling design.

Jacobs [30] used laser ultrasonic techniques to monitor material degradation like changes in stiffness in a thick, glass-reinforced, vinylester (thermosetting) fiber-reinforced polymer (FRP) composite material.

2.3 BEHAVIOUR OF COMPOSITES UNDER IMPACT LOAD

Composite materials are very sensitive to out-of-plane loading (i.e., loading transverse to plies or reinforcement) because they are much weaker in the thickness direction than in the plane of lamination. Consequently, composite materials subjected to transverse impact may suffer significant damage, resulting in deterioration of its overall load-carrying capacity. The response of composite materials to these impact loadings is complex, as it depends on the structural configuration as well as the intrinsic material properties. Further, it depends on the material, geometry, and velocity of the impactor. Each plays an important role in characterizing the overall effect of transverse impact.

The various forms of damage modes possible under impact loading range from nonvisible or barely visible to penetration of the impactor. Low velocity impacts may not cause any visible damage on the laminate but may cause internal damage in the form of matrix cracking, delamination, and/or fiber cracking inside the laminate. This may lead to significant reduction in strength. Stiffness reductions are also possible but not generally dramatic. A common example of low velocity impact is the accidental dropping of a tool on the composite component or structure during manufacturing, service, or maintenance. Generally, impact with impactor speeds less than 100 m/s are classified as low velocity impact. But there are several other definitions of low velocity impact, with no universal agreement. Sometimes low velocity impact is used in the context of low energy impact, i.e., less than 136 J (100 ft-lb). Low velocity impact normally involves deformation of the entire structure during the contact duration of the impactor, and this situation is considered quasi-static with no consideration of the stress waves that propagate between

the impactor and the boundary of the impacted component. On the other hand, high velocity or hypervelocity impacts involve impactor speeds greater than 1 km/s. This is sometimes also referred to a situation where complete penetration of target (i.e., composite structure) occurs. Usually, the deformation of the composite structure in high velocity impact is localized in a small zone surrounding the contact area during the duration of contact with the impactor.

Several types of test techniques have been used to generate impact. These can be classified generally into three categories:

- Drop Weight Impact Tests
- Pendulum Tests
- Ballistic Tests

Currently, however, increasing use is being made of instrumented impact tests with drop weight impact testers to characterize the low velocity impact of composite structures. This is usually done on drop weight impact machines, where the striker is instrumented to measure the applied load. These machines have means of measuring displacement or acceleration. Thus the history of the load, displacement, and acceleration during the impact event is recorded, and these can be converted to give impact load-time and impact energy-time histories. From these, features such as peak load and absorbed energy can be related to fracture processes occurring in the material.

A typical load history in an impact test is schematically shown in Figure 2.1. The load-time history can be divided into two distinct regions, a region of fracture initiation and a region of fracture propagation. As the load increases during fracture initiation

phase, elastic strain energy is accumulated in the specimen and no gross failure takes place; but failure mechanisms on a microscale for example, microbuckling of the fibers on the compression side or debonding at the fiber-matrix interface are possible. When a critical load is reached at the end of the initiation phase, the composite specimen may fail either by a tensile or a shear failure depending on the relative values of the tensile and interlaminar shear strengths. At this point the fracture propagates either in a catastrophic "brittle" manner or in a progressive manner continuing to absorb energy-at smaller loads.

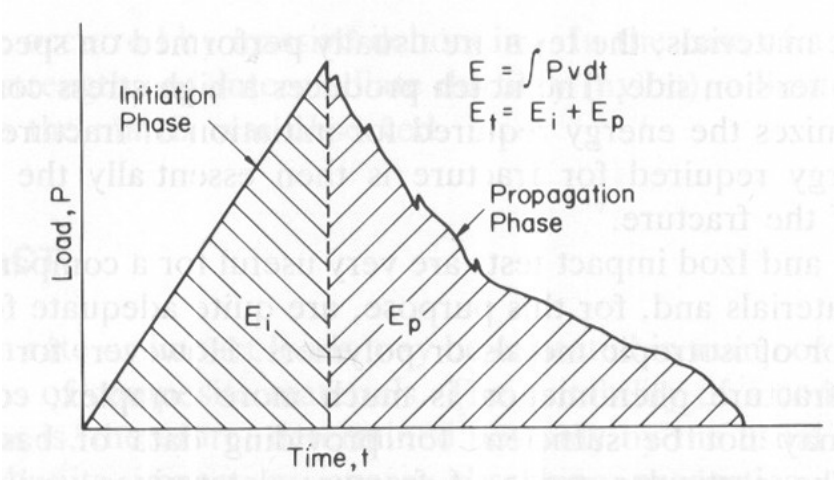

Figure 2.1 Typical load history during impact test. Shyr and Pan [35]

The total impact energy, E_t as recorded on the impact machine or on the energy-time curve on the oscilloscope is thus the sum of the initiation energy, E_i and propagation energy, E_p. A high-strength brittle material which has a large initiation energy but a small propagation energy and a low-strength ductile material which has a small initiation energy but a large propagation energy-may have the same total impact energy.

Nahas [31] conducted radial impact loading on a plug that can slide inside the GRP test tube which is water filled. He found that two phases of fracture occurs fracture

initiation phase and fracture propagation phase. Ratio of initiation energy to propagation energy is ductility. High ratio more ductile and low ratio more brittle**.**

Alderson and Evans [32] conducted static and single-bounce low velocity (up to 10m/s) drop weight impact tests on the pipes by two support conditions - floor supported along the pipe length and simply supported in half circumference end cradles. Filament-wound E-glass/epoxy resin pipes with winding angle of ± 55°, external diameter 162 mm, wall thick 6 mm, length 500 mm were tested to full specimen damage (the tup insert was about to penetrate the lower resin layer of the pipe) and partial damage tests were conducted.

- The damage areas were found to increase with the increase in intial energies then decreases near total penetration and remain almost constant.
- The pipes tested exhibit a two-part failure process i.e., an elastic region is followed by failure due to delamination initiation and local crushing.

Ambur and Starnes [33] studied effect of curvature on the impact damage characteristics and residual strength of graphite epoxy composite plates and found that impact energy required to initiate damage increases, then decreases with increase in radii. The impact causes a dent to form on the impacted surface of the plate and causes the surface ply on the back surface of the plate opposite to the impact location to crack and separate from the plate. Measured dent depth is 0.05” for 16-ply. The damage initiation and barely visible damage were discussed.

Curtis et al. [34] taking four layered ± 55° filament-wound E-glass fiber reinforced epoxy composite tubes did lateral indentation and low speed impact tests and then were tested under internal pressure to determine their residual burst strength. Drop in the burst pressure increases with increase in the deflection of the pipe due to impact. Tubes that have been subjected to a deflection of above 48 mm show a dramatic reduction (60-70 %) in burst strength. Tubes that subjected to low indentation or impact energy failed catastrophically within the test section whilst tubes that had been subjected to high energy indentation burst at the indentation buckling sites.

Shyr and Pan [35] studied the impact behaviour and the damage characteristics in different fabric structures with various thickness of the laminates, under low velocity, medium-heavy incipient impact energy conditions using a guided drop weight test rig Dynatup Model 8250 with a pair of adjustable rebound catchers to prevent multiple impacts on the E-glass fabrics test specimens. It was found that in the load-time curve the first drop is the matrix cracks failure. A small indentation cone, matrix cracks, and delamination damage can be observed from the perpendicular cross-section surface of the impacted laminate. The tests were conducted for different energies to have initial damage, major damage and finally penetration.

Zuleyha Aslan et al. [36] studied the low-velocity impact of cross-ply E-glass/epoxy laminated composite plates with a vertical drop-weight testing machine at two different tup weights of 1350 and 2600 g. Transverse impact first initiates critical matrix cracks in

a layer within laminated composites with a brittle matrix. These cracks generate delaminations immediately along the bottom or upper interface of the cracked layer.

Kalthoff [37] characterized the strength and toughness of a glass fiber reinforced vinylester by means of instrumented impact tests utilizing charpy V-notch specimens. The edge-on specimens bends slightly backwards towards its original shape whereas in side-on delamination of specimens takes place. The graphs of force-displacement and energy-displacement are studied and force and energy is greater for edge-on compared to side-on specimens.

Baucom and Zikry [38] studied the response of stitched and unstitched E-glass/epoxy laminates subjected to transverse impacts by impacting the specimens repeatedly with a energy of 18 J for each impact, until complete perforation has occurred. Photography, SEM and analysis of contact force evolution are utilized to assess the progression of damage. The peak force first increases with the increase in strikes but later decreases after 3^{rd}, 2^{nd}, 6^{th} strikes for 2D, 3D, warp-knit respectively. Perforation has taken place on 5^{th}, 10^{th}, 8^{th} strikes for 2D, 3D, warp-knit specimens.

Gning et al. [39] studied the damage development in thick ± 55° filament wound glass/epoxy tubes of 55 mm internal diameter and 6 mm thick tubes intended for underwater applications by drop weight impact tests using a 4 m height drop tower.

- The mean damage threshold value was found to be 3 to 4 J.
- At low incident speed or energies a small local indentation at the contact point is noted of about 0.3 mm thickness has been damaged.

- After threshold energy level is reached, delmainations occur through the thickness.
- For energies upto 7 J, numerous transverse intra-layer cracks appear, weakening the already delaminated plies.
- For low energies the damage area is circular for high energies its expands to elliptical shape.
- Some samples were sectioned and polished and true damage area was revealed by a dye penetrant technique. This has given the true damage area is roughly 10 times the projected area.

Morais et al. [40] studied the variation of the resistance to low energy repeated impacts of glass, carbon, and aramid fabrics-reinforced composites as a function of the laminate thickness. It was found that the resistance to low energy impacts increases only with laminate thickness, irrespective of the fiber reinforcement used whereas for higher energies is dependent on the fiber used. The performance of glass fabrics was attributed to the fineness of glass fibers compared to aramid and carbon fibers. The front face shows dome fracture, resulting from the localized matrix crushing and fiber shearing under the indentator. At the rear face the damage had the characteristic pattern of cracks following the direction of the fibers on the fabrics and main damage event occurring are fiber deformation and rupture.

Strait et al. [41] using instrumented impact test data obtained from penetration tests studied the effects of seawater immersion on the impact resistance of two glass fiber reinforced epoxy composites were characterized by. In the conventional epoxy system,

the energy for incipient damage increased significantly following seawater immersion due to plasticization of the matrix by the absorbed moisture. Both glass/epoxy systems experienced substantial reductions in total energy absorbed, peak load and energy absorbed at peak load as a result of moisture-induced degradation of the fibers and fiber/matrix interface.

Liu et al [42] studied the impact perforation resistance of laminated and assembled E-glass fibers and epoxy matrix composite plates. Study of the force-deflection close curve represent the absorbed energy of the composite laminate for the specific impact and when the curve is no longer a closed one then perforation has occurred. When penetration took place, the absorbed energy was approximately equal to the impact energy. When perforation occurred, the absorbed energy was again smaller than the impact energy. Experimental results revealed that the equal-energy interval, which was the difference between the penetration threshold and perforation threshold, increased as the thickness of composite plates increased.

Belingardi and Vadori [43] examined the behavior of glass fiber epoxy composite laminates plates subjected to low velocity impact loading. The force displacement curves allow to identify two thresholds: the first material damage force and the maximum force. For first one the curve sharply changes its look and large oscillations are visible and for the second one its reaches its maximum force then drops suddenly. These two parameters have been compared showing that their values remain substantially constant with impact energy.

Dear and Brown [44] investigated the impact behaviour of E-glass polyester composite material by using a drop-weight impact facility and it was observed that the onset of through-thickness damage can occur before there is visual evidence of surface damage at the point of contact between the striker and the specimen. A linear relationship has been observed between impact energy absorbed and peak load and the composite with higher glass fiber weight fraction absorbs most impact energy. The materials exhibited the same propensity to have well hidden through-thickness impact damage before damage to the front and rear faces was visible.

Corbett and Reid [45] studied the deformation and failure mechanisms in glass-reinforced epoxy/phenolic resin composite pipes and demonstrated that such pipes are vulnerable to local impact loading, even at low impact energies. The consequence of this damage was a reduction in the pressure-carrying capacity of the pipes and the damaged pipes weep or leak from the impacted zone when exposed to internal fluid pressure

Reid and Ashton [46] conducted extensive experimental programme on local loading of E-glass fiber epoxy composite pipes. Internally pressurized GRP pipes were impacted by hemispherical nosed projectiles of 1 kg mass, with pipes pressurized with water at 0, 4 and 15 MPa respectively.

- The damage (delamination) areas of the impacted pipes under internal pressure reduced substantially with an increase of internal pressure.
- The burst pressure of 4.3 mm thick virgin GRP pipes varied between 40 and 50 MPa.

- Residual pressure strength ratio was calculated which is the ratio of the maximum pressure sustained by a damaged pipe (failing by leakage or burst) divided by the maximum pressure for an undamaged pipe and its varied between 1 to 0 with an increase with impact energies.
- Two types of failure that occurred in the pressure tests were burst and weepage.

Dai and Harris [47] carried out acoustic emission study of impact-damaged 100 mm bore and 5.5 mm wall thickness GRP pipes and found that damage caused by severe impacts, of net energies up to 43 J on the pipes caused severe microstructural damage, but they did not reduce the load-bearing capacity of the pipes. The mean burst pressure of undamaged pipes was found to be 9.6 MPa.

Park and Jang [48] investigated the impact behaviour of aramid fiber/glass fiber vinylester resin hybrid composites by the analysis of delamination area. The impact velocity was fixed at 4.0 m/sec and the incident impact energy was 160 J and the delamination area of each layer was determined by the process of penetrant injection and de-plying. When the aramid layer was at impacted surface, the laminate exhibited the higher delamination area and total impact energy. The indentation depth of pure aramid composite was very large compared to glass-aramid and aramid-glass composites.

2.4 MOTIVATION FOR PRESENT INVESTIGATION

Many researchers, have studied mechanical behaviour of the composite materials. They focused mainly on the mechanical properties like tensile, fatigue, fracture,

hydrostatic burst pressure and impact characteristics of the GFRP materials and pipes. Incidental damage due to low-velocity impacts, either in service or during handling, can adversely affect their mechanical performance, reducing structural integrity and causing fluid leakage. Normally in the previous studies, pipes were impacted and carried out hydrostatic burst tests which resulted in a huge amount of pressure drop. Moreover concentration of many researches was on the hydrostatic burst pressure performance of the composite pipes after impact and the effect of environmental conditions like natural exposure and seawater exposure including the accelerated testing like dry heat, salt spray and humidity. All the studies showed that there is good amount of degradation of the mechanical properties after exposures. However, it became necessary to focus on the testing of the pipes after being exposed to natural and accelerated environmental conditions. In particular, the dry heat and seawater exposures, due to the exposure to high temperatures and salt water as the pipe will encounter such environment in service. Seawater exposures have been shown to result in the most severe degradation of the material properties.

The GFRP pipes were exposed to salt spray, dry heat and humidity ambient along with 100% accelerated conditions, as its simulate outdoor exposures like heat, air oxidation, ocean spray, intense sunlight and cold weather. Accelerated exposure tests can usually reach the same degradation as natural exposure tests. Therefore many experimental investigations have been conducted in order to determine the degradation of the pipes due to various factors.

2.5 OBJECTIVE OF THE PRESENT STUDY

In the present experimental work, the effect of environmental conditions on the hydrostatic pressure and impact performance on the glass fiber reinforced thermoset pipes is being investigated along with the hydrostatic pressure performance after the impact test. In the present work we have studied the effect of the seawater immersion and natural exposures on the oil filled GFRP pipes.

- Natural outdoor environmental exposure of 3 months and 12 months
- Seawater exposure of 3 months and 12 months

Four different accelerated natural conditions were considered as follows

- Dry Heat 40ºC for 300h and 1000h
- Salt Spray for 300h and 1000h
- Humidity Ambient and 100% for 300h and 1000h

Hydrostatic burst tests were conducted using a self designed an in-house and fabricated hydrostatic pressure test stand. The impact test characteristic was studied by using Dynatup 9250G impact tester.

CHAPTER 3

EXPERIMENTAL SETUP AND PROCEDURE

3.1 HYDROSTATIC BURST TEST

Hydrostatic burst testing is conducted to determine a material's performance. Burst Testing (ASTM D1599) is conducted to determine a material's short term strength. Pipe samples are pressurized such that a ductile failure occurs in 60 - 70 seconds. The pressure required for such a failure is known as the 'burst pressure'. Actual pipe samples are pressurized with water as the internal medium and either air or water as the external medium. The internal pressure in the pipe samples results in both an axial and a hoop stress. As the hoop stress is twice the axial stress, it is the stress in the hoop direction that cause the burst.

The schematic of the experimental facility is depicted in Figure 3.1. The design can handle a maximum pressure of 600 bars. The test rig used to carry out the hydrostatic burst test was manufactured using

1. Test stand
2. High Pressure Hand pump
3. C-clamps
4. Endcaps
5. Safety stand

The brief test description is as follows, the pipe specimen was closed at both the ends using two endcaps one of which has a provision for hose to inject water into the pipe. This complete pipe assembly along with the endcaps is fastened in between two flat endplates supported by 12 threaded slender tie-bars fastened by nuts. High pressure hand pump was used to pump high pressure into the pipe specimen. Water supply was given to the high pressure pump through a tap and is then supplied to the pipe specimen. This complete setup was then placed on the safety stand covered by a rectangular Plexi-glass shield to avoid any injuries while working at high pressures. The description of each individual part used in the experimental facility is discussed in detail in the following sections.

3.1.1 Test Stand

The test stand was manufactured using two aluminium magnesium alloy square plates of dimensions 40 cm × 40 cm × 2.6 cm with a through thickness hole of diameter 7.5 cm to accommodate the end-caps assembly mounted into the pipe specimen. In a previous design of burst test apparatus by Curtis et al. [34] the tube specimen was subjected to hoop loading only, the axial loads being carried by the tie-bars. The plates will be subjected to shear strength equal to the pressure applied on the pipe. The tensile strength and shear strength of the alloy plate are given in the Table 3.1, taking into consideration a factor of safety of 4 for the plate shear failure. A groove of 0.3 cm thickness and 17.5 cm diameter was machined on the inside of the each endplate to support the pipe.

Table 3.1 Properties of Aluminium-Magnesium alloy of 2.7 cm thickness plate

Ultimate Tensile Strength	360 MPa	52200 psi
Shear Strength	215 MPa	31200 psi

Design Calculations for selection of endplates and tie-bars

Endplates

Maximum pressure acting on the plates = 55 MPa

Maximum Shear strength of each alloy plate = 215 MPa

Factor of the safety for the plates

$$F.S = \frac{215}{55}$$

$$F.S \cong 4$$

Tie-Bars

Long galvanized stainless steel tie-bars of diameter 2.7 cm were used to support the two endplates with the help of nuts fastened both inside and outside of the plates as shown in Figure 3.2 (a). With the help of the tie-bars the pipe specimens were subjected to hoop loading only, where as the axial loads or tensile loads were carried by the tie-bars. The tensile strength of the galvanized steel tie-bars is given in the Table 3.2.

Table 3.2 Tensile Properties of Galvanised steel tie-bars

Ultimate Tensile strength	330 MPa	47900 psi
Yield Tensile strength	285 MPa	41300 psi

Maximum pressure acting on the endplates = 55 MPa

Total number of tie-bars = 12

Diameter of the endcap = 15 cm

Stress or Pressure is force acting per unit area $P = \frac{F}{A}$

Pressure exerted by endcaps on the plates = 8000*0.0069

= 55.2 MPa

= 5520 N/cm^2

Area of the endcap which exert pressure on the plates = $\frac{\pi}{4} * 15^2$

Force acting on each plate

$$F = P * A$$

$$F = 5520 * \frac{\pi}{4} * 15^2$$

$$F = 975.5 \text{ KN}$$

Force acting on each tie-bar $F_X = \frac{975.5}{12} = 81.3$ KN

Cross sectional area of the each tie-bar = $\frac{\pi}{4} * 2.7^2$

Tensile Strength acting on each tie-bar

$$P = \frac{F_X}{A}$$

$$P = \frac{81300}{\frac{\pi}{4} * 2.7^2}$$

$$P = 14200 \text{ N/cm}^2$$

$$P = 20580 \text{ psi} = 142 \text{ MPa}$$

From the table the yield tensile strength of the bar = 285 MPa

Factor of Safety for the tie-bars

$$F.S = \frac{285}{142}$$

$$F.S \cong 2$$

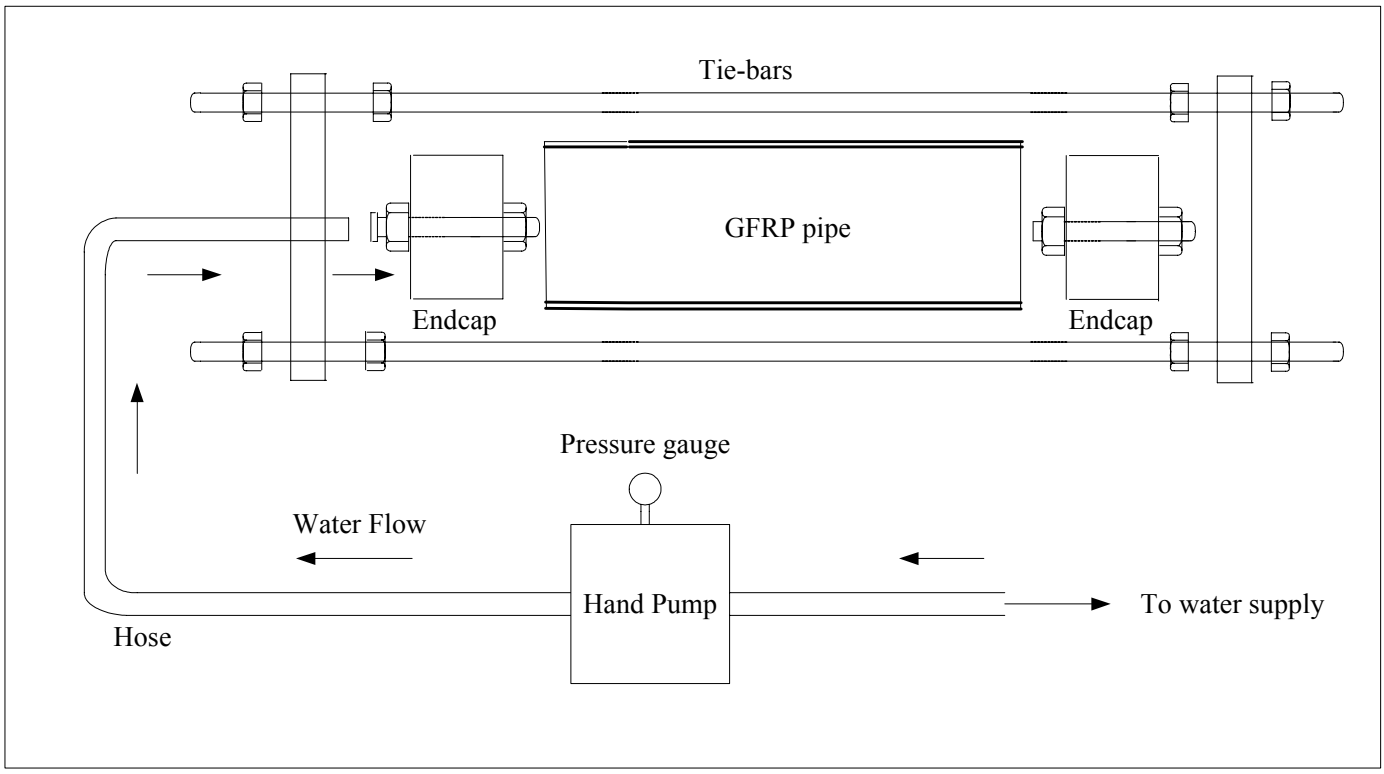

Figure 3.1 Schematic of the test section

(a)

(b)

Figure 3.2 (a) Test stand and (b) Base plate

3.1.2 High Pressure Hand Pump

The pipe specimens were pressurized using a high pressure hand pump of pressure rating 0-70 MPa (0 – 10,000 psi) as shown in Figure 3.3. The inlet of the pump was connected to the water tap and the outlet to the pipe using a high pressure rated hose. The pump was operated so as to maintain uniform pressure rate until the failure or burst take place.

3.1.3 C-Clamps

The ends of the pipe specimen are often subjected to hoop failures at high pressures. To avoid the hoop failure of the current pipe specimens at the ends a pair of C – clamps were designed to hold the pipe at both the ends as shown in the Figure 3.4. C – clamps were manufactured using carbon-steel with a width of 10 cm thickness 2.0 cm and diameter of 15 cm. With the C – clamps fastened at the end of the pipe is now subjected to the failure away from the ends.

3.1.4 End Caps

The most critical part in the present Hydrostatic Burst test rig is the end-cap, because it has to resist a high pressure before a catastrophic failure occurs or leaks develop in the pipe. Commercial endcaps were used as shown in the Figure 3.5, for the first time and the failure of the pipe were found to be at endcaps due to weak grip of the endcap gripper. The fibers were damaged under the endcaps area due to steel gripper and the pipe became weak on both sides of the pipe and failed.

Figure 3.3 High Pressure Hand Pump

Figure 3.4 C-clamps

The pipe is needed to be failed at the middle. Therefore the design of the end-caps was done with utmost care. The end-caps assembly consists of the following parts,

1. Solid Aluminium cap
2. O - rings
3. Shaft
4. Teflon washer
5. Rubber washer
6. Steel Disc

3.1.4 (a) Solid Circular Aluminum Cap

Figure 3.2 (a) shows the aluminium cap. The main component of the end cap assembly is a solid circular aluminium cap of diameter 14.8 cm and thickness 8 cm. A through hole of 3.8 cm diameter was drilled at the center of the aluminium cap to accommodate a shaft for the end-cap assembly as shown in the Figure 3.6 (a).

3.1.4 (b) O – Rings

The O-rings used are shown in the Figure 3.6 (b), which are mounted in the grooves 0.45 cm depth and 0.54 cm width machined on the solid aluminum cap. The manufacturer, Parker, has provided O-rings of diameter 14.2 cm and a thickness of 0.54 cm, with an O-ring supporter of thickness 0.2 cm and width 0.485 cm of same diameter as O-ring.

Figure 3.5 Commercial GT-588T EST 6” High pressure Endcaps

Figure 3.6 Designed Endcap Assembly

(a) (b)

Figure 3.7 (a) Solid Aluminum Cap (b) O-rings with supporters

(a) (b)

Figure 3.8 (a) Shaft and nuts for the endcap (b) Teflon Washer

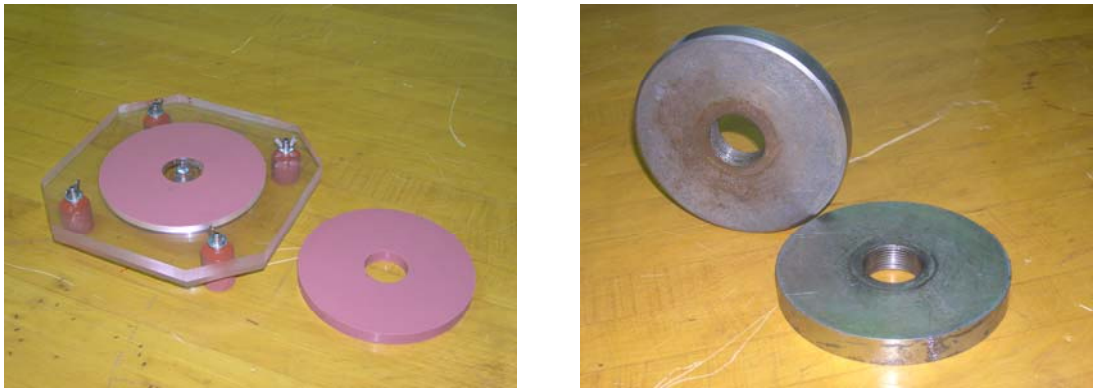

(a) (b)

Figure 3.9 (a) Rubber Washer with moulding equipment (b) Steel Disc

3.1.4 (c) Shaft

The shaft is made of mild steel with a diameter of 3.8 cm and length 21 cm. A through hole of diameter 1.05 cm is drilled on one of the shaft for access of water. The other endcap is left solid without any hole. The shaft along with the nuts is shown in the Figure 3.8 (a).

3.1.4 (d) Teflon Washer

A Teflon washer of 1.2 cm thickness and diameter of 14.7 cm as shown in Figure 3.8 (b) is used in the endcap assembly. This Teflon washer was mounted on the shaft after the solid aluminum cap. The Teflon washer will help in expansion of the rubber washer when the nut of the shaft is tightened.

3.1.4 (e) Rubber Washer

The rubber washer was mould using Plexi-glass molding equipment as shown in the Figure 3.9 (a). The rubber washer was prepared using liquid rubber with a hardener. The rubber washer plays a vital role for the endcaps to avoid the leakage of water at high pressures along with the O-Rings. It is mounted in between the steel disc and the Teflon washer so that it can squeeze and expand to make the pipe and endcap assembly air-tight. The rubber washer was of 1.2 cm thick with a outer diameter of 14.7 cm.

3.1.4 (f) Steel Disc

Endcap assembly consists of a steel disc between the rubber washer and the inside nut of the shaft as shown in the Figure 3.9 (b). The steel disc has outer diameter of 14.6 cm, 2 cm thick and a chamfer of 0.25 cm towards rubber side. A threaded hole of diameter 3.7 cm was drilled at the center to mount the steel disc on to the shaft.

3.1.5 Safety Stand

The whole test section assembly was mounted into a safety stand, with the pipe assembly being horizontal. It consists of a hard wooden trolley of dimensions 150 cm × 70 cm, on which a rectangular safety shield made of Flexi-glass was fixed to have protection while working at high pressures. The dimensions for the Flexi-glass shield were 50 cm × 50 cm × 150 cm, that can be fastened to the trolley using nuts as shown in the Figure 3.10.

3.1.6 Test Procedure

1. The endcaps assembly is prepared carefully mounting first the solid aluminium cap then the Teflon washer, new rubber washer, steel disc and finally the nut onto the shaft. The nuts of the shaft both inside and outside are not completely fastened while the endcap assembly is prepared at the first.

Figure 3.10 Safety stand with Flexi-glass shield

Figure 3.11 Endcap inserted into the pipe specimen

(a)

(b)

Figure 3.12 (a) The pipe-endcap assembly is being slided into the test stand (b) The test stand is fastened with nuts to hold the pipe between the endplates.

2. The pipe specimen of length 100 cm is used for the Hydro burst test. It is chamfered to about 1 mm on both the inside edges of the pipe ends to slide the endcap assembly into the pipe easily as shown in the Figure 3.10. The outside surface of endcap should be in same level as the pipe. The outside nut on the endcap assembly is fasten tightly which makes the rubber washer gets squeezed and expand to make the pipe air-tight.

3. The pipe-endcap assembly is now slided into test stand, placing the pipe exactly into the groove provided on the endplates as shown in the Figure 3.12 (a). The whole test stand is fastened with nuts on the tie-bars to hold the pipe and endcap assembly able to handle high pressures as shown in the Figure 3.12 (b).

4. A hose is connected from a high pressure hand pump to the pipe. The hose should be long enough so that test setup is far away from pump. The pipe is filled with water, through the hole provided on one of the endcap shaft.

5. The pipe-test stand assembly is now placed on a safety stand with the help of a manual crane. The Flexi-glass shield is fixed over the test stand assembly to avoid any injuries while working at high pressures.

6. Now the pipe is hydrostatically pressurized with the hand pump. The test shall be carried out at ambient temperature. The maximum pressure achieved during the test shall be recorded as the burst pressure, as indicated on the pressure gauge provided on the pump. The pressurization rate throughout the test shall not exceed

1379 KPa/s or 1.5 MPa/s (less than 200 psi per second). The duration of the test shall be between 50-70 seconds as according to ASTM 1599.

Parameters to monitor and record

1. Burst pressure
2. Description of failure
3. Hoop pressure

Calculate the pipe hoop stress as follows:

For outside diameter controlled pipe

$$S = \frac{P(D-t)}{2t} \tag{3.1}$$

or

For inside diameter controlled pipe

$$S = \frac{P(d+t)}{2t} \tag{3.2}$$

3.2 IMPACT TEST

The Dynatup 9250G impact tester was used for low velocity impact tests for this study as shown in the Figure 3.13. The 9250G model is gravity-based system, which generates maximum velocities up to 5 meters per second and impact energies up to 1000 Joules. The impactor, which was used to strike the pipe samples, is a hemispherical indenter (tup) with a 1.27 cm diameter spherical head. The ranges of impact energies can

be obtained by choosing suitable combinations of crosshead mass and drop height. The contact force is measured with a load transducer located between the cross head and hemispherical tup nose. Instrumented impact test records contain the entire impact event so that the full impact force versus time profile can be analyzed. The Dynatup impulse data acquisition system is the heart of impact testing system. It captures load information at very high speed from impact tests then data is analyzed graphically.

The objective of impact testing is to determine an object's ability to resist high-rate loading, which is measured by the energy absorbed to fracture a test piece at high strain rate. Impact strength along with impact resistance is one of the most commonly measured properties and to quantify. The impact resistance of a part is, in many applications, a critical measure of service life. More importantly these days, it involves the perplexing problem of product safety and liability.

Drop weight impact testing has been described as an “energy technology”. In this study, low velocity impact tests were conducted using an instrumented drop weight impact testing machine (DYNATUP 9250G) to examine fracture surfaces of the tested specimens. Force/absorbed energy-time plots were generated for each impact test.

With the height and weight known, impact energy can be calculated. Since the falling weight either stopped dead on the test sample, or destroyed it completely in passing through, the only results that could be obtained were of a pass/fail nature. It is unidirectional with no preferential direction of failure. Failure can be defined by deformation, crack initiation, or complete fracture, depending on the requirements.

Failures originate at the weakest point in the sample and propagate from there. If insufficient energy is delivered to damage the sample, there is option to either maintain that mass and increase the height or vice versa. The force vs time curve can be characterized by the peak force, the energy to peak force, total energy, and displacement to maximum load.

Maximum (peak) load is the highest point in the load-time curve. Often the point of maximum load corresponds to the onset of material damage or complete failure. Energy to maximum load is the energy that the sample has absorbed up to the point of maximum load. It is the area under the load/deflection curve from the test start to the maximum load point. Total energy is the energy that the sample has absorbed up to the end of the test, when the load reaches zero again. It is the area under the load/deflection curve from the test start to the test end. Deflection to maximum load is the distance the impactor traveled from the point of impact to the point of maximum load.

3.2.1 Design of V-block

The V-block for the testing of the pipe was designed as per the ASTM D 2444. The V-block holder is twice as long as the specimen being tested and have a 90° included angle. It has been fabricated using steel. The side supports is of sufficient depth to support the specimen in the V and not on the top edges of the V-block.

Figure 3.13 Dynatup 9250G equipped with Impulse for Impact testing

3.3 NATURAL AND ACCELERATED CONDITIONS

3.3.1 Natural Exposure

Natural (outdoor) environment exposure site available at KFUPM campus was selected to avoid any obstacles for exposure. Impact test samples have been mounted on test racks. In addition to the impact test samples 20 crude oil-filled pipes sections of 125 cm each from GFRV1 material has been placed on a wooden platform to receive natural exposure. The GFRV pipes were first closed air tight using strong glue at one end with the PVC endcaps, after being confirmed that the glued side is dried the crude oil is poured into the pipe as shown in the Figure 3.14. Then the pipes are closed from the other side also and placed on the racks as shown in the Figure 3.14. Care has been taken that the pipes should not get disturbed or damaged and being checked regularly.

For seawater immersion tests, special frames were designed and fabricated from CPVC plates and sheets. Each frame is capable to hold fifteen 125 cm long pipe sections. Two such frames containing 30 GFRV1 pipes have been submerged in Arabian Gulf seawater at KFUPM beach shoreline, for seawater exposures.

3.3.2 Accelerated Conditions

Accelerated exposure conditions have been targeted for GFRV2 material. Pipe samples of 16.0 cm length were exposed to different accelerated conditions as follows

- Dry heat at 40^{o}C
- Salt Spray
- Humidity Ambient
- Humidity 100%

(a)

(b)

(c)

(d)

Figure 3.14 (a) Crude oil filled into the GFRV pipe (b) Oil filled pipe after glued at both ends, (c) and (d) Pipes placed on racks for natural exposure.

3.3.2 (a) Dry Heat 40ºC

The effect of dry heat on materials is important in operations using composites in a desert region, such as the Saudi Arabia. LBB Series Despatch oven has been used for this accelerated condition, which has an efficient forced circulating oven to maintain a constant temperature of 40ºC. The oven uses an indicating microprocessor based digital control that displays the actual chamber temperature at the sensing point. Pipe specimens were placed on the steel racks in the oven as shown in the Figure 3.15.

3.3.2 (b) Salt Spray

Salt spray exposure testing was designed to provide a controlled, high humidity, high temperature, and corrosive environment. This test has been used extensively to provide relative corrosion or deterioration resistance data. The apparatus is a Q-Fog CCT 600 model as shown in the Figure 3.15 indended for salt spray. The test temperature was set to 95ºF (35ºC) and salt fog was introduced. A 5% wt. salt solution was continuously atomized into the chamber. The pH was measured at room temperature after collection of the condensate and followed procedures stated in ASTM B 117 (Standard practice for operating Salt Spray apparatus).

3.3.2 (c) Humidity Ambient and 100%

Humidity also plays a very important role in the degradation of the composite pipes. Singleton Corrosion Test Cabinet model DIN FJ32H1-N-N-23 as shown in the Figure 3.15 is used for the exposure of the pipe to humidity for both the ambient and 100%. Humidity testing manual ASTM D 2246-65 (reapproved 1981) or D 2247-86a is followed for the carrying out the exposure tests.

(a)

(b)

(c)

Figure 3.15 (a) Salt spray exposure (b) Humidity exposure and (c) Dry Heat 40ºC exposure

CHAPTER 4

RESULTS AND DISCUSSION

Hydrostatic burst tests and Impact tests were conducted on the GFRV and GFRE pipes. The **ASTM 1599** "Standard test method for resistance to short-time hydraulic pressure of plastic pipe, tubing, and fittings" for carrying out hydrostatic burst test where as the **ASTM D 2444-99** "Standard Test Method for Determination of the Impact Resistance of Thermoplastic Pipe and Fittings by Means of a Tup (Falling Weight)" for carrying out impact tests. Instrumented drop weight impact testing machine (DYNATUP 9250G) was used to evaluate the impact strength of tested composites pipes. The bursting and impact behaviors of Glass Fiber Reinforced Vinylester (GFRV) thermoset pipes were found to be completely different from those of Glass Fiber Reinforced Epoxy (GFRE) thermoset pipes.

4. 1 BASELINE TESTS

4.1.1 Hydrostatic Burst Tests

The baseline tensile strengths of the GFRV and GFRE composite pipes are shown in the Table 4.1.

Table 4.1 Baseline Tensile Strengths of GFRV and GFRE

	GFRV1	GFRV2	GFRE
Tensile Strength (MPa)	253 MPa	202.6 MPa	327 MPa

Several preliminary burst tests were performed to reach a stage where the test set up started to perform satisfactorily. The burst test results for GFRV1, GFRV2 and GFRE pipes are provided in Table 4.2. The average burst pressure was found to be 28.9 MPa (4200 psi) for GFRV1 pipes, 31.0 MPa (4500 psi) for GFRV2 and 40.0 MPa (5800 psi) for GFRE.

A depiction of the failed pipes is provided in Figure 4.1. The failure behavior of GFRV2 was ductile yielding that occurs when the stress in the pipe wall exceeds the yield stress of the material. It was observed that the fibers were twisted and buckled, and the pipe finally busted at about 33.8 MPa (4900 psi).

The stress on the pipe wall increases with increase in pressure. When the yield stress of the polymer exceeds, localized yielding occurs that results in the thinning of the wall in a localized region of the pipe (typically at the point where the wall thickness is lowest). This is followed by localized expansion (or "ballooning") leading to final failure at the newly oriented polymer structure in the 'balloon' to result in the typical "Parrot's Beak Failure".

Another failure mode was that of the twisting of the pipe and delamination. A portrayal of this failure mode is shown in Figure 4.2. The failure pressure was 31.0 MPa (4500 psi) in this case. In contrast to failure by yielding, failure by delamination did not have such a point where the wall thickness is lower than the original thickness of 6 mm i.e., the failure is uniform along the length of the tested pipe.

The failure of GFRV1 occurred at a pressure of 28.3 MPa (4100 psi) which is little lower than that of GFRV2 pipes and the location of failure was at end caps as shown in Figure 4.3. The end caps were of the type commercial end caps. Another type of failure,

as shown in Figure 4.4, was same as that of GFRV2 twisted bending. It was observed that this failure occurred at a higher value of 29.6 MPa (4300 psi). This failure is similar to the one shown in Figure 4.1, but in this case leakage was observed just before the burst. A comparison of the GFRV pipes subjected to hydrostatic burst tests is shown in Figure 4.5.

The general observation of GFRE pipes was that they failed at greater pressure than the GFRV1 and GFRV2 pipes exhibiting brittle behavior. Large holes of about 10 cm diameter were created at 40.0 MPa (5800 psi) due to burst. This test is depicted in Figure 4.6. Bending and large number of longitudinal cracks were observed on the surface of the GFRE pipe with a small leak at a site where seeping of the water took place at 35.9 MPa (5200 psi). The longitudinal cracks are an indication that failure would be the burst if the pipe had tolerated some more pressure. The failure of GFRV was found to be of ductile nature whereas for GFRE it was brittle. The failure pressure of GFRV is around 25 % less than the failure pressure of GFRE.

Table 4.2 Burst pressure and type of failure of GFRV1, GFRV2 and GFRE

Specimen No.	Pipe	Burst/Failure/Max Pressure MPa (psi)	Failure Type	Hoop Stress MPa (psi)	Remarks
1	GFRV1	28.3 (4100)	Burst	367.9 (53300)	Commercial Endcaps
2		29.6 (4300)	Burst	385.4 (55900)	Designed Endcaps
3		28.9 (4200)	Leak at Endcap	375.8 (54600)	End slipped
4	GFRV2	33.8 (4900)	Burst at Middle	439.2 (63700)	
5		31.0 (4500)	Pipe bend and fibers delaminated	403.4 (58500)	
6		31.0 (4500)	Pipe bulks at the middle	403.4 (58500)	End slipped
7	GFRE	40.0 (5800)	Leak	519.9 (75400)	Number of continuous cracks along the length of the pipe
8		35.9 (5200)	Leak	466.0 (67600)	The pipe got bend little away from middle of the pipe
9		40.0 (5800)	Burst in the middle	519.9 (75400)	The pipe got burst at the middle creating a hole of about 10 cm diameter

(a)

(b)

(c)

Figure 4.1 (a) Burst pipe with complete test set up (b) Close up of burst failure. (Visible fiber breakage) (c) Interior of the burst failed GFRV2 pipe.

(a)

(b)

(c)

Figure 4.2 (a) Twisted failed GFRV2 pipe. (b) Delaminated failed pipe. (c) Interior of failed pipe.

(a) (b)

Figure 4.3 (a) Detachment of a whole layer of failed GFRV1 pipe. (b) Close up of burst failure.

(a) (b)

Figure 4.4 (a) Failed GFRV1 pipe by twisting in the middle (b) Interior of the failed pipe.

(1) (2) (3) (4) (5) (6)

Figure 4.5 Beginning from left is specimen GFRV pipe (pipe 1) before hydro burst test. 2 and 3 are GFRV1 after the test. 4, 5 and 6 are GFRV2 after burst test

(a)

(b)

Figure 4.6 (a) GFRE burst failed pipe with complete test set up (b) Close-up of burst failure showing hole created by burst.

(a)

(b)

(c)

Figure 4.7 (a) Failed GFRE pipe by bending (b) Close view of pipe where failure occurred (leakage point) (c) Longitudinal cracks on the pipe.

Before After

Figure 4.8 Beginning from left is GFRE pipe before hydro burst test and the failed pipes after the test.

4.1.2 Impact Testing

Low-velocity impact tests were carried out using an instrumented drop weight impact test machine (DYNATUP 9250G) to evaluate the impact strength of tested composites pipes. The impactor is a hemispherical indenter (tup) with a 1.27 cm diameter spherical head. Force/absorbed energy-time plots were generated for each impact test. When the height and weight known, impact energy can be calculated. The tests were performed on 150 mm internal diameter 6 mm thick 300 mm long pipes supported on a V-block. The mass of drop weight was 10 kg for low impact energy up to 50 J and 25 kg for higher energies. Inspection of fractured pieces was done after each test.

The above procedure of varying mass and energy was carried out till the energy required to just initiate the fracture in the pipe samples and the total penetration of the pipe occurred. Tests were done for intermediate energies to predict the failure trend of the pipe samples. With the height and weight known calculations were carried out to obtain maximum (peak) load, energy to maximum load, impact energy, deflection to maximum load, and impact velocity for GFRP composite pipes as listed in Table 4.4

4.1.2 (a) GFRV2

Glass fiber reinforced vinylester composite pipes were tested using DYNATUP 9250G impact machine. The load-time and energy-time traces of GFRV2 for impact energies of 6 J, 30 J, 70 J and 100 J are shown in the Figure 4.9 and Figure 4.10. The curve is characterized by the peak force, the energy to peak force, total energy, and

displacement to maximum load. Energy to peak force is the energy that the specimen has absorbed up to the point of maximum load. Deflection at peak load is the distance that the specimen deforms as a result of the force supplied by the drop weight. It is the deflection value at the point where the load curve reaches it peak. First the specimen undergoes a linear elastic deformation and then shatters after an initial fracture or damage, which can be seen from the first fall of the load-time graph. For Low energy of 6 J the specimen failure is abrupt, with no plastic deformation. Instead, there is a region of fiber breakage and pullout ending with an abrupt break. The fiber breakage region is characterized by oscillations in the load capacity. In this region, load may remain essentially flat, drift up, or drift down. It can be observed that as the impact energy increases the oscillations (flat region), mainly due to fiber breakage region

The fiber breakage region is characterized by oscillations in load capacity. For higher energies of 70 J and 100 J there is plastic deformation of the specimen before it reaches break point as shown in the Figure 4.9. The peak load (the sample can resist the progress of the impactor and it is taken as the impact strength.) is the point in force Vs time curve. Higher the impact energy higher will be the maximum force required to propagate the crack on large scale i.e., at 6 J the damage is minimal (initiation) and at 100 J it is total penetration.

The maximum force is a measure of the ease at which cracks begin to propagate on a large scale. Higher the impact energy higher is the maximum force required to propagate the crack on a large scale. For the total penetration the surface plies opposite to the impact location cracked and separated from the inner surface of the pipe. The peak force

and energy to peak force for each impact was found to first increase up to 70 J and then remained constant. This can be explained as after some limit the energy-absorbing capacity reaches a saturation level from where it will absorbs same force, as shown in the Table 4.3.

Table 4.3 Impact Properties of GFRV2 composite pipe

Specimen	Peak Force (kN)	Deformation at Peak Force (mm)	Energy to Peak Force (J)	Total Penetration Energy (J)	Test Height (mm)
V2/BL/IM/6J/1	3.22	2.08	3.82	4.92	50.00
V2/BL/IM/6J/2	3.29	1.47	2.39	4.97	50.30
V2/BL/IM/6J/3	3.29	1.49	2.60	4.37	50.30
AVERAGE	**3.27**	**1.68**	**2.94**	**4.75**	**50.20**
V2/BL/IM/30J/1	5.47	7.08	27.39	28.10	298.00
V2/BL/IM/30J/2	5.38	7.11	26.80	27.76	302.50
V2/BL/IM/30J/3	5.01	7.42	26.15	28.36	296.70
AVERAGE	**5.28**	**7.20**	**26.78**	**28.07**	**299.07**
V2/BL/IM/70J/1	6.58	11.29	51.50	66.83	303.00
V2/BL/IM/70J/2	6.57	11.54	51.23	66.90	303.80
V2/BL/IM/70J/3	6.53	13.51	62.33	68.69	302.00
AVERAGE	**6.56**	**12.11**	**55.02**	**67.47**	**302.93**
V2/BL/IM/100J/1	6.57	16.59	79.10	96.22	403.00
V2/BL/IM/100J/2	6.58	12.48	58.05	96.35	401.80
V2/BL/IM/100J/3	6.57	14.40	44.69	95.13	404.50
AVERAGE	**6.57**	**14.49**	**60.61**	**95.90**	**403.10**

4.1.2 (b) GFRE

Glass fiber reinforced epoxy (GFRE) composite pipes were also impact tested using DYNATUP 9250G impact machine. The impact behavior of GFRE was completely different from that of GFRV2. The load-time and energy-time traces of the GFRE for impact energies of 12 J, 35 J, 80 J and 110 J are shown in the Figure 4.11 and Figure

4.12. The mean impact energy was found to be 12 J and 110 J to initiate damage (threshold impact energy) and the total penetration respectively.

For 12 J impact energy it is found that the peak load is about 6.3 KN and its remains same for 35 J, 80 J and 110 J impact energies with a value of 6.6 KN. This can be explained with regard to GFRE pipe's greater load bearing capacity. For the total penetration the surface plies opposite to the impact location cracked and separated from the inner surface of the pipe. The peak force and deformation at the peak force for each impact was found to remain constant, as shown in the Table 4.4.

Table 4.4 Impact Properties of GFRE composite pipe.

Specimen	Peak Force (kN)	Deformation at Peak Force (mm)	Energy to Peak Force (J)	Total Penetration Energy (J)	Test Height (mm)
E/BL/IM/12J/1	6.55	3.19	10.36	9.54	120.60
E/BL/IM/12J/2	6.55	3.70	12.91	9.63	121.30
E/BL/IM/12J/3	5.81	3.88	12.39	8.78	121.90
AVERAGE	**6.30**	**3.59**	**11.89**	**9.32**	**121.27**
E/BL/IM/35J/1	6.72	3.02	10.10	31.18	353.80
E/BL/IM/35J/2	6.66	3.06	9.83	32.45	346.30
E/BL/IM/35J/3	6.54	3.01	9.66	31.52	355.20
AVERAGE	**6.64**	**3.03**	**9.87**	**31.72**	**351.77**
E/BL/IM/80J/1	6.62	2.97	10.36	80.60	324.30
E/BL/IM/80J/2	6.66	3.19	10.73	80.25	322.60
E/BL/IM/80J/3	6.59	3.12	11.48	81.12	324.10
AVERAGE	**6.62**	**3.09**	**10.86**	**80.66**	**323.67**
E/BL/IM/110J/1	6.62	6.11	28.66	114.47	445.80
E/BL/IM/110J/2	6.56	5.58	25.42	115.14	442.40
E/BL/IM/110J/3	6.58	5.10	23.02	115.30	446.60
AVERAGE	**6.59**	**5.59**	**25.70**	**114.97**	**444.93**

4.1.3 Impact – Hydrostatic Burst Testing

The Impact – Hydrostatic burst testing were carried out, as it will give important information regarding the behavior of the GFRP pipes after impact. The pipes may be subjected to any damage like the dropping of the heavy items or instruments while installation, impact of vehicles or heavy bodies from outer atmosphere like meteoroids.

4.1.3 (a) Impact – Hydrostatic Burst behavior of GFRV2

The GFRV2 specimens of 1000 mm (1 m) long were used to carry out the impact testing. Later hydrostatic burst tests were conducted to assess the damage caused by impact. The load-time and energy-time traces of the GFRV2 for impact energies of 20 J, 40 J, 75 J and 100 J are shown in the Figure 4.13 and Figure 4.14.

For 20 J impact energy the peak load is about 4.38 KN and it increases to 5.7 KN for 40 J and reaches to 6.53 KN for 75 J and 6.57 KN for 100 J. The peak force and energy to peak force for each impact was found to first increase up to 75 J and then remain constant, as shown in the Table 4.5.

Table 4.5 Impact Properties of GFRV2 composite pipe for Hydro Burst Testing

Specimen	Peak Force (kN)	Deformation at Peak Force (mm)	Energy to Peak Force (J)	Total Penetration Energy (J)	Test Height (mm)
V2/IM-HB/20J	4.38	5.95	20.10	19.20	197.10
V2/IM-HB/40J	5.70	9.20	37.55	36.92	406.70
V2/IM-HB/75J	6.53	11.85	54.46	72.23	301.80
V2/IM-HB/100J	6.57	10.56	47.76	97.70	402.20

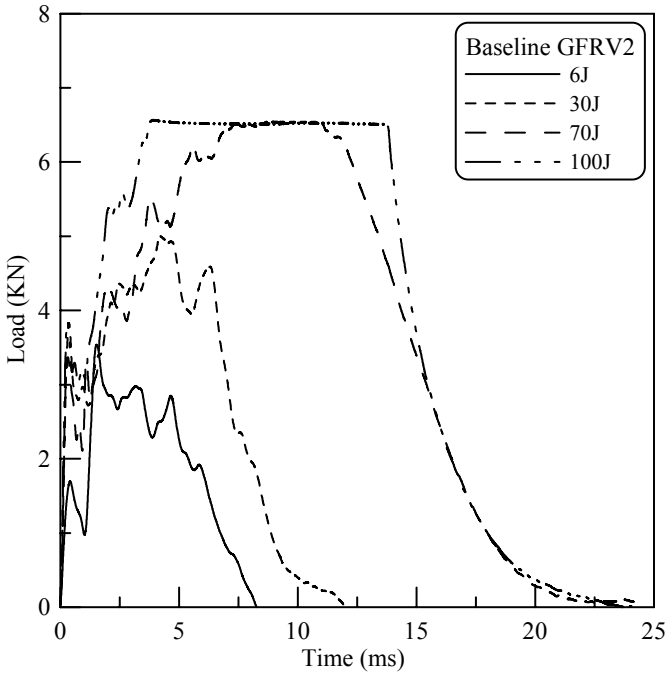

Figure 4.9 Load Vs Time plot for GFRV2 at impact energies of 6 J, 30 J, 70 J, 100 J

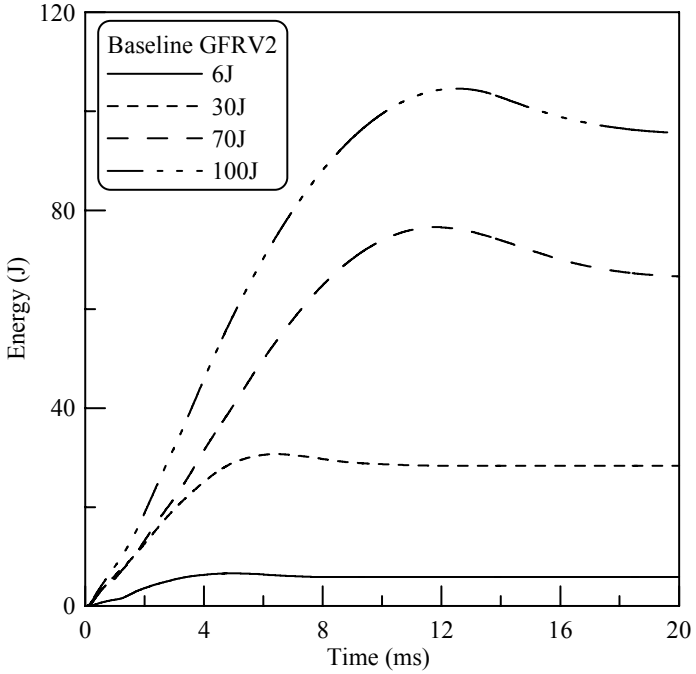

Figure 4.10 Energy Vs Time plot for GFRV2 at impact energies of 6 J, 30 J, 70 J, 100 J

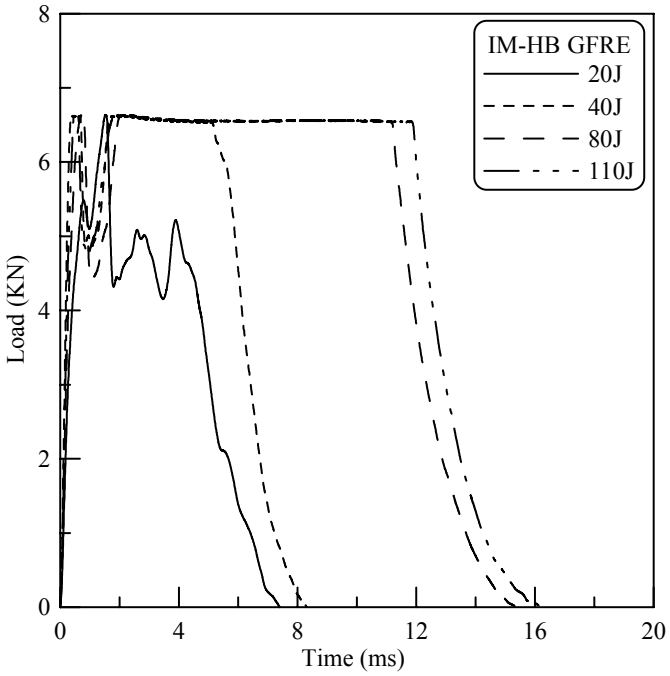

Figure 4.11 Load Vs Time plot for GFRE at impact energies of 20 J, 40 J, 80 J, 110 J

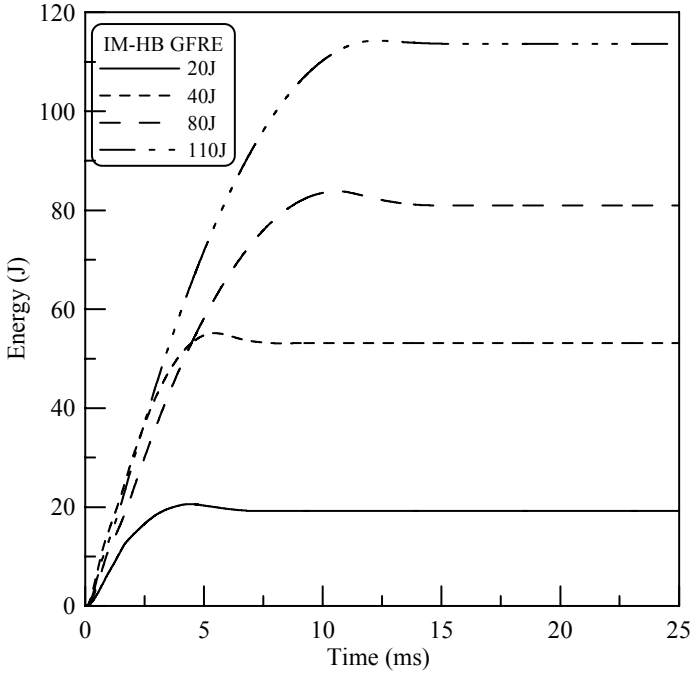

Figure 4.12 Energy Vs Time plot for GFRE at impact energies of 20 J, 40 J, 80 J, 110 J.

4.1.3 (b) Impact – Hydrostatic Burst behavior of GFRE

The GFRE specimens of 1000 mm (1 m) long were used to carry out the impact testing followed by hydrostatic burst tests were conducted to assess the damage caused by impact. The load-time and energy-time traces of the GFRE for impact energies of 20 J, 40 J, 80 J and 110 J are shown in the Figure 4.15 and Figure 4.16.

The maximum force was observed to be same for all the impacted GFRE pipes and it is about 6.62 KN. The peak force and deformation at peak force for each impact was found to remain constant, as shown in the Table 4.6. The deformation or defection at the peak force remained approximately constant for all impact energies indicating that GFRE pipes are more impact resistant than GFRV.

Table 4.6 Impact Properties of GFRE composite pipe for Hydro Burst Testing.

Specimen	Peak Force (kN)	Deformation at Peak Force (mm)	Energy to Peak Force (J)	Total Penetration Energy (J)	Test Height (mm)
E/IM-HB/20J	6.64	2.62	11.46	19.22	199.40
E/IM-HB/40J	6.62	1.85	8.54	53.11	406.60
E/IM-HB/80J	6.63	4.87	24.27	80.95	323.30
E/IM-HB/110J	6.63	1.39	5.20	113.65	442.70

Figure 4.13 Experimental setup for Impact test (DYNATUP 9250G)..

Figure 4.14 GFRV2 impact specimens of 20 J, 40 J, 75 J and 100 J before hydro burst test

Figure 4.15 GFRV2 impact specimens of 20 J (from left), 40 J, 75 J and 100 J after hydro burst test. The impacted site and the failure after hydro burst test are shown.

(a) (b)

Figure 4.16 (a) Leakage of water at about 45° away from impact site for 75 J impact energy (b) The leaks on the opposite side (180°) of the impact site.

Figure 4.17 GFRE impact specimens of 20 J (from left), 40 J, 80 J and 110 J after hydro burst test. The impacted site and the failure after hydro burst test are shown.

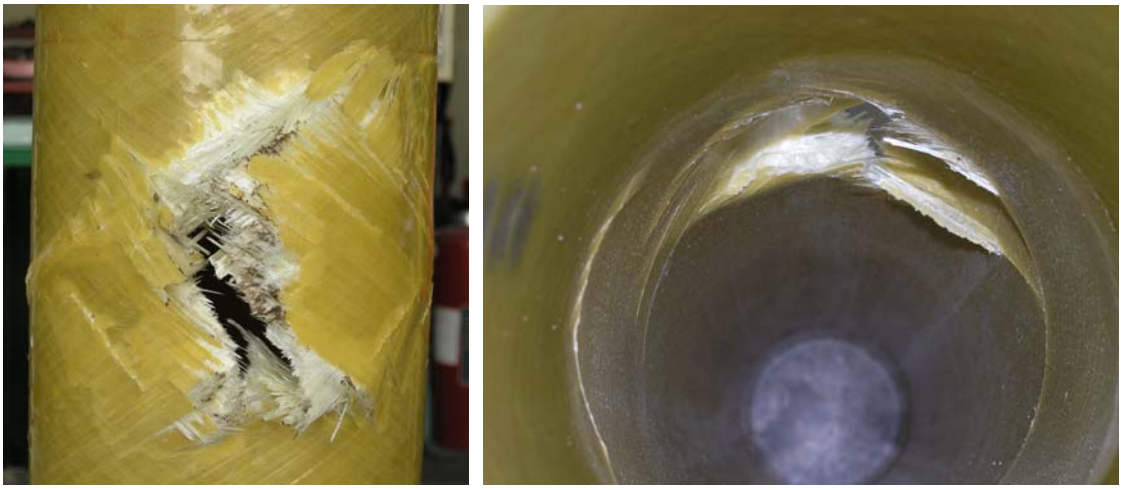

(a) (b)

Figure 4.18 (a) The burst failure at impact site for 40 J impact energy (b) Inside view of the failed pipe.

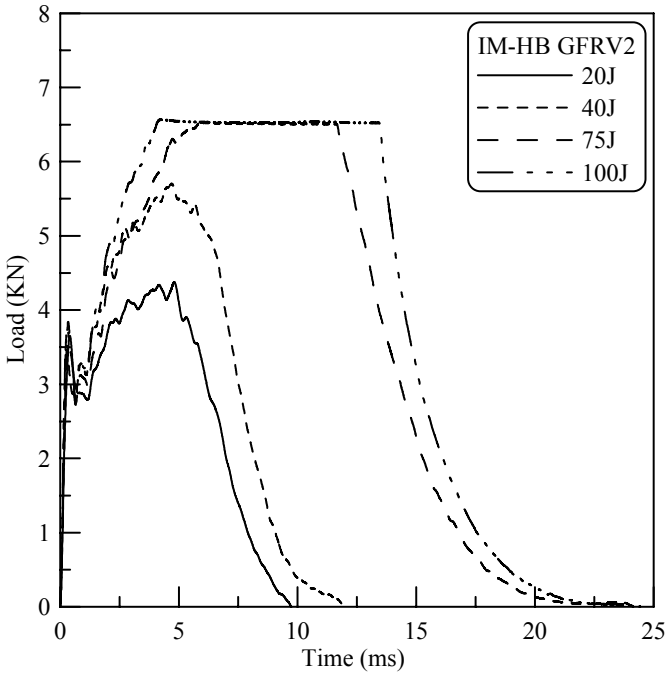

Figure 4.19 Load Vs Time plot for GFRV2 Impact-Hydro burst (IM-HB) pipe specimens at impact energies 20 J, 40 J, 75 J and 100 J.

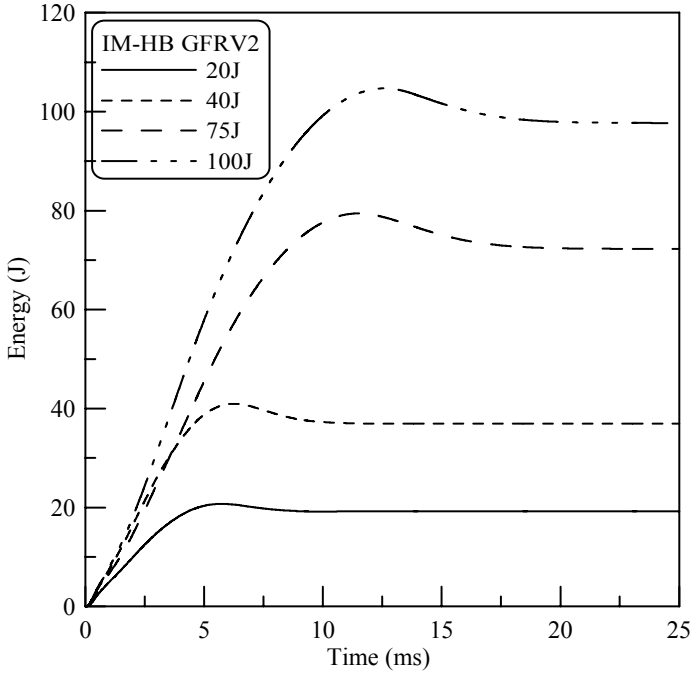

Figure 4.20 Energy Vs Time plot for GFRV2 IM-HB pipe specimens at impact energies of 20 J, 40 J, 75 J, 100 J.

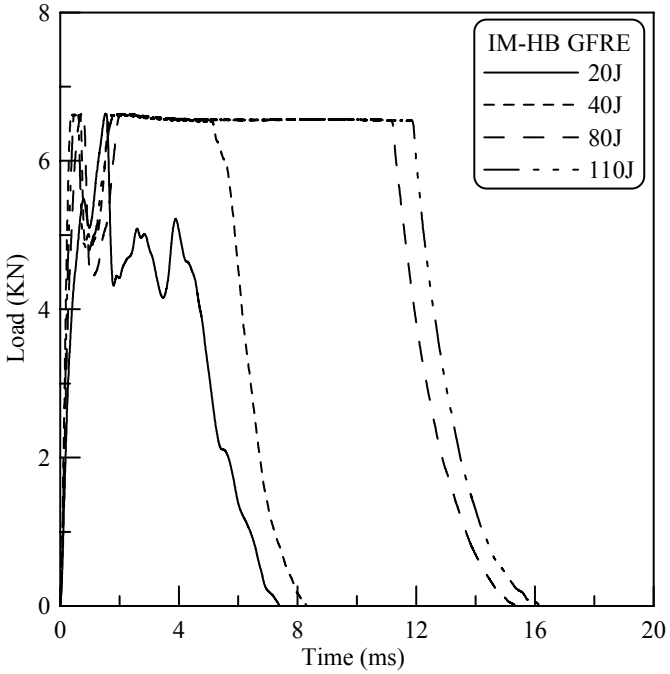

Figure 4.21 Load Vs Time plot for GFRE IM-HB at impact energies of 20 J, 40 J, 80 J, 110 J.

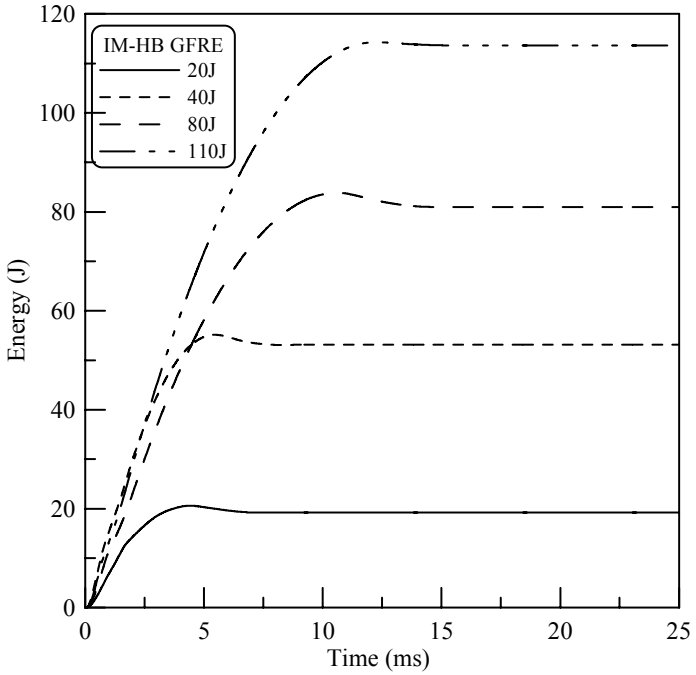

Figure 4.22 Energy Vs Time plot for GFRE IM-HB at impact energies of 20 J, 40 J, 80 J, 110 J.

4.1.3 (c) Residual Burst Strengths of GFRP Pipes

The assessment of residual strength of impacted pipes was made by subjecting all of the GFRV2 and GFRE pipes to a gradually increasing internal fluid pressure (using water) until leakage or burst of the pipes occurred. The tests were terminated when the rate of weepage through the damage zones was equal to the delivery from the pump or when burst occurred. An important parameter to assess the increased damage upon the residual pressure capacity of the pipes is the residual strength ratio, which is defined as the ratio of the maximum pressure sustained by a damaged pipe (failing by leakage or burst) divided by the maximum pressure for an undamaged pipe. The failure pressures for different impact energies and residual pressure strength ratios are calculated and illustrated as shown in the Table 4.7.

The overa11 results from the pressure tests are shown in Table 4.6. It can be seen that the residual strength tends to decrease with increasing impact energy delivered to the pipes. A typical curve of residual strength Vs impact energy is characterized by three main regions, which can be identified by the gradient of the residual strength curve as shown in the Figure 4.23 and Figure 4.24. Region I (0 J - 40 J) is characterized by a rapid reduction of residual strength by 70-80% due to the impact, fiber breakage and fiber-resin bond gets damaged and creates a point on the pipe where the stress is minimum and thus pipe pressure performance decreases drastically. Region II (40 J - 80 J), where the residual strength tends to remain constant (a 'plateau' zone), and finally region III (80 J – 110 J), in which there is further gradual fall of residual strength to zero as the total penetration of the pipe has created a small hole at the impact site resulting in zero failure pressure. There was a leak before applying the pressure at the impact energies of 100 J

and 110 J for GFRV2 and GFRE respectively, which is considered as zero. Comparing the curves for the GFRV2 and GFRE pipes impacted, it can be seen that GFRE have greater residual strength when compared to GFRV2.

The two types of failures that occurred in the pressure tests were burst and weepage. Burst was a catastrophic failure that occurred in an explosive manner with substantial fiber fracture around the impact damage zone. Weepage occurred in a gradual manner as fluid leaked through the impact damage zone. The test results indicated that for low impact energy, the damage size is small and leakage or weeping or even burst tends to occur from regions located 90° circumferentially away from the impact zone (and occasionally at about 45°) or on the opposite side (180°) to the impact damage zone of the GFRP pipe. This is probably due to the formation of more intense bending regions that result in resin cracking and delamination rather than plastic flow. However, for relatively high impact energy, the impact damage zones become large and weeping tends to occur through them.

Table 4.7 Failure or burst pressures of the impacted specimens of GFRV2 and GFRE and Residual Pressure Strength Ratio.

S.No.	GFRV2			GFRE		
	Failure Pressure (MPa)	Impact energy (J)	Residual Pressure Strength Ratio	Failure Pressure (MPa)	Impact energy (J)	Residual Pressure Strength Ratio
1	31.03	0	1.000	40.00	0	1.000
2	19.31	20	0.622	29.00	20	0.724
3	3.10	40	0.100	6.20	40	0.155
4	3.08	75	0.067	2.41	80	0.060
5	0.0	100	0.000	0.0	110	0.000

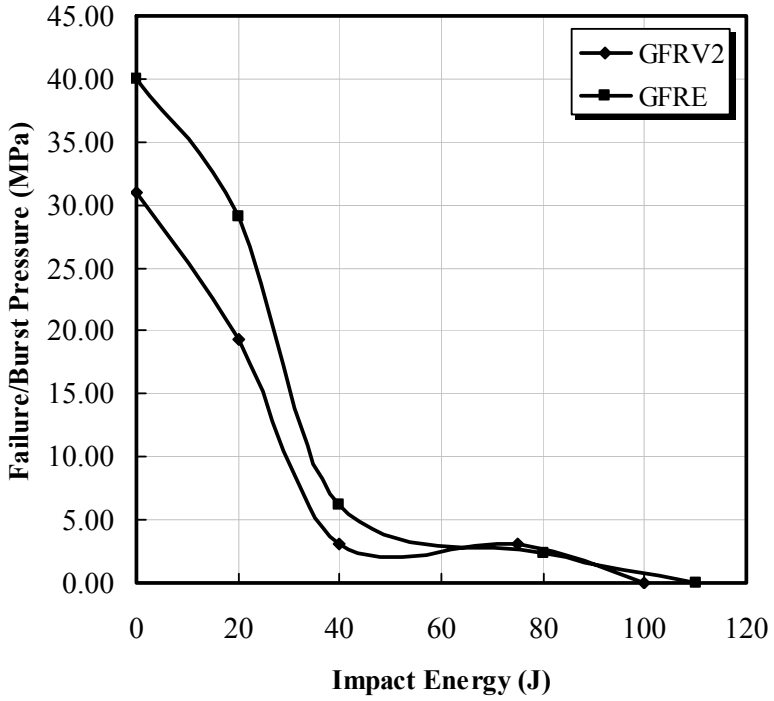

Figure 4.23 Failure/Burst Pressure of impacted GFRV2 and GFRE pipes

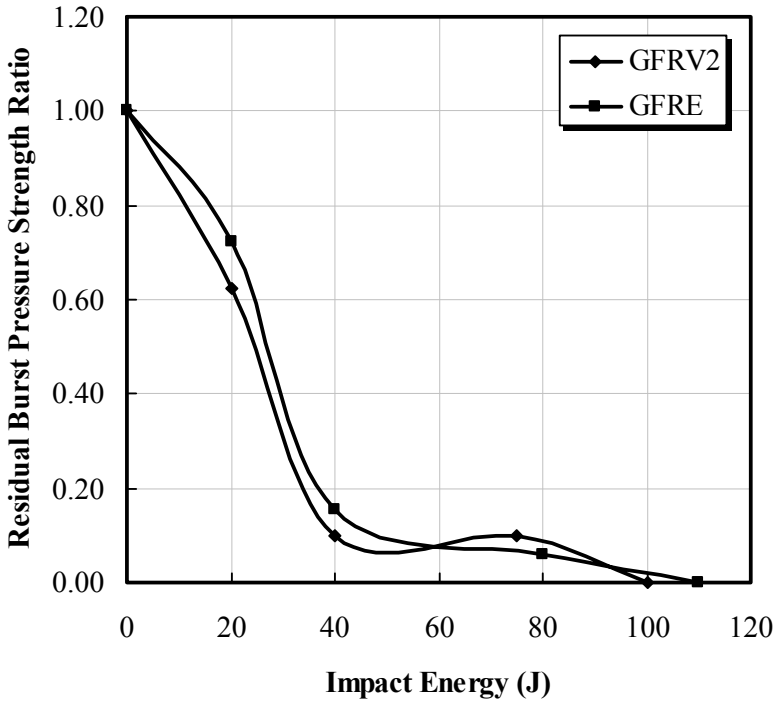

Figure 4.24 Residual Pressure Strength Ratio Vs Impact Energy of impacted GFRV2 and GFRE pipes.

4.2 EFFECT OF NATURAL AND ACCELERATED CONDITIONS

4.2.1 Hydrostatic Burst Tests

The GFRV1 composite pipes were immersed in seawater and exposed to outdoor conditions filled with crude oil. For seawater exposure, pipes were immersed in Arabian Gulf water at a site located at KFUPM beach. Pipe sections of 1.25 m in length filled with crude oil have been exposed to natural environment at exposure site located at KFUPM campus. These specimens were placed on a wooden platform.

The above natural exposures conditions were chosen so as to depict the conditions the pipe will generally encounter in the transportation of the crude oil. This helps to take necessary precautions and estimate the replacement period of the pipes due to degradation. The failure pressures for different exposure conditions are shown in the Table 4.8.

Table 4.8 Effect of environmental conditions on Hydrostatic pressure performance

S. No.	Exposure	Burst/Failure Pressure MPa (psi)	Failure Type	Hoop Stress MPa (psi)
1	Sea Water Immersion: 3 Months	24.8 (3600)	Leak	323.0 (46800)
2		31.7 (4600)	Leak and delaminated fibers	412.6 (59800)
3	Sea Water Immersion: 12 Months	31.7 (4600)	Twisted and Busted	412.6 (59800)
4		31.7 (4600)	Burst	412.6 (59800)
5	Oil Filled outdoor Exposure: 3 Months	30.3 (4400)	Leak	394.7 (57200)
6		33.1 (4800)	Leak and delaminated fibers	430.6 (62400)
7	Oil Filled outdoor Exposure: 12 Months	34.5 (5000)	Burst	448.0 (65000)
8		34.5 (5000)	Burst	448.0 (65000)

For the natural outdoor exposure of GFRV1 pipes for 3 months the burst/failure pressures were recorded as 30.3 MPa (4400 psi). The failure was in the form of three cracks on one pipe and for the other pipe delamination was observed at a pressure of 33.1 MPa (4800 psi). The average failure pressure was 31.7 MPa i.e., approximately 10% increase in the burst pressure as compared to the virgin hydro burst pressure. The failure was a burst for 12 months natural outdoor exposure at a pressure of 34.5 MPa (5000 psi), approximately 20% increase in the burst pressure.

Degradation may occur when polymers are irradiated, but cross-linking is the predominant reaction. The modulus increases with cross-linking. Although cross-linking is a useful reaction in making vinyl ester materials, undesirable consequences may occur after the materials are in service, as observed after the exposure of the oil filled composite pipes. An increase in the burst strength for the pipe exposed for 12 months is shown in the Figure 4.25. The fall in the pressure may be observed for further exposure period, which is beyond the scope of the present study.

The Hydrostatic burst pressure for the virgin pipe of GFRV1 was about 28.9 MPa (4200 psi) whereas for the seawater exposure of 3 months for a specimen, the burst pressure was observed to be 24.8 MPa (3600 psi). The mode of failure for one pipe was a crack and for another pipe the failure was delamination at approximately the same pressure of 31.7 MPa (4600 psi) as shown in Figure 4.26.

The 12 months seawater exposure of the GFRV1 pipe is shown in the Figure 4.27. The burst pressure of 1-year exposure pipe is 31.7 MPa (4600 psi) which is more than that of virgin pipe and 3 months exposure pipes. The failure is purely burst at the center of the pipe as a result of moisture-induced degradation of the fibers and fiber-matrix interface. The average burst pressure for the seawater immersion of 3 months exposure is around 4% less than the baseline burst pressure. A similar observation was made by Ghorbel and Spiteri [22]. In their study, exposure for 3000 hours (12 months) decreases burst pressure for ECR glass fiber vinyl ester resin composite pipe and 10% increase for the exposure period of 12 months. Vinyl-esters containing the ester group in their chain molecules are susceptible to hydrolysis of the side group, which might lead to cross-linking. The increase in the strength of the GFRV pipe is due to plasticization of the matrix by the absorbed water.

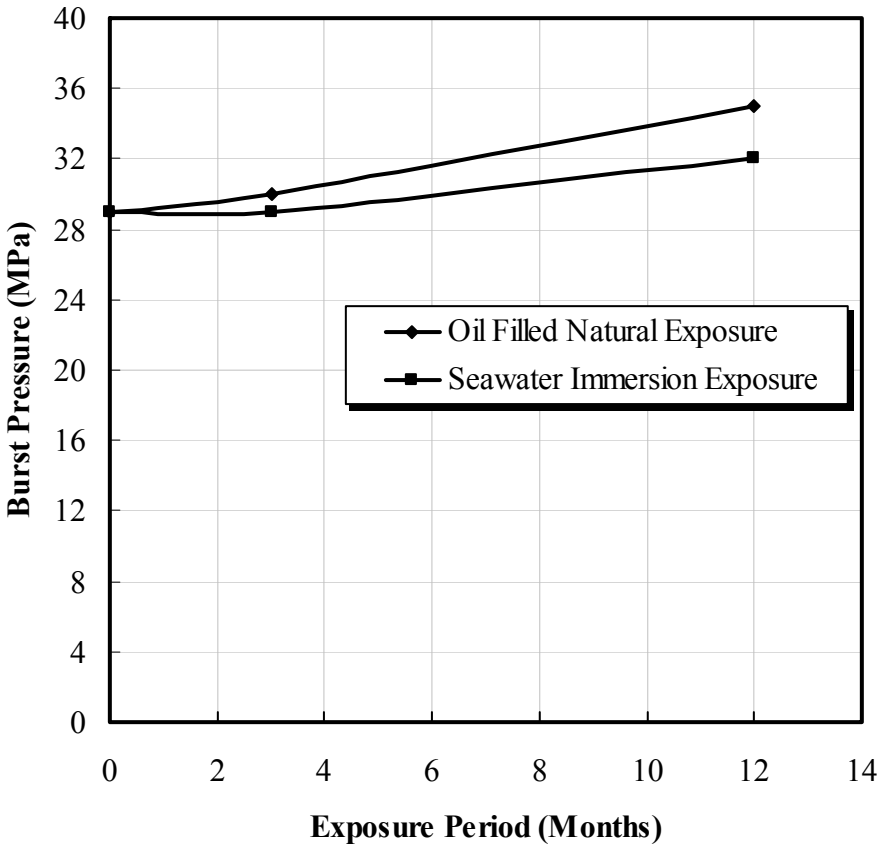

Figure 4.25 Burst Pressure Vs Exposure Period for the Oil filled Natural and Sea water exposures of 3 and 12 months.

Figure 4.26 GFRV1 exposed to Natural outdoor atmosphere for a period of 3 months. (Failure Mode: Burst)

Figure 4.27 GFRV1 exposed to Seawater Immersion for a period of 3 months. (Failure Mode: Burst)

(a)

(b)

(c)

Figure 4.28 (a) Seawater immersed pipe after 12 months of exposure (b) Close-up view of the pipe showing the deposited algae (c) Interior of the pipe

(a)

(b)

(c)

Figure 4.29 (a) Burst failure of the GFRV1 pipe after 12 months exposure to seawater immersion (b) Inside view of the failed pipe (c) Visible fiber breakage

4.2.2 Impact Testing

Impact testing of the GFRE pipes was carried out after being exposed to different accelerated environmental conditions as shown below

- Dry Heat at 40ºC
- Salt Spray
- Humidity Ambient
- Humidity 100%

For low velocity impact testing, the load-time and energy-time traces can yield important information concerning damage initiation and growth.

4.2.2 (a) Dry Heat 40ºC

The effect of dry heat on materials is important in operations using composites pipes in a desert region like Saudi Arabia. The impact tests were conducted on the 160 mm long GFRV2 pipe of diameter 150 mm and thickness 6 mm, after being exposed to the accelerated condition of dry heat at 40ºC in an oven. The pipes were kept in the oven for two different periods of 300 hours and 1000 hours.

For comparison, impact behavior of the GFRV2 pipes exposed to different dry heat exposure periods at energy levels of 6 J, 30 J, 70 J and 100 J are studied. The load-time and energy-time are plotted as shown in the Figures 4.30 through 4.33. It was observed that the impact time or contact time of the indentator with the pipe increases with an increase in exposure periods.

For a impact energy of 6 J, it is found that the peak load for 0h exposure is 3.27 KN and it increases to 3.39 KN for 300h and drops down to 3.30 KN for 1000h as in Table 4.9. The peak in the load-time curves is representative of the point at which the specimen can no longer resist the progress of penetration. This point is also representation of the fiber fracture and fiber pullout beginning on the tensile face of the specimen accompanied by unstable propagation of matrix cracks and delaminations. The increase followed by the decrease in peak load is due to the curing of the pipe for 300h as the degradation of the pipe takes place due to higher thermal effects. For higher impact energies the peak load for 300h and 1000h is same as that of unexposed pipe because the pipe reaches its maximum energy-absorbing capacity, which can be observed from Figure 4.34. There is a region of fiber breakage and pullout ending with an abrupt break. The fiber breakage region is characterized by oscillations in the load capacity. In this region, load may remain essentially flat, drift up, or drift down. It can be observed that as the impact energy increases the oscillations (flat region), mainly due to fiber breakage region, and shifts from right of the peak load to left.

The deformation or deflection at the peak force for 6 J is nearly 1.68 mm for virgin pipe and increases to 2.31 mm for 300 hrs exposure then drops down to 1.50 mm for 1000 hrs. This indicates that the material became strong due to curing. For total penetration at about 100 J the deformation decreases from 14.5 mm to 9.36 mm as shown in the Figure 4.35, due to decrease in the strength of the pipe material after exposure.

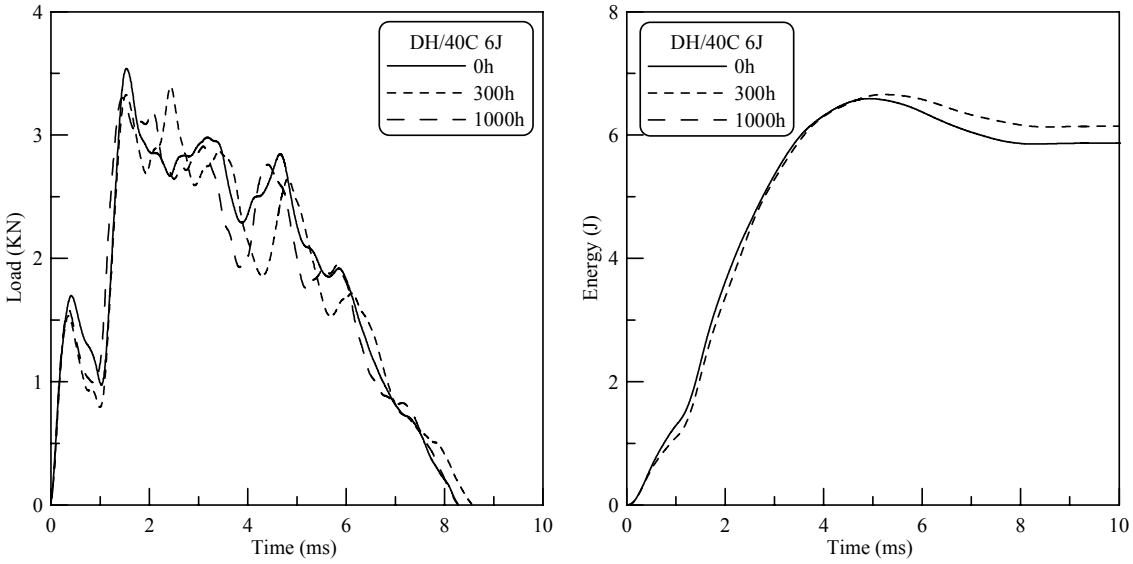

(a) (b)

Figure 4.30 (a) Load Vs Time and (b) Energy Vs Time plots for an impact energy 6 J exposed to Dry Heat 40°C of period 0h, 300h and 1000h.

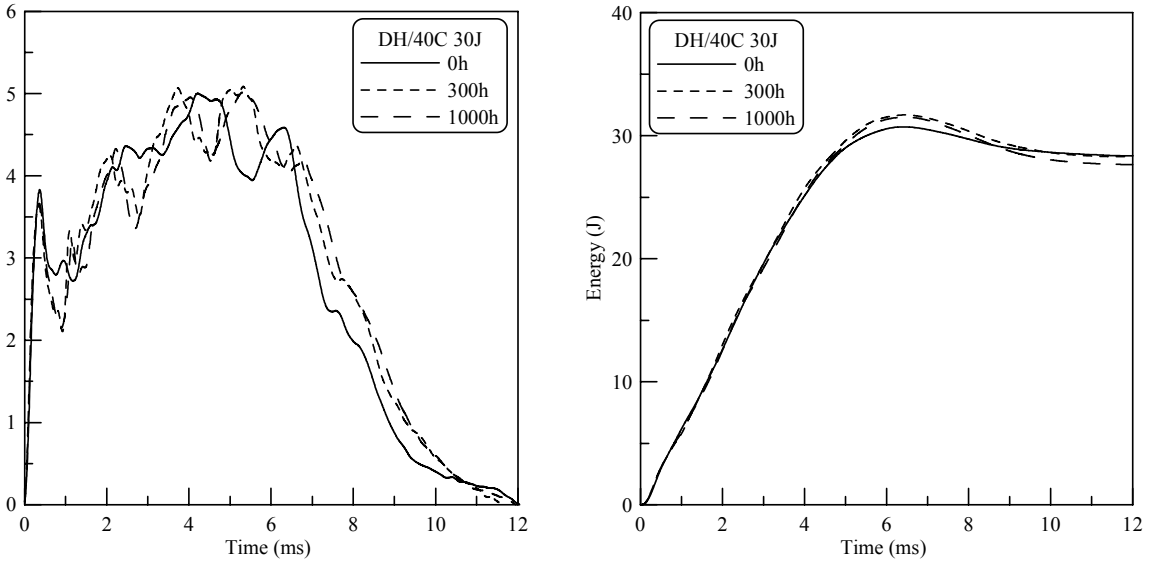

(a) (b)

Figure 4.31 (a) Load Vs Time and (b) Energy Vs Time plots for an impact energy 30 J exposed to Dry Heat 40°C of period 0h, 300h and 1000h.

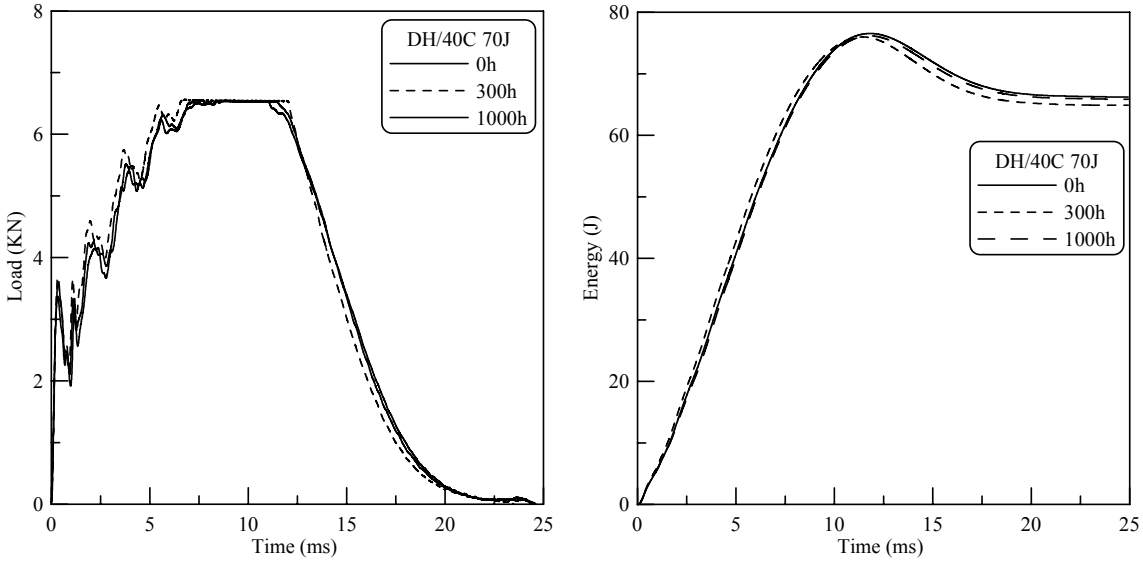

(a) (b)

Figure 4.32 (a) Load Vs Time and (b) Energy Vs Time plots for an impact energy 70 J exposed to Dry Heat 40°C of period 0h, 300h and 1000h.

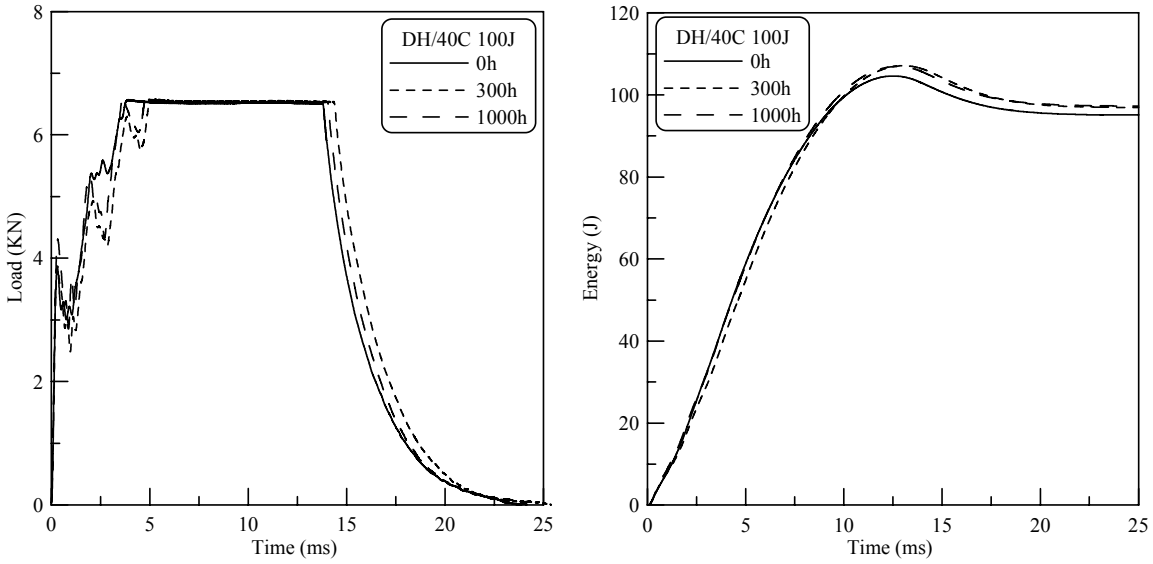

(a) (b)

Figure 4.33 (a) Load Vs Time and (b) Energy Vs Time plots for a impact energy 100 J exposed to Dry Heat 40°C of period 0h, 300h and 1000h.

Table 4.9 Impact properties of GFRV2 pipes exposed to Dry heat 40ºC

Specimen	Peak Force (kN)	Deformation at Peak Force (mm)	Energy to Peak Force (J)	Total Penetration Energy (J)
V/DH/40/0h/6J	3.27	1.68	2.94	4.75
V/DH/40/300h/6J	3.39	2.31	4.32	6.13
V/DH/40/1000h/6J	3.30	1.50	2.23	6.15
V/DH/40/0h/30J	5.28	7.20	26.78	28.07
V/DH/40/300h/30J	5.09	8.46	30.49	28.31
V/DH/40/1000h/30J	5.02	8.60	30.14	27.66
V/DH/40/0h/70J	6.56	12.11	55.02	67.47
V/DH/40/300h/70J	6.56	12.66	57.77	64.91
V/DH/40/1000h/70J	6.56	13.80	60.88	65.87
V/DH/40/0h/100J	6.57	14.49	60.61	95.90
V/DH/40/300h/100J	6.58	12.95	58.25	96.94
V/DH/40/1000h/100J	6.59	9.36	40.42	97.29

The energy absorbed at peak load is the critical parameter for applications that require no visible surface damage following impact.

The energy to peak force increases from 0h to 300h with increase in the total penetration energy of 6 J and then decreases for 1000h as shown in the Figure 4.36 due to the curing process. As the impact energy is increased to 70 J the difference between the energy at peak load and total penetration energy decreases, indicating curing effect. For the impact energy of 100 J, energy absorbed at peak load decreases indicating the degradation of the pipe due to 1000h dry heat exposure.

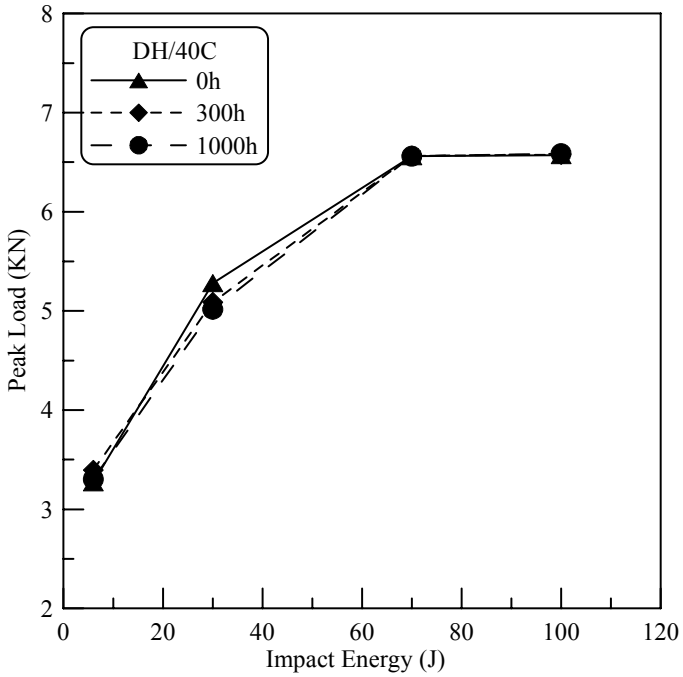

Figure 4.34 Peak Load Vs Impact Energy traces for accelerated GFRV2 Dry Heat 40° exposures for different impact energies.

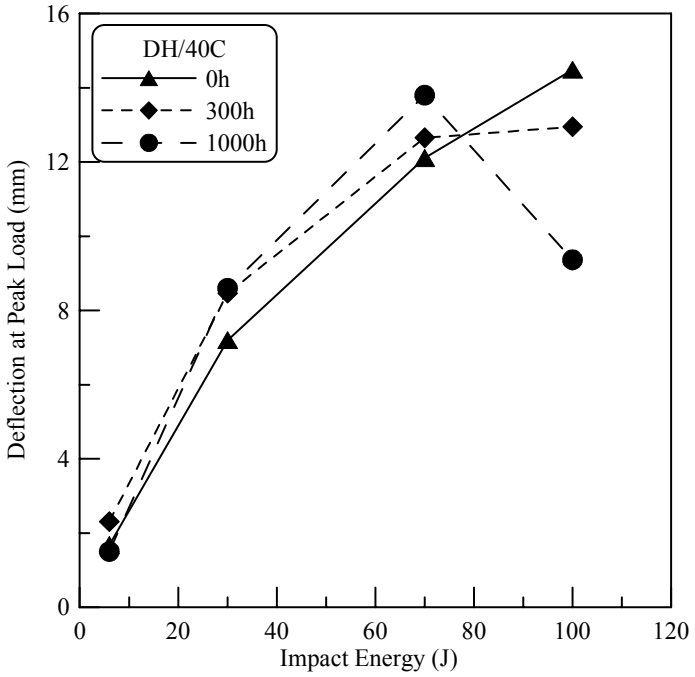

Figure 4.35 Deflection at peak load Vs Impact energy plot for accelerated GFRV2 Dry Heat 40° exposures for different impact energies.

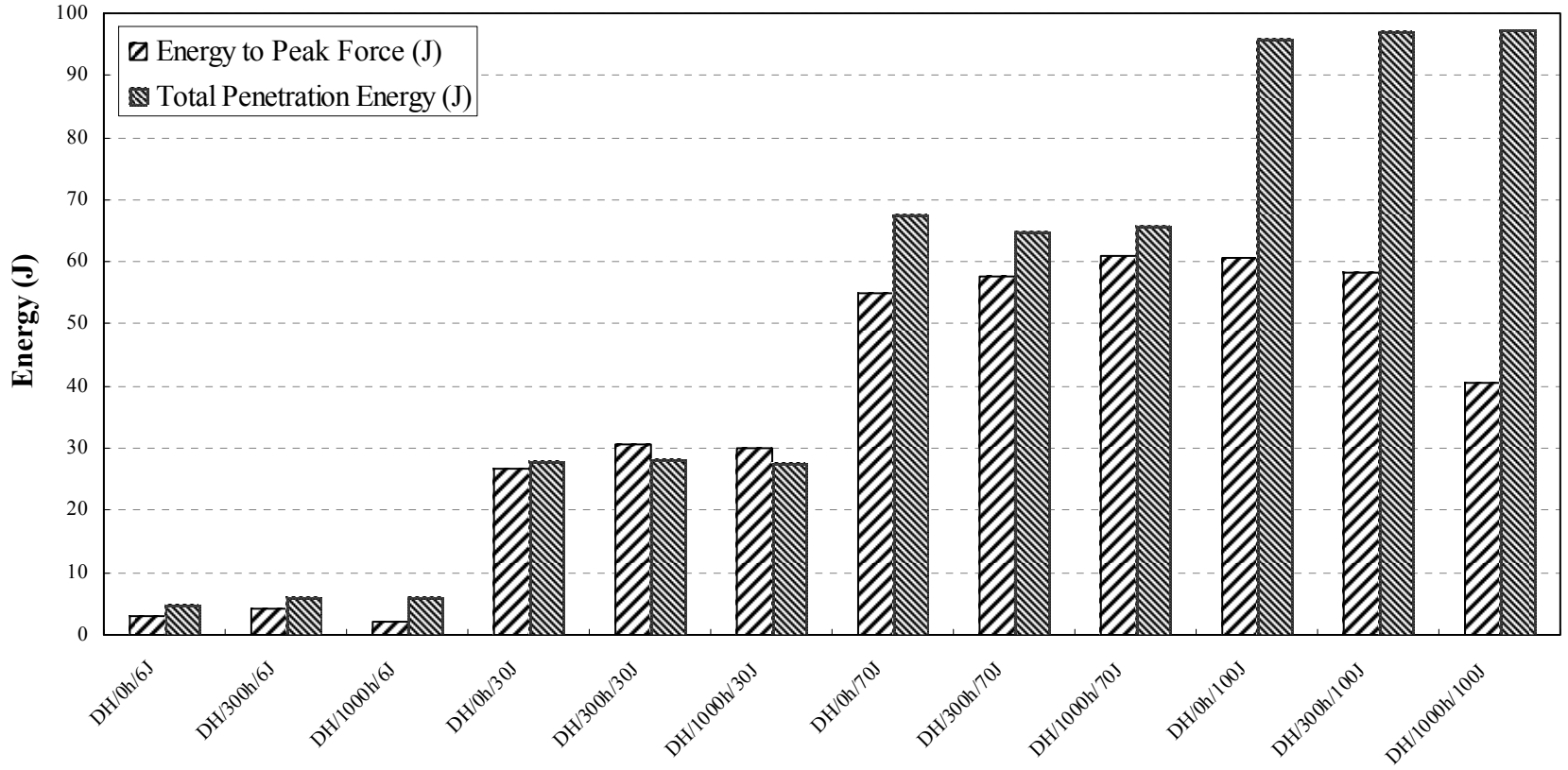

Figure 4.36 Comparison between the energy at peak force and total penetration energy for impact tested GFRV2 pipes exposed to different accelerated dry heat 40ºC conditions.

4.2.2 (b) Salt Spray

Salt spray exposure testing was designed to provide a controlled, high humidity, high temperature, and corrosive environment, which had been used extensively to provide relative corrosion or deterioration resistance data. The impact tests were carried out on the 160 mm long GFRV2 pipe of diameter 150 mm and thickness 6 mm, after being exposed to the accelerated condition of salt spray in Q-Fog CCT salt spray chamber. The pipes were kept in the chamber for 300 hours and 1000 hours.

For comparison, the impact behavior of the GFRV2 pipes exposed to different salt spray exposure periods at energy levels of 6 J, 30 J, 70 J and 100 J were studied. The load-time and energy-time curves are plotted as shown in Figures 4.37 through 4.40. It can be observed that as the impact energy increases the oscillations (flat region), mainly due to fiber breakage region, shifts from right of the peak load to the left.

For an impact energy of 6 J with 0h exposure the peak load is 3.27 KN, which increases to 3.39 KN for 300h and drops drastically to 3.23 KN for 1000h as shown in Table 4.10. A similar observation was made by Amateau et al. [9]. Glass fibers in this environment are severely degraded due to combination of mechanisms ranging from pitting, hydroxylation, hydrolysis, and leaching. Although the presence of resins in GFRP pipes around filaments protect the fibers from such attack, the salt spray will accelerate the degradation of bond and some resin themselves. For higher impact energies, as shown in Figure 4.41, the peak load for 300h and 1000h is same as unexposed pipe indicating that the material does not absorb the salt.

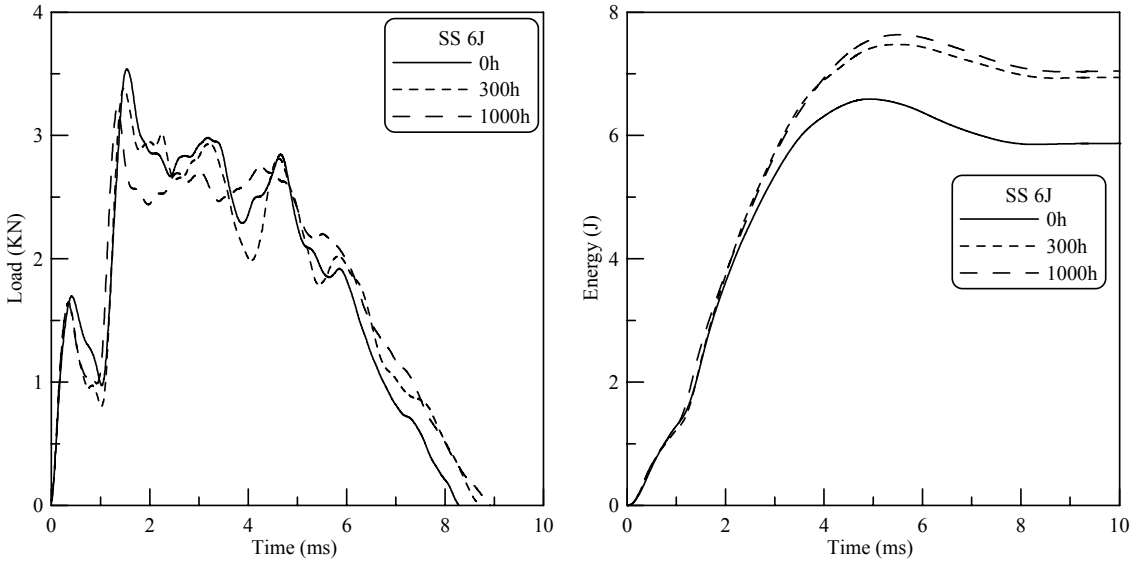

(a) (b)

Figure 4.37 (a) Load Vs Time and (b) Energy Vs Time plots for impact energy of 6 J exposed to Salt Spray of period 0h, 300h and 1000h

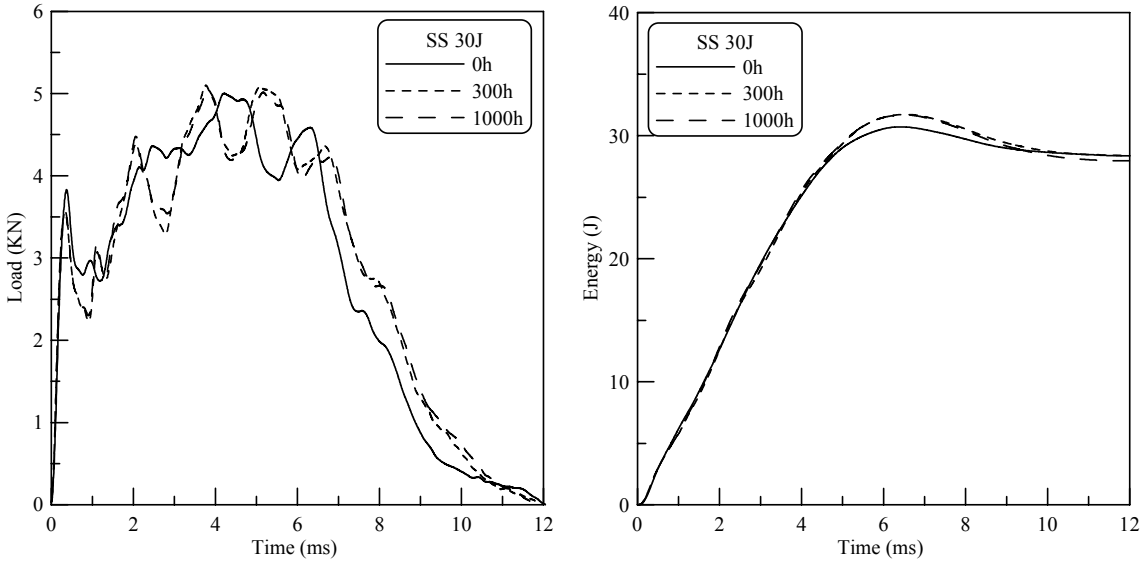

(a) (b)

Figure 4.38 (a) Load Vs Time and (b) Energy Vs Time plots for impact energy 30 J exposed to Salt Spray of period 0h, 300h and 1000h.

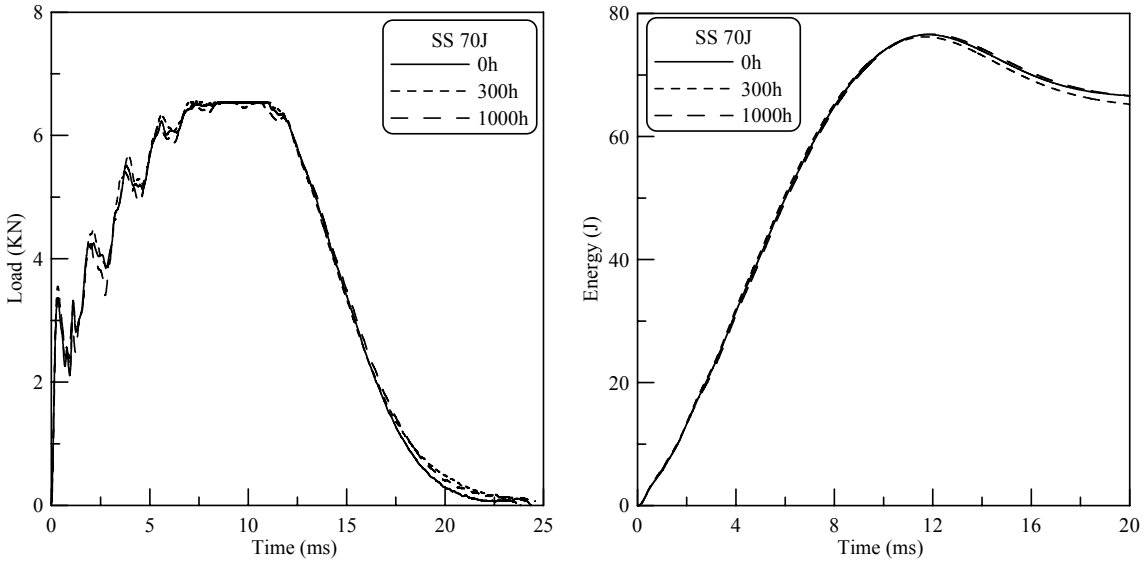

(a) (b)

Figure 4.39 (a) Load Vs Time and (b) Energy Vs Time plots for impact energy 70 J exposed to Salt Spray of period 0h, 300h and 1000h.

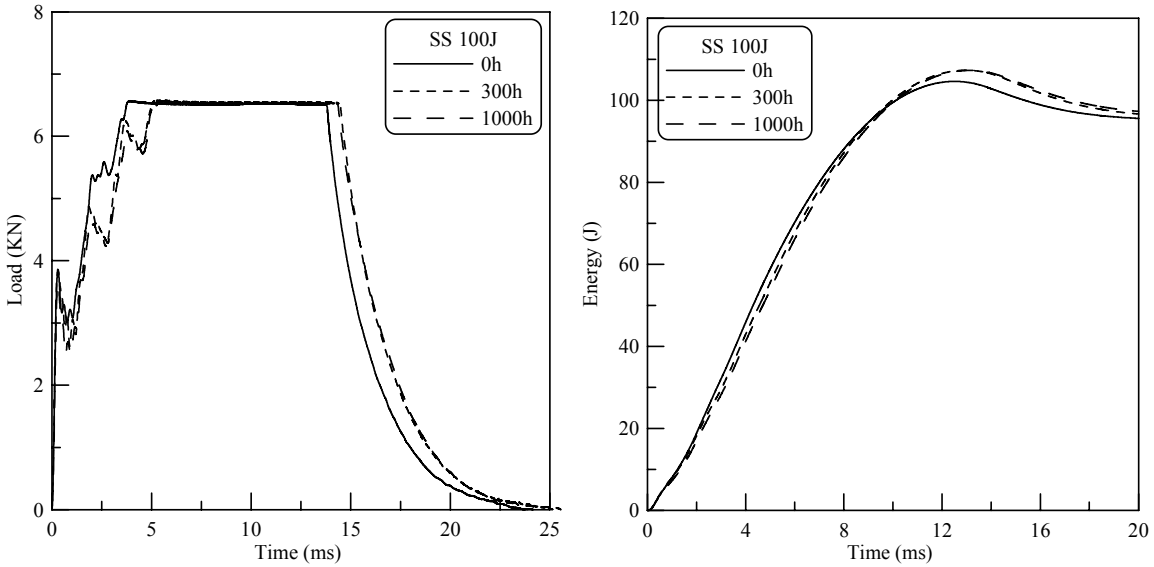

(a) (b)

Figure 4.40 (a) Load Vs Time and (b) Energy Vs Time plots for impact energy 100 J exposed to Salt Spray of period 0h, 300h and 1000h.

The deformation or deflection at the peak force for 6 J is nearly 1.68 mm for virgin pipe that decreases to 1.64 mm and 1.52 mm for 300h and 1000h exposure respectively. Also, it was observed that for total penetration at about 100 J the deformation decreased from 14.5 mm to 13.43 mm as shown in the Figure 4.42. The decrease in deformation is attributed to the degradation of the pipe due to salt spray.

Table 4.10 Impact properties of GFRV2 pipes exposed to Salt Spray

Specimen	Peak Force (kN)	Deformation at Peak Force (mm)	Energy to Peak Force (J)	Total Penetration Energy (J)
V/SS/0h/6J	3.27	1.68	2.94	4.75
V/SS/300h/6J	3.39	1.64	2.24	6.93
V/SS/1000h/6J	3.23	1.52	2.11	7.03
V/SS/0h/30J	5.28	7.20	26.78	28.07
V/SS/300h/30J	5.10	7.24	23.97	28.40
V/SS/1000h/30J	5.05	7.28	24.51	27.97
V/SS/0h/70J	6.56	12.11	55.02	67.47
V/SS/300h/70J	6.55	13.47	60.54	64.51
V/SS/1000h/70J	6.54	14.92	67.72	65.90
V/SS/0h/100J	6.57	14.49	60.61	95.90
V/SS/300h/100J	6.58	12.82	58.20	95.77
V/SS/1000h/100J	6.58	13.43	59.82	96.46

The energy to peak force decreases from 0h to 1000h with increase in the total penetration energy for impacted specimens of 6 J as shown in the Figure 4.43. This is due to the salt injection into the fiber-matrix interphase, resulting in loss of integrity at that level.

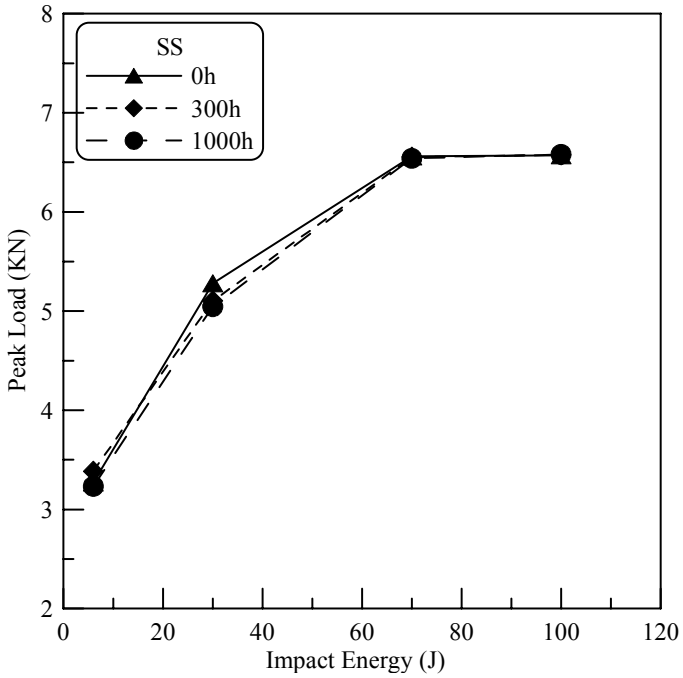

Figure 4.41 Peak Load Vs Impact Energy trace for accelerated GFRV2 salt spray exposure for different impact energies.

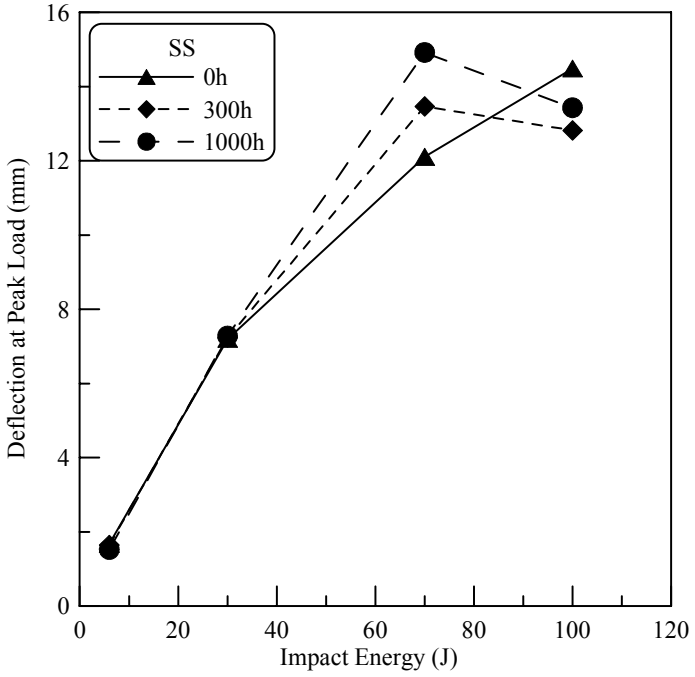

Figure 4.42 Deflection at peak load Vs impact energy plot for accelerated GFRV2 salt spray exposure for different impact energies.

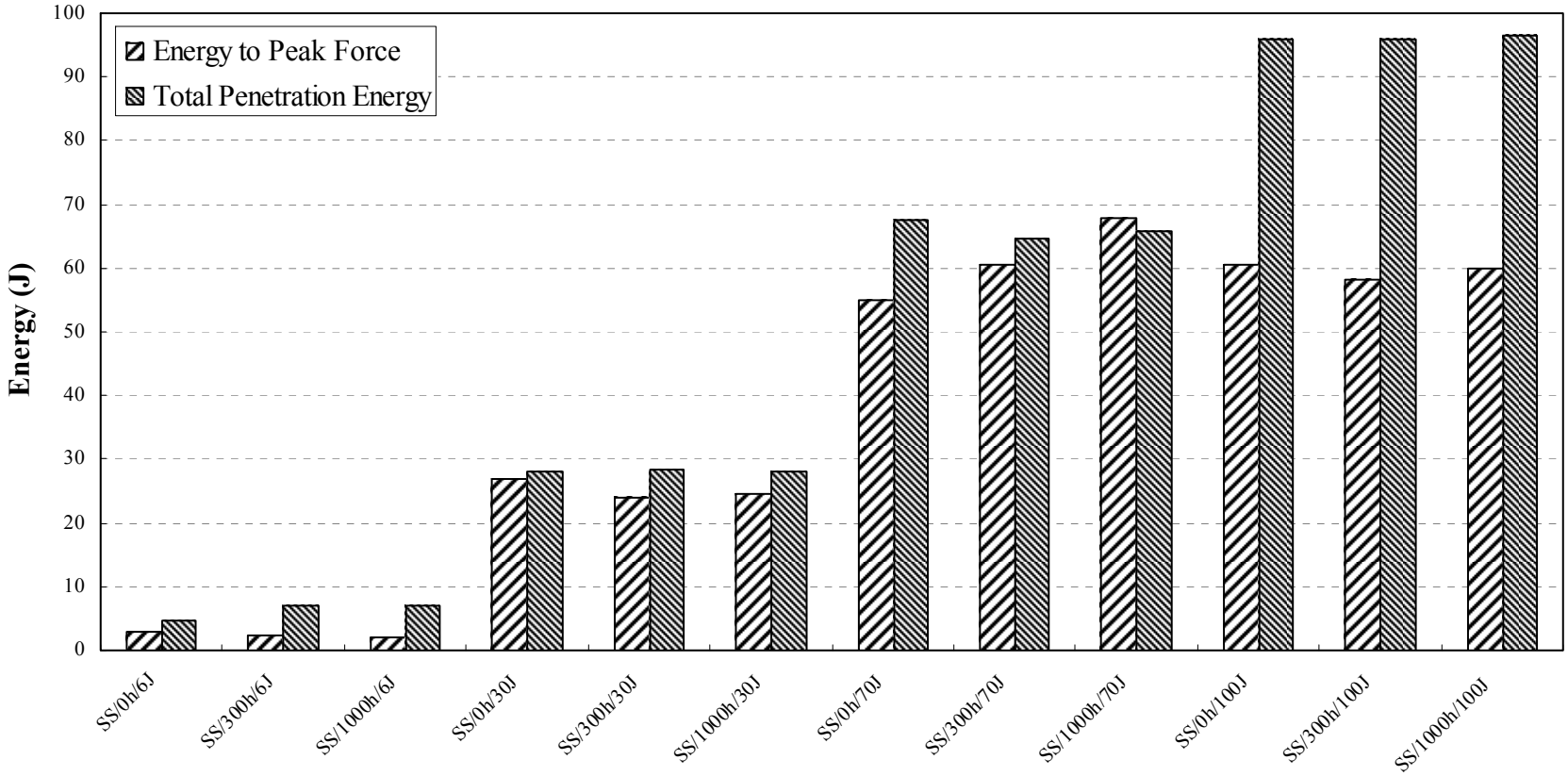

Figure 4.43 Comparison between the energy at peak force and total penetration energy for impact tested GFRV2 pipes exposed to different accelerated Salt spray conditions.

4.2.2 (c) Humidity Ambient

Humidity ambient exposure testing was designed to provide a controlled moisture/aqueous environment. Moisture and humidity has primary effect of causing the degradation at the fiber as well as resin level. The impact tests were carried out on the 160 mm long GFRV2 after being exposed to the accelerated condition of humidity ambient in Singleton Corrosion Test Cabinet. The pipes were kept in the chamber for 300 hours and 1000 hours exposure periods. To compare the impact behavior of the GFRV2 pipes exposed to different humidity ambient exposure periods at each energy level of 6 J, 30 J, 70 J and 100 J, the load-time and energy-time curves are plotted as shown in the Figures 4.44 through 4.47.

At impact energy of 30 J it was observed that peak load for 0h exposure is 5.28 KN that decreases to 5.25 KN and 5.11 KN for 300h and 1000h respectively as shown in Table 4.11 and Figure 4.48. The decrease in peak load is due to the moisture absorption leading to the weakening of the resin-fiber bond. Moisture weakens the fiber/matrix interface not only through chemical attack and reaction, but also through mechano-chemical effects such as osmotic pressure. Moisture diffuses and separates out in voids of resin and dissolves soluble materials of polymer. The resin acts as a semi-permeable membrane and osmotic pressure develops inside the void because of continuous water diffusion.

The deformation at the peak force for 6 J is nearly 1.68 mm for virgin pipe and that increases to 2.33 mm for 300h exposure then decreases to 1.56 mm for 1000h. For 100 J the deformation decreases from 14.5 mm to 13.59 mm. This is explained mainly due to moisture absorption leading to the weakening of the fiber/resin bond.

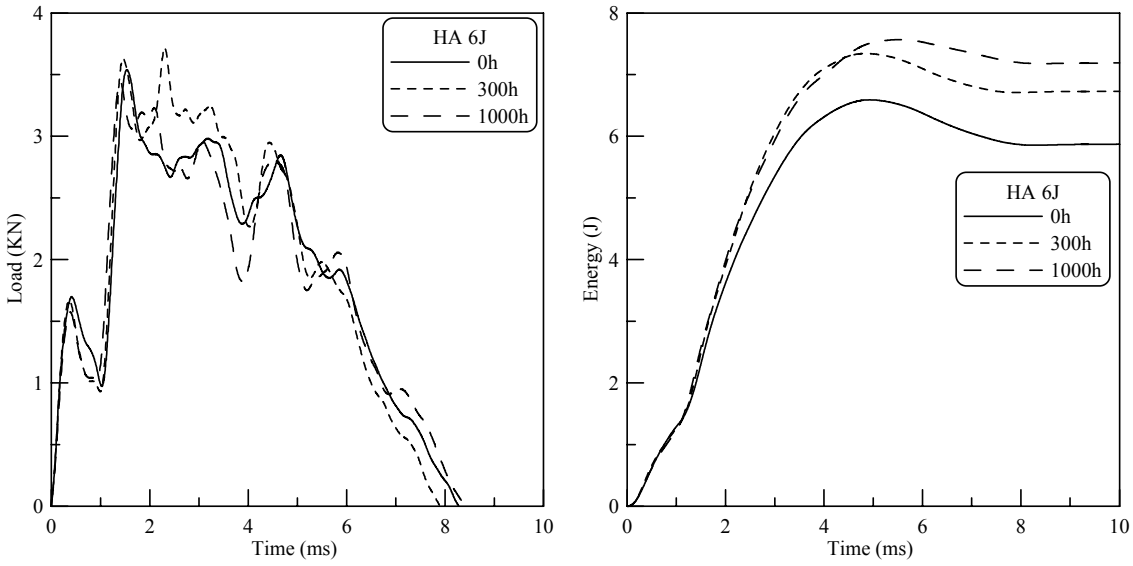

(a) (b)

Figure 4.44 (a) Load Vs Time and (b) Energy Vs Time plots for impact energy 6 J exposed to Humidity Ambient of period 0h, 300h and 1000h.

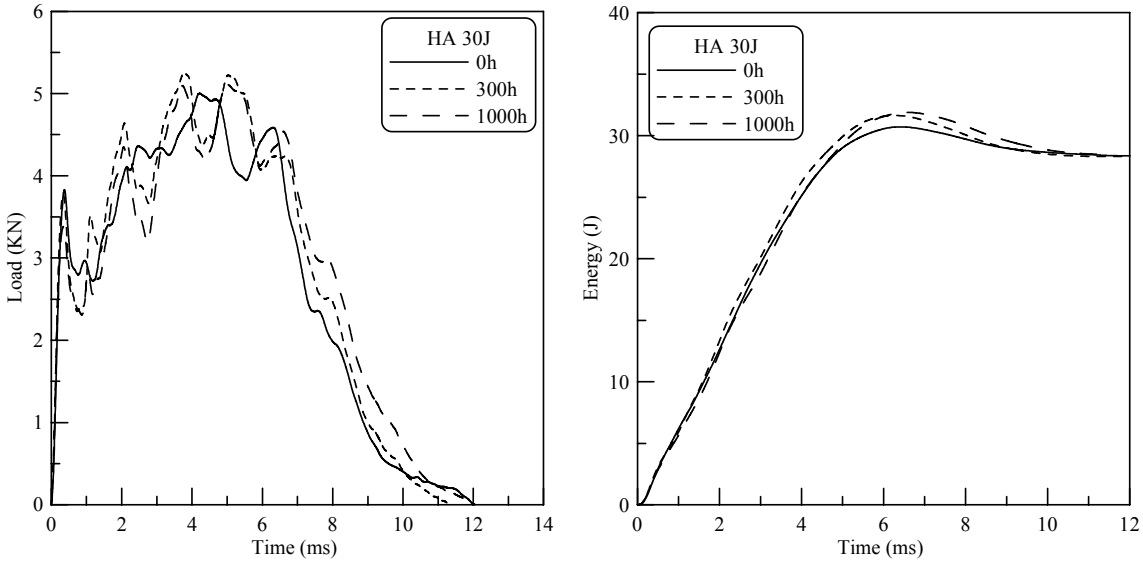

(a) (b)

Figure 4.45 (a) Load Vs Time and (b) Energy Vs Time plots for impact energy 30 J exposed to Humidity Ambient of period 0h, 300h and 1000h.

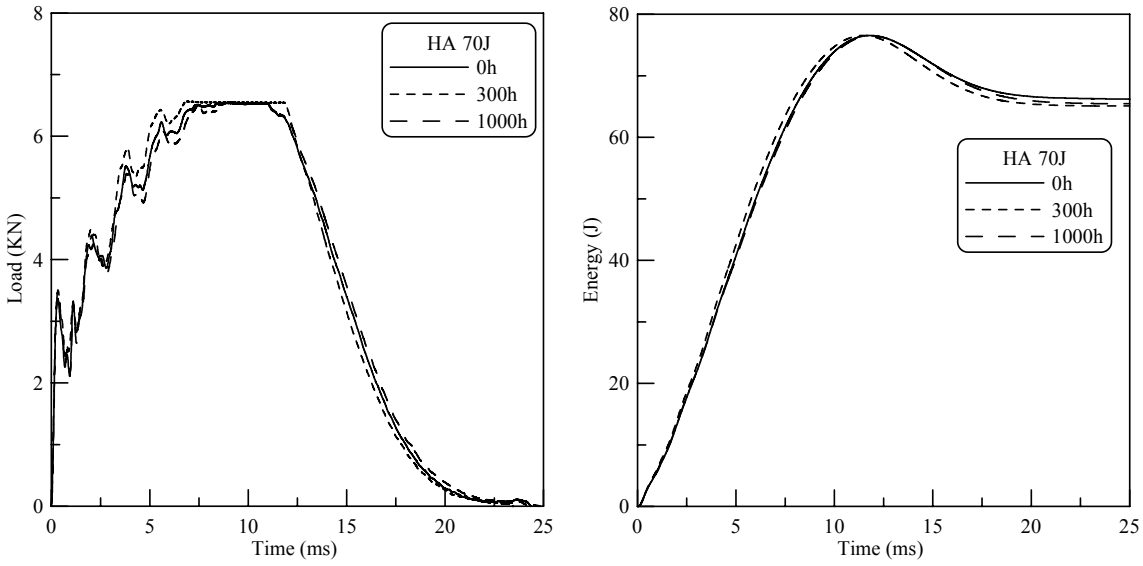

(a) (b)

Figure 4.46 (a) Load Vs Time and (b) Energy Vs Time plots for impact energy 70 J exposed to Humidity Ambient of period 0h, 300h and 1000h.

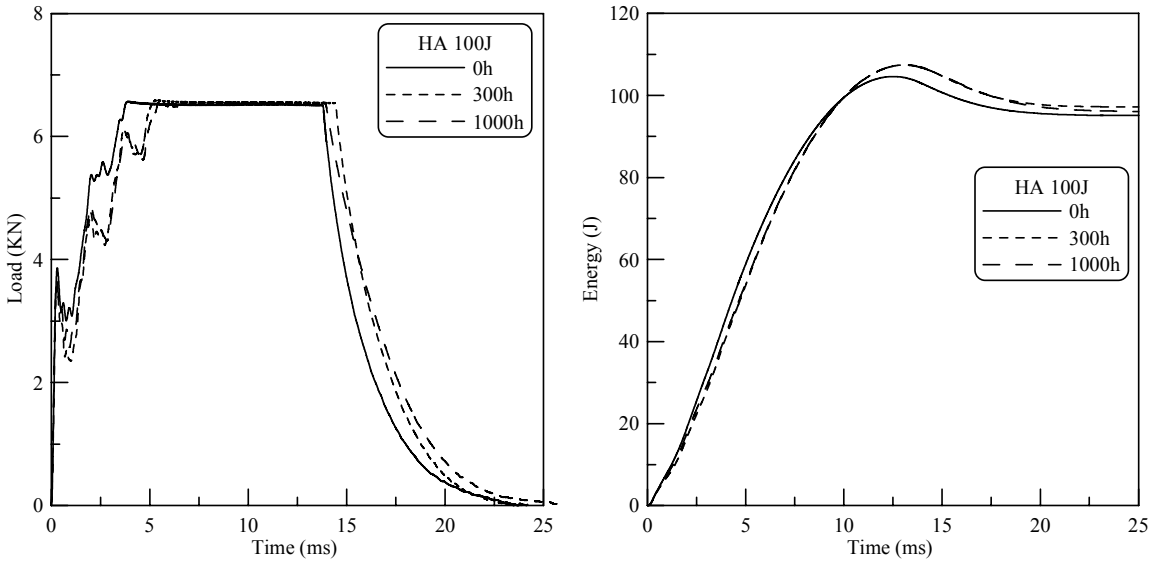

(a) (b)

Figure 4.47 (a) Load Vs Time and (b) Energy Vs Time plots for impact energy 100 J exposed to Humidity Ambient of period 0h, 300h and 1000h.

Table 4.11 Impact properties of GFRV2 pipes exposed to Humidity Ambient

Specimen	Peak Force (kN)	Deformation at Peak Force (mm)	Energy to Peak Force (J)	Total Penetration Energy (J)
V/HA/0h/6J	3.27	1.68	2.94	4.75
V/HA/300h/6J	3.72	2.33	4.65	6.71
V/HA/1000h/6J	3.45	1.56	2.23	7.18
V/HA/0h/30J	5.28	7.20	26.78	28.07
V/HA/300h/30J	5.25	7.10	25.06	28.32
V/HA/1000h/30J	5.11	8.49	29.37	28.43
V/HA/0h/70J	6.56	12.11	55.02	67.47
V/HA/300h/70J	6.57	13.01	59.04	65.10
V/HA/1000h/70J	6.55	15.23	69.66	65.45
V/HA/0h/100J	6.57	14.49	60.61	95.90
V/HA/300h/100J	6.59	13.21	58.18	97.24
V/HA/1000h/100J	6.58	13.59	61.24	96.06

The energy to peak force increases for 0h to 300h with increase in the total penetration energy of 6 J and then decreases for 1000h as shown in the Figure 4.50. This is due to moisture absorption. For the impact energy of 30 J, the energy at peak load decreases for 300h and then increases for 1000h. For the impact energy of 70 J, the difference between the energy at peak load and total penetration energy decreases and energy at peak load exceeds at 1000h. For the impact energy of 100 J, energy absorbed at peak load seems to remain constant, showing no degradation due to the exposure of humidity ambient. Moisture weakens the fiber/matrix interface, but the moisture didn't diffuse in this case and thus the impact resistance is not affected.

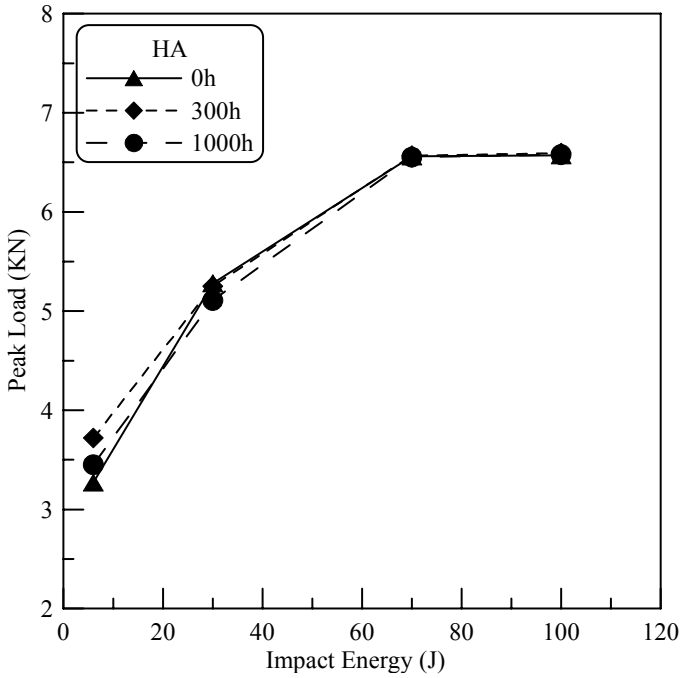

Figure 4.48 Peak Load Vs Impact Energy trace for accelerated GFRV2 Humidity Ambient exposures for different impact energies.

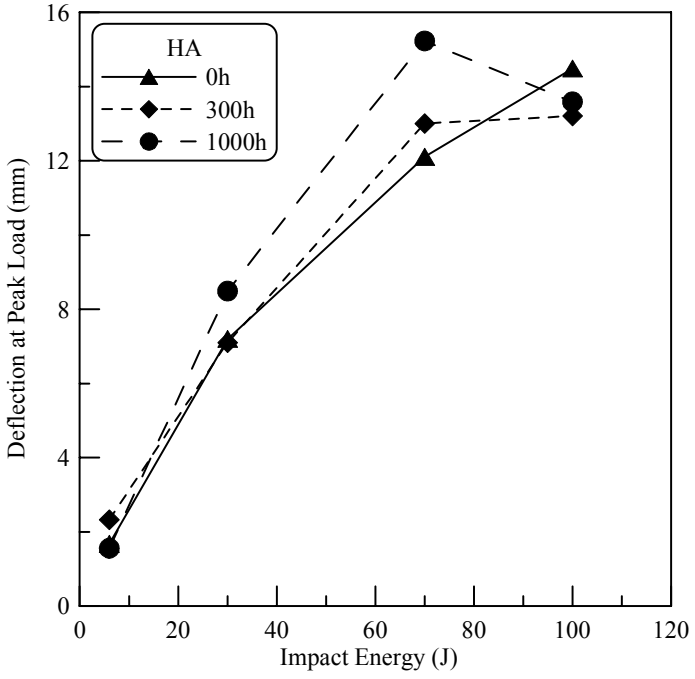

Figure 4.49 Deflection at peak load Vs impact energy traces for accelerated GFRV2 Humidity Ambient exposures for different impact energies.

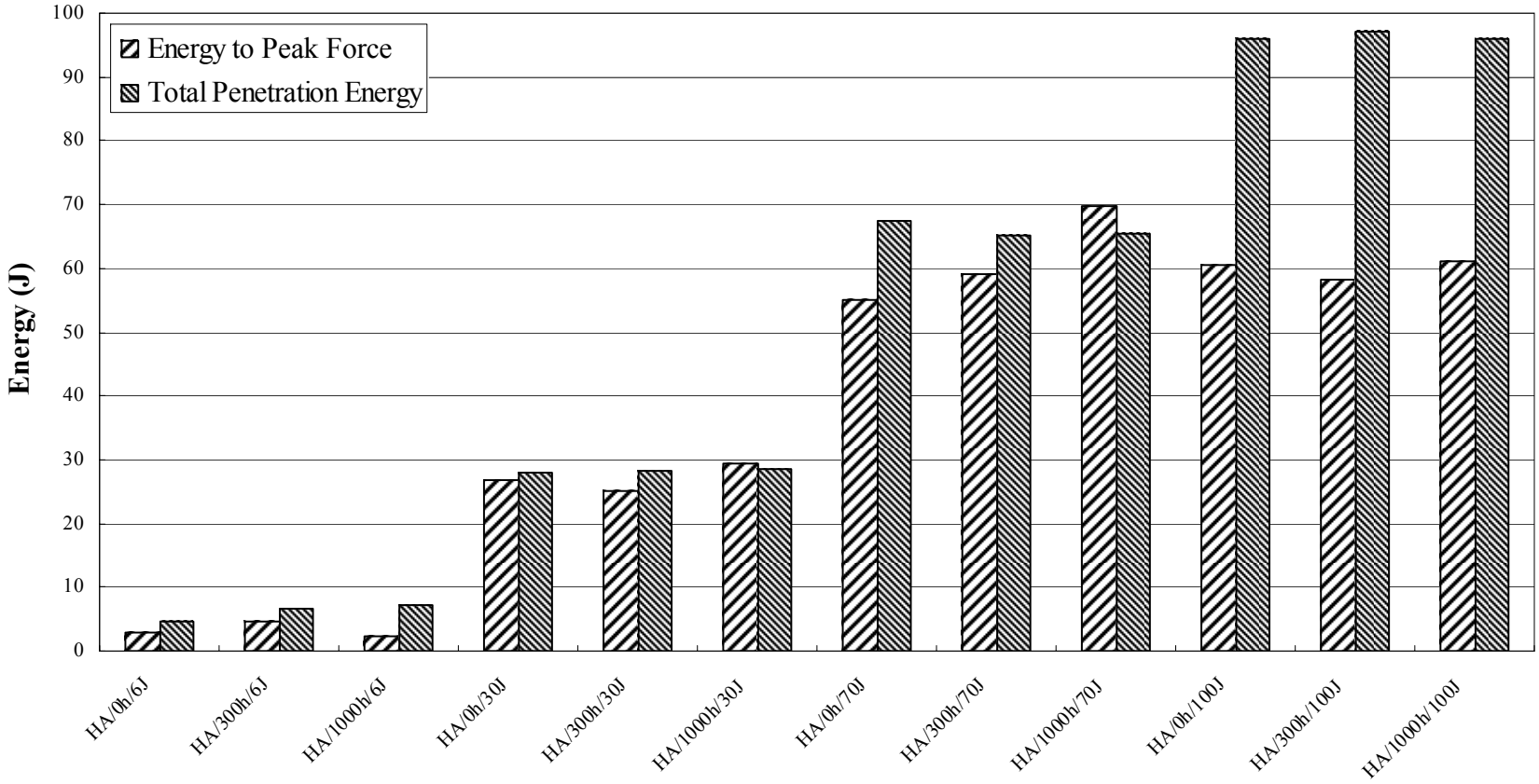

Figure 4.50 Comparison between the energy at peak force and total penetration energy for impact tested GFRV2 pipes exposed to different accelerated Humidity ambient conditions.

4.2.2 (d) Humidity 100%

Humidity 100% exposure testing was designed to provide a controlled moisture/aqueous environment. The impact tests were carried out on the 160 mm long GFRV2 pipe of diameter 150 mm and thickness 6 mm, after being exposed to accelerated condition of humidity 100% in Singleton Corrosion Test Cabinet. The pipes were kept in the cabinet for two different periods of 300 hours and 1000 hours. Comparison of impact behavior of GFRV2 pipes exposed to different Humidity 100% exposure periods at energy levels of 6 J, 30 J, 70 J and 100 J. The load-time and energy-time are shown in Figures 4.51 through 4.54.

At impact energy of 6 J, it is observed that the peak load for 0h exposure is 3.27 KN, which increases to 3.48 KN and 3.58 KN for 300h and 1000h respectively as shown in Table 4.12 and Figure 4.55. The increase in peak load indicates that there is no effect of humidity on impact resistance at low energies.

The deflection at the peak force is constant for all the exposure periods because of negligible effect of humidity for 30 J. For impact energy of 70 J the deflection is constant for all the exposures. For total penetration at about 100 J the deformation decreases from 14.50 mm to 14.05 mm, due to the absorbed moisture weakening the bond of fiber and resin.

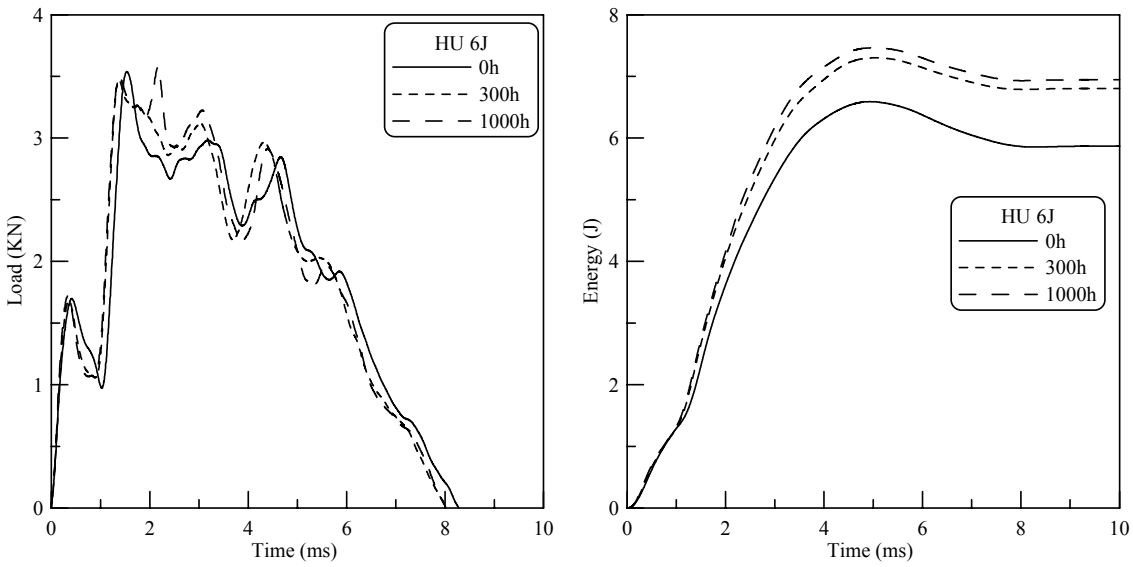

(a) (b)

Figure 4.51 (a) Load Vs Time and (b) Energy Vs Time plots for impact energy 6 J exposed to 100% Relative Humidity of period 0h, 300h and 1000h

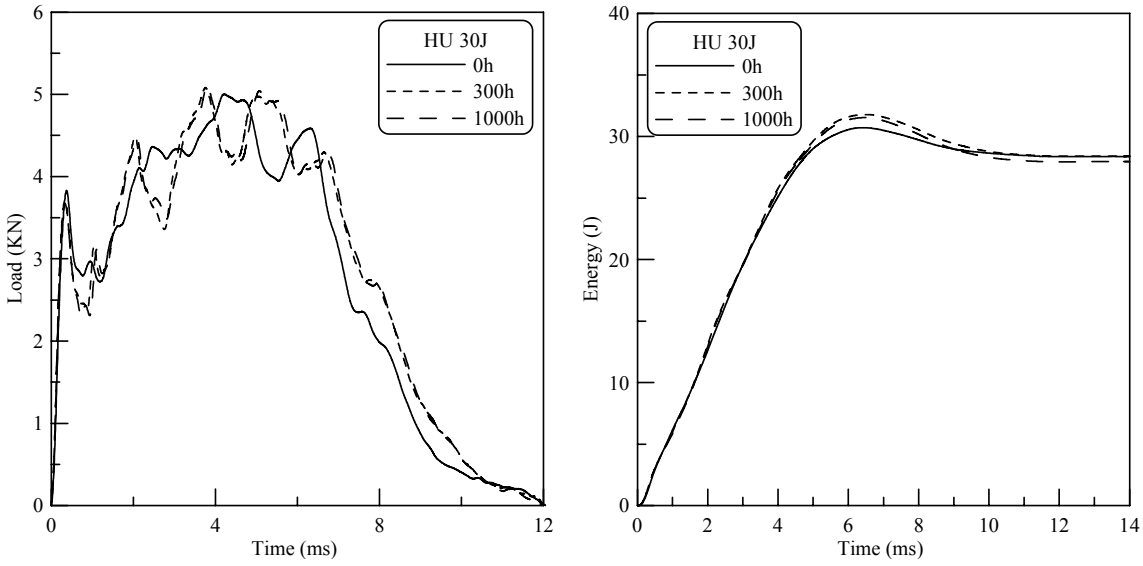

(a) (b)

Figure 4.52 (a) Load Vs Time and (b) Energy Vs Time plots for impact energy 30 J exposed to 100% Relative Humidity of period 0h, 300h and 1000h

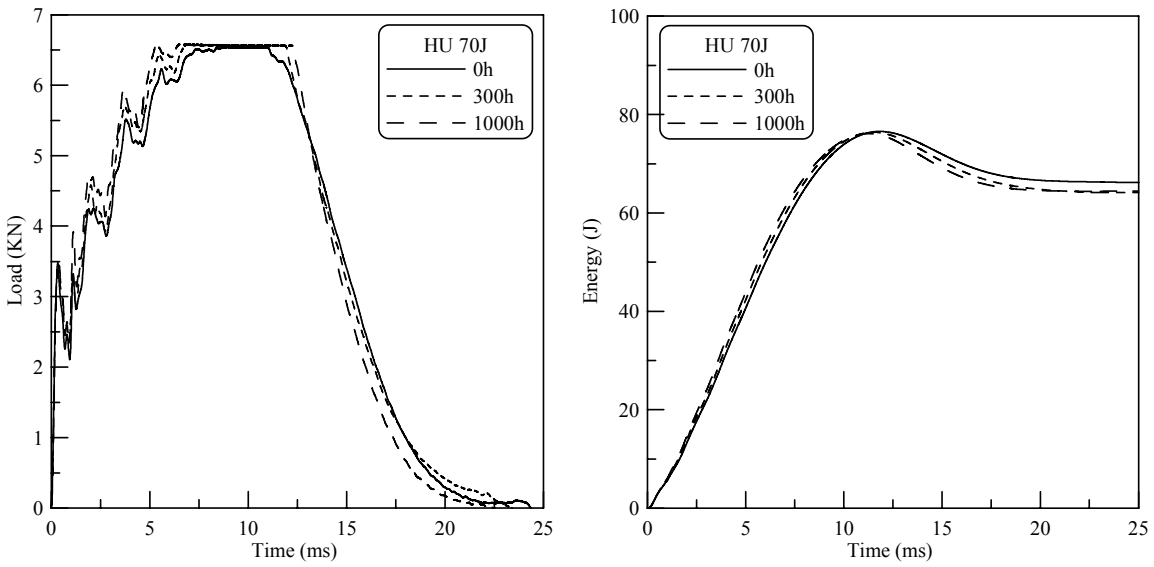

(a) (b)

Figure 4.53 (a) Load Vs Time and (b) Energy Vs Time plots for impact energy 70 J exposed to 100% Relative Humidity of period 0h, 300h and 1000h

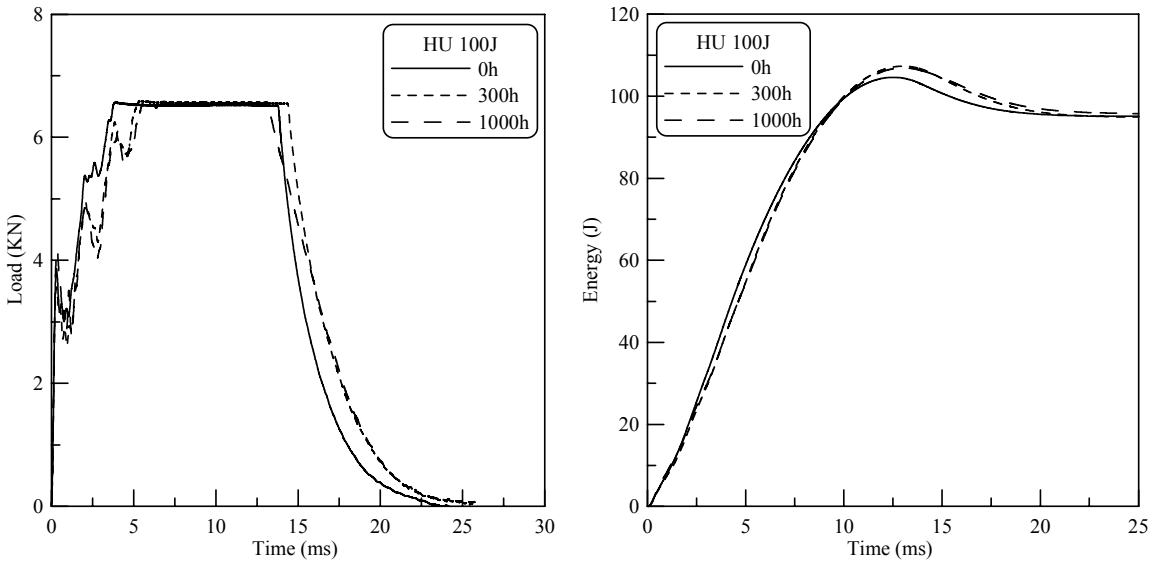

(a) (b)

Figure 4.54 (a) Load Vs Time and (b) Energy Vs Time plots for impact energy 100 J exposed to 100% Relative Humidity of period 0h, 300h and 1000h

Table 4.12 Impact properties of GFRV2 pipes exposed to Humidity 100%

Specimen	Peak Force (kN)	Deformation at Peak Force (mm)	Energy to Peak Force (J)	Total Penetration Energy (J)
V/HU/0h/6J	3.27	1.68	2.94	4.75
V/HU/300h/6J	3.48	1.50	2.23	6.79
V/HU/1000h/6J	3.58	2.21	4.59	6.93
V/HU/0h/30J	5.28	7.20	26.78	28.07
V/HU/300h/30J	5.08	7.20	24.41	28.40
V/HU/1000h/30J	5.10	7.25	24.49	27.94
V/HU/0h/70J	6.56	12.11	55.02	67.47
V/HU/300h/70J	6.59	13.02	59.14	64.15
V/HU/1000h/70J	6.58	12.35	57.41	64.40
V/HU/0h/100J	6.57	14.49	60.61	95.90
V/HU/300h/100J	6.59	13.26	59.71	94.88
V/HU/1000h/100J	6.59	14.05	64.82	95.71

The energy to peak force increases from 0h to 1000h with increase in the total penetration energy of 6 J as shown in the Figure 4.57. This is because the effect of humidity exposure cannot be seen at low impact energies due to negligible absorption of water into the pipe specimen. For the impact energy of 30 J the energy at peak load decreases due to the degradation of the pipe. Moisture weakens the fiber/matrix interface Moisture diffuses and separates out in voids of resin and dissolves soluble materials of polymer. The resin acts as a semi-permeable membrane and osmotic pressure develops inside the void because of continuous water diffusion, leading to weakening of fiber/resin bond.

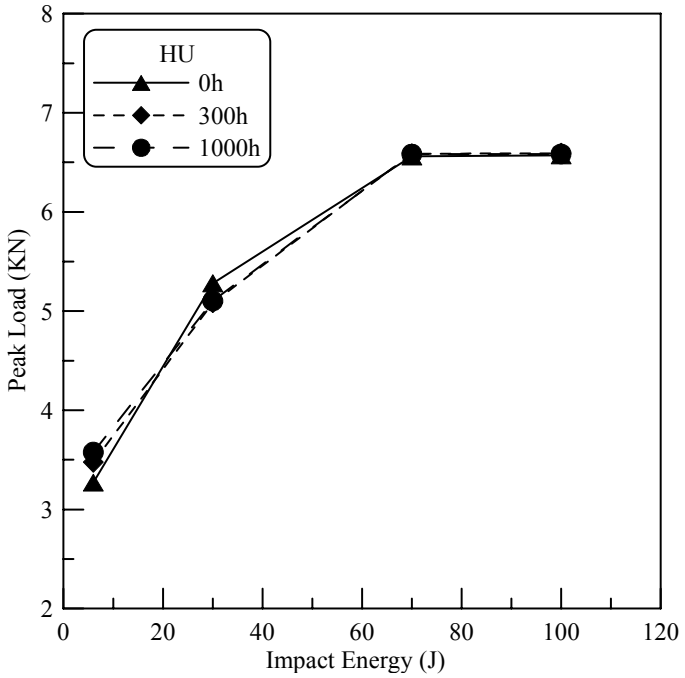

Figure 4.55 Peak Load Vs Impact Energy trace for accelerated GFRV2 Humidity 100% exposures for different impact energies

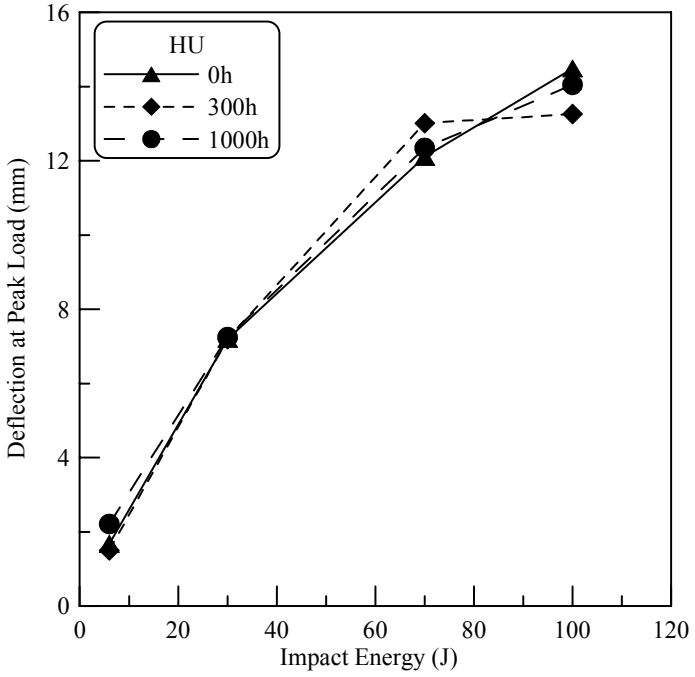

Figure 4.56 Deflection at peak load Vs impact energy plot for accelerated GFRV2 Humidity 100% exposures for different impact energies.

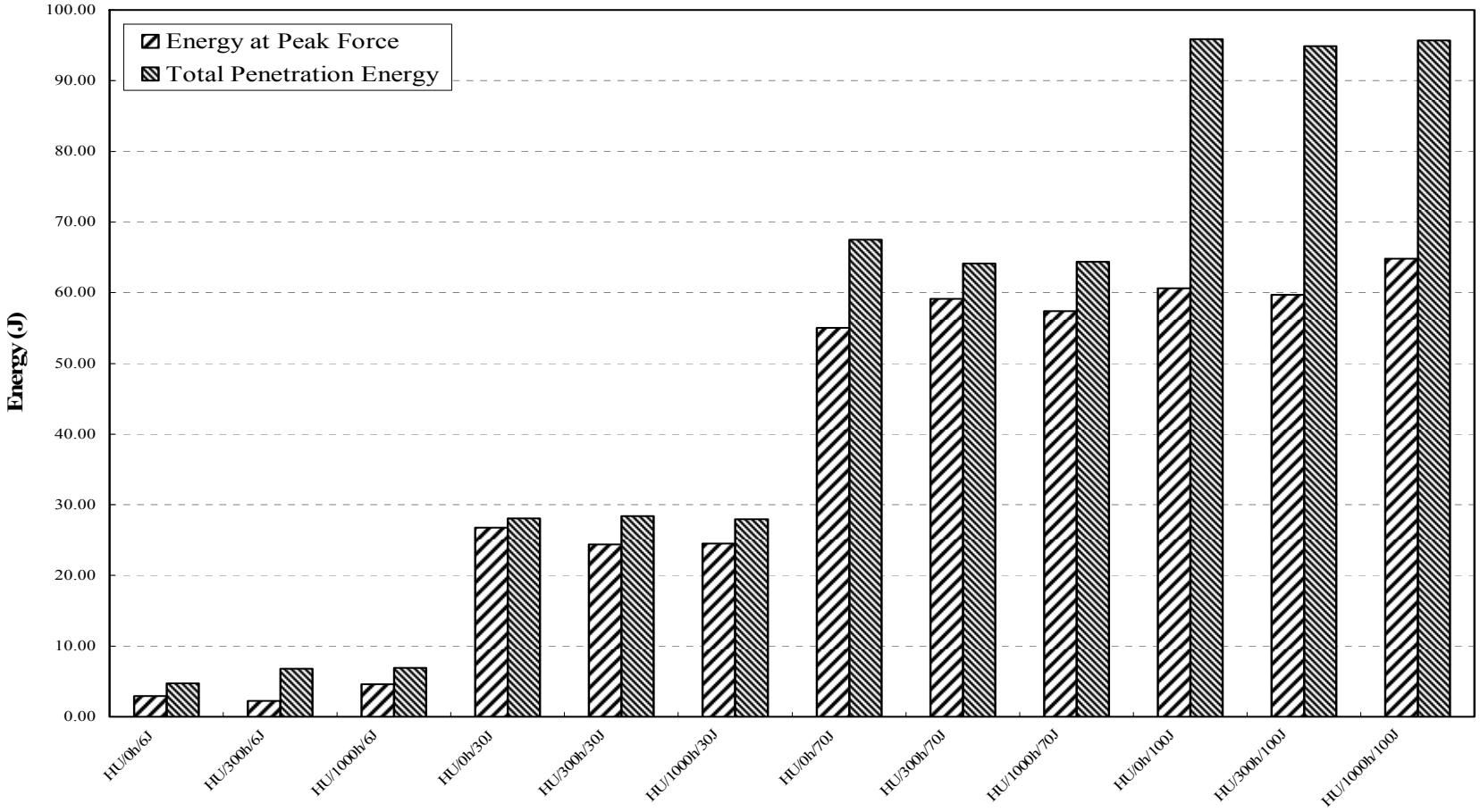

Figure 4.57 Comparison between energy at peak force and total penetration energy for impact tested GFRV2 pipes exposed to different accelerated Humidity 100% conditions.

CHAPTER 5

CONCLUSIONS AND RECOMMENDATIONS

5.1 CONCLUSIONS

This chapter presents the conclusions drawn from the analysis of the experimental data of hydrostatic burst tests and low velocity impact tests conducted on the glass fiber reinforced thermoset pipes. The following were extracted

1. Burst and low velocity impact behavior of two vinylester based (GFRV1 and GFRV2) and one epoxy based (GRFE) filament wound glass fiber reinforced thermoset pipes were investigated.
2. The GFRV2 pipes exhibit 6% higher pressure carrying capacity than the GFRV1, where as the burst pressure for GFRE pipes averaged approximately 25% higher than the GFRV pipes. The burst failure mode of GFRV was ductile in nature whereas for GFRE it was found to be brittle.
3. The burst failure of vinylester based and epoxy based GFRP pipes typically occurred at the points of minimum wall thickness or at the point where material defects (not visible to naked eye) were present. Failure occurred by expansion or ballooning resulting in the typical parrot's beak failure.
4. Delamination and twist failure of the GFRV composite pipe is observed in the case where the wall thickness of the pipe is according to the specifications and the

pipe is free of any defects. Whereas in GFRE composite pipes the failure for the pipe without any defects creates long cracks along the length of the pipe.

5. The impact energy required to just initiate damage for GFRE was double the energy needed for GFRV pipes. The energy for total penetration of the GFRE is 10% more than the energy needed to penetrate the GFRV pipe specimen. The maximum peak load was same for both types of GFRP pipes. The deflection for total penetration of the pipe was about twice the thickness of the pipe.
6. Post impact pressure strength ratio for GFRE pipes is higher than the GFRV pipes. Low impact energies, where the impact damage zone was small, leakage, weeping or burst occurred from regions located circumferentially 90° away from the impact zone (and occasionally at about 45°) or on the opposite side (180°) to the impact damage zone of the GFRP pipe. This is probably due to resin cracking and delamination which may have occurred due to bending during impact tests rather than plastic flow. However, at relatively high impact energies, where the impact damage zones was relatively large and the failure occurred by weeping.
7. The GFRV1 pipe exposed to seawater immersion exhibits increase in the burst pressure but the failure was purely in the form of burst at the center of the pipe. The 3 months and 12 months exposed pipes showed a 10% increase in burst pressure on an average when compared to virgin pipes. The increase in the strength of the GFRV pipe is due to plasticization of the matrix by the absorbed water.
8. For the natural outdoor exposure containing crude oil the burst pressure increases with increase in the exposure periods. The 3 months and 12 months exposure

resulted in the increase of burst pressure by 10% and 20% respectively. Degradation may occur when polymers are irradiated, but cross-linking is the predominant reaction. The modulus increases with cross-linking. Although cross-linking is a useful reaction in making vinylester materials, there may occur undesirable consequences after the materials are in long service.

9. There is an improvement in the impact resistance for the specimens exposed to dry heat 40ºC initially for 300 hrs. The strength decreases as the time progresses for 1000 hrs exposure period. This was mainly attributed to curing process and the possible reason might be that the post cure was fully achieved after 300 hrs.
10. Under salt spray conditions, the GFRV2 composite pipes showed a decrease in the peak force absorbed by the specimens due to the salt injection into the fiber-matrix interphase, resulting in loss of integrity.
11. The behavior of the composite pipe exposed to ambient humidity results in a decrease in the peak load i.e., impact resistance. This decrease may be due to the moisture absorption leading to the weakening of the resin-fiber bond. Moisture weakens the fiber/matrix interface not only through chemical attack and reaction, but also through mechanochemical effects such as osmotic pressure.
12. Due to negligible effect of exposure the impact resistance of GFRV2 composite pipes when exposed to 100% humidity, increases for 1000 hrs of exposure. This behavior is expected to change for higher exposure periods, when the moisture gets absorbed into the fiber/matrix interface.

5.2 RECOMMENDATIONS

Following are some of the recommendations for any future work to be carried out on GFRP and effect of environmental conditions:

1. Hydrostatic burst test rig can be made computer-controlled and to design the pneumatic controlled endcaps.
2. Tensile testing can be done after the impact so as to assess the post impact damage.
3. Microscopic analysis of the impact damaged specimens can be carried out to have an in-depth failure analysis.
4. Accelerated exposures for higher periods can be investigated to explain further degradation of the pipes.

REFERENCES

1. Liao, K., Schultheisz, C.R., Hunston, D.L., Brinson, L.C., *Long-Term Durability of Fiber Reinforced Polymer Matrix Composite Materials for Infrastructure Applications: A Review.* Journal of Advanced Materials, 1998. **30**(4): p. 3-40.
2. Martin, J.W., Chin ,J. W., Byrd, W. E., Embree, E., Kraft, K. M., *An integrating sphere-based ultraviolent exposure chamber design for the photodegradation of polymeric materials.* Polymer Degradation and Stability, 1999. **63**: p. 297-304.
3. Sampath, P.K., Ganti, A.S., *Environmentally influenced degradation of fiber-reinforced composites.* Materials Performance, May 1997. **36**(5): p. 65-69.
4. Signor, A.W., Chin, J. W. *Effects of ultraviolet radiation exposure on vinylester matrix resins: Chemical and Mechanical Characterization*. in *American Society for composites, 16th technical conference proceedings*. 2001.
5. Liau, W.B., Tseng, F. P., *The effect of long-term ultraviolet light irradiation on polymer matrix composites.* Polymer Composites, Aug 1998. **19**(4): p. 440-445.
6. Marsh ,L.L., Lasky, R., Seraphim, D. P., Springer. G. S., *Moisture solubility and diffusion in epoxy and epoxy-glass composites.* IBM Journal of Research Development, Nov 1984. **28**(6): p. 655-661.
7. Springer, G.S., Sanders, B. A., Tung, R. W., *Environmental effects on glass fiber reinforced polyester and vinylester composites.* Journal of Composite Materials, July 1980. **14**: p. 213-232.
8. Sarkar, B.K., Bose, N. R., Roy, R., *Effects of moisture on the mechanical properties of glass fibre reinforced vinylester resin composites.* Building Materials Science, Feb 2001. **24**(1): p. 87-94.

9. Amateau, M.F., Karasek, M. L., Strait, L. H., *Effects of Seawater immersion on the impact resistance of glass fiber reinforced epoxy composites.* Journal of Composite Materials, 1991 :(14)26 .p. 2118-2133.

10. Zheng, Q., Morgan, R. J., *Synergistic thermal-moisture damage mechanisms of epoxies and their carbon fiber composites.* Journal of Composite Materials, 1993. **27**(15): p. 1465-1478.

11. Monney, L., dubois, C., Perreux, D., Burtheret ,A., Chambaudet, A., *Mechanical behaviour of an epoxy-glass composite under photo-oxidation.* Polymer Degradatio and Stability, 1999. **63**: p. 219-224.

12. Kumar, B.G., Singh, R. P., Nakamura, T., *Degradation of carbon fiber-reinforced epoxy composites by ultraviolet radiation and condensation.* Journal of Composite Materials, 2002. **36**(24): p. 2713-2733.

13. Fernand Ellyin, R.M., *Environmental effects on the mechanical properties of glass-fiber epoxy composite tubular specimens.* Composite Science and Technology, 2004. **64**: p. 1863-1874.

14. Kwang-Bok Shin, C.-G.K., Chang-Sun Hong,, *Correlation of accelerated aging test to natural aging test on graphite-epoxy composite materials.* Journal of Reinforced Plastics and Composites, 2003. **22**(09): p. 849-861.

15. Chin, J.W., Nguyen, T., Aouadi, K., *Effects of environmental exposure on fiber-reinforced plastic (FRP) materials used in construction.* Journal of Composites Technology and Research, Oct 1997. **19**(4): p. 205-213.

16. Lixin Wu, K.M., Vistasp M. Karbhari, James S. Zhang, *Short-Term effects of Sea Water on E-Glass/Vinylester Composites.* Journal of Applied Polymer Science. **84**: p. 2760-2767.

17. Karbhari. V. M. , R.J., Zhang. J., *Low- temperature hygrothermal degradation of ambient cured E-glass/vinylester systems.* Journal of Applied Polymer Science, 2002. **86**: p. 2255-2260.

18. Kootsookos, A., Mouritz, A. P., *Seawater durability of glass and carbon-polymer composites.* Composites Science and Technology, 2004. **64**: p. 1503-1511.

19. Mizoguchi, M., Morii, T., Fujii ,Y., Hamada, H. *Study on acid stress corrosion in E glass and C glass reinforced vinylester composites*. in *13th International Conference on Composite Materials*. 2001.

20. Muscati, A., Blomfield, J. A., *Full scale burst tests on GRP pipes.* IMechE, 1977: p.10-7 .

21. Nakai, Y., Kurahasi, H. *Hydrostatic burst test of pipe with HIC*. in *The international corrosion forum, National association of corrosion engineers*. 1982. Houston, TX.

22. Ghorbel, I.S., P., *Durability of closed-end pressurized GRP pipes under hygrothermal conditions. Part I: Monotonic tests.* Journal of Composite Materials, 1996. **30**(14): p. 1562-1580.

23. Nagesh, *Finite-element analysis of composite pressure vessels with progressive degradation.* Defence Science Journal, 2003. **53**(1): p. 75-86.

24. Chang, D.J., Valenzuela, P. R., Albright, T. V., *Burst tests of filament-wound graphite-epoxy tubes*. Dec 2000, The aerospace Corporation, Propulsion science and experimental mechanics department, space materials laboratory: Los Angeles.

25. Glover, A.G ,.Smith, N., Tyson, W., Chakravarti, A., Malik, L., *Fracture predication of a burst test on a vessel containing flaws.* ASME, 1992. **239**: p. 197-202.

26. Chang, D.J., Katzman, H. A., Nokes, J. P., Adams, P. M., Amimoto, S. T., *Burst testing of filement-wound graphite-epoxy composite cylindrical tubes*. Nov 2002, Aerospace Corporation, Lab Operations: El Segundo, CA. p. 80.

27. Smith, J.H., Rana, M. D., Hall, C., *The use of "Fitness for service" assessment procedures to establish critical flaw sizes in high pressure gas cylinders.* Journal of Pressure Vessel Technology, May 2003. **125**(2): p. 177-181.

28. Yang, C., Pang, S. S, Zhao, Y., *Buckling analysis of thick-walled composite pipe under external loading.* Journal of Composite Materials, 1997. **31**(4): p. 409-42.6

29. Yang, C., *Design and analysis of composite pipe joint under tensile loading.* Journal of Composite Materials, 2000. **34**(4): p. 332-349.

30. Jacobs, L.J., Dokun, O. D., Haj-ali, R. M., *Ultrasonic monitoring of material degradation in FRP composites.* Journal of Engineering Mechanics, 2000. **126**(7): p. 704-710.

31. Nahas, M.N., *Radial impact strength of fibre-reinforced composite tubes.* Journal of Materials Science, 1987. **22**: p. 657-662.

32. Alderson, K.L., Evans, K. E., *Low-velocity transverse impact of filament-wound pipes: Part I. Damage due to static and impact loads.* composite Structures, 1992. **20**: p. 37-45.

33. Ambur, D.R., Starnes, J. H. *Effect of curvature on the impact damage characteristics and residual strength of composite plates*. in *39th AIAA/ASME/ASCE/AHS/ASC Structues, Structural Dynamics, and Materials Conference*. 1998. Long Beach, CA: AIAA.

34. Curtis, J., Hinton, M. J., Li, S., Reid, S. R., Soden, P. D., *Damage, deformation and residual burst strength of filament-wound composite tubes subjected to impact or quasi-static indentation.* Composites: Part B, 2000. **31**: p. 419-433.

35. Shyr, T.W., Pan, Y.H., *Impact resistance and damage characteristics of composite laminates.* composite Structures, 2003. **62**: p. 193-203.

36. Aslan, Z., Karakuzu ,R., Okutan, B., *The response of laminated composite plates under low-velocity impact loading.* composite Structures, 2003. **59**: p. 119-127.

37. Kalthoff, J.F., *Characterization of the dynamic failure behaviour of a glass-fiber/vinylester at different temperatures by means of instrumented charpy impact testing.* Composites: Part B, 2004. **35**: p. 657-663.

38. Baucom, J.N., Zikry, M. A., *Low-velocity impact damage progression in woven E-glass composite systems.* Composites: Part A, 2005. **36**: p. 658-664.

39. Gning ,P.B., Tarfaoui, M., Collombet, F., Riou, L., Davies, P., *Damage development in thick composite tubes under internal loading and influence on implosion pressure: experimental observations.* Composites: Part B, 2005. **36**: p. 306-318.

40. Morais, W.A., Monteiro, S. N., Almeida, J. R. M., *Effect of the laminate thickness on the composite strength to repeated low energy impacts.* Composite Structures, 2005. **70**: p. 223-228.

41. Strait, L.H., Karasek, M. L., Amateau, M. F., *Effects of seawater immersion on the impact resistance of glass fiber reinforced epoxy composites.* Journal of Composite Materials, 1992. **26**(14): p. 2118-2133.

42. Liu, D., Raju, B. B., Dang, X., *Impact perfortion resistance of laminated and assembled composite plates.* International Journal of Impact Engineering, 2000. **24**: p. 733-746.

43. Belingardi, G., Vadori, R., *Low velocity impacts tests of laminate glass-fiber-epoxy matrix composite material plates.* International Journal of Impact Engineering, 2002. **27**: p. 213-229.

44. Dear, J.P., Brown ,S. A., *Impact damage processes in reinforced polymeric materials.* Composites: Part A, 2003. **34**: p. 411-420.

45. Corbett, G.G., Reid, S. R., *Failure of composite pipes under local loading with a hemispherically tipped indenter.* International Journal of Impact Engineering, 1994. **15**: p. 465-490.

46. Reid, S.R., Ashton, J. N., *Tolerance of composite pipes to local impact damage.* Proc Instn Mech Engrs, 1996. **210**: p. 181-192.

47. Dai, Z.Z., Harris, B., *Acostic emission study of impact-damaged GRP pipes.* NDT International, 1988. **21**(4): p. 259-265.

48. Park. R., J., J., *Impact behavior of aramid fiber/glass fiber hybrid composite: Evaluation of impact behavior using delamination area.* Journal of Composite Materials, 2000. **34**(13): p. 1117-1134.

VITAE

- Born in Hyderabad, India on September 13, 1977.
- Pursued B. Engg in Mechanical Engineering in 2001 from Osmania University, Hyderabad, India.
- Pursued M.S. in Mechanical Engineering (Materials Science) in 2005 from King Fahd University of Petroleum and Minerals, Dhahran, Saudi Arabia.
- Email: md_khaliq619@yahoo.com